Zeitschrift: IABSE congress report = Rapport du congrès AIPC = IVBH Kongressbericht

Band: 4 (1952)

Rubrik: AI3: Consideration of the actual conditions for deformation (plasticity, creep, etc.)

AI 3

The calculation of plastic collapse loads for plane frames

Le calcul des charges plastiques de rupture des cadres plans

Die Berechnung der plastischen Brucklasten ebener Rahmentragwerke

B. G. NEAL and P. S. SYMONDS

Engineering Department, Cambridge University

Brown University, Providence, R.I., U.S.A.

INTRODUCTION

Plastic design methods have been developed with a view to providing a more rational and economical approach to the design of framed structures whose members possess a high degree of ductility.[1] The methods are applicable to cases in which the members of a frame possess a relation between bending moment and curvature of the form illustrated in fig. 1. The important features of this type of relation are:

(i) If the curvature increases indefinitely, the bending moment tends to a limiting value $\pm M_p$, termed the fully plastic moment, regardless of the previous history of loading.

(ii) An increase of curvature is always accompanied by an increase of bending moment of the same sign, unless the bending moment has attained its fully plastic value.

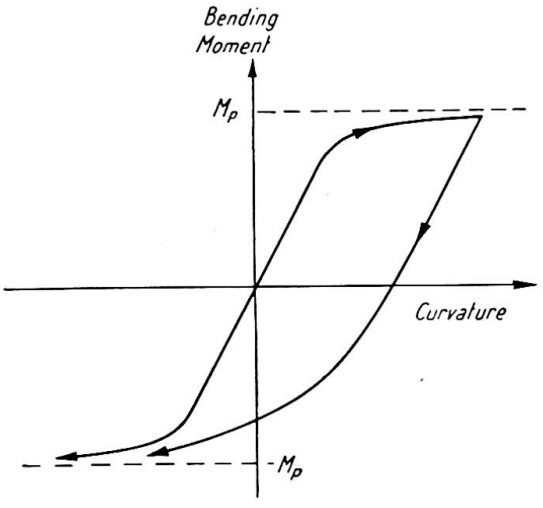

Fig. 1

The behaviour of mild steel beams conforms quite closely to these assumptions, and experimental investigations have confirmed the validity of applying plastic methods of design to framed structures of mild steel.[2] As yet, little consideration has been given to the possibility of applying the plastic methods

[1] For references see end of paper.

to framed structures of other ductile materials, such as certain of the light alloys.

When the fully plastic moment is attained at a particular cross-section of a member, the curvature at this cross-section is indefinitely large, so that a finite change of slope can occur over an indefinitely short length of the member at this cross-section. The member therefore behaves as though a hinge existed at this cross-section, rotation of the hinge being possible only when resisted by the fully plastic moment. This concept of a plastic hinge was first introduced by Maier-Leibnitz,[3] and it is of great value in considering the behaviour of framed structures under load.

For the sake of simplicity, consider first a framed structure subjected to several loads, each load maintaining the same proportion to each of the other loads. If the loads are steadily increased, the structure will first support the loads by wholly elastic action. Eventually a plastic hinge will form at the most highly stressed cross-section. If the loads are increased still further, this plastic hinge will rotate under a constant bending moment, its fully plastic moment, and further plastic hinges will form and rotate in other parts of the structure. Finally, a condition will be reached in which a sufficient number of plastic hinges have formed to transform the structure into a mechanism. The structure will then continue to deform to an indefinite extent while the loads remain constant, until the geometry of the structure is changed appreciably. Such changes may either check the growth of the deflections, or cause a catastrophic collapse by accentuating the effects of the loads. In practice, strain-hardening also checks the growth of deflections. The theoretical condition of indefinite growth of deflection under constant loads is termed plastic collapse.

The methods of plastic design are used in conjunction with a load factor. The structure is designed so that the most unfavourable combination of the working loads, when multiplied by the chosen load factor, would just cause a failure by plastic collapse. This procedure is justifiable even when the loads do not necessarily maintain the same proportions to one another, for it has been shown that plastic collapse of a structure will occur at the same set of loads regardless of the sequence in which the individual loads were brought up to their collapse values. It is clear that the load factor has a very precise meaning in plastic design, for it represents the margin of safety which is provided against an actual physical failure of the structure.

Several methods for computing plastic collapse loads have been suggested.[4, 5] These methods have been capable, in principle, of determining plastic collapse loads for framed structures of any degree of complexity. In practice, however, their application has been limited by the amount of time required for the necessary computations. In the present paper a method is presented which enables plastic collapse loads and their corresponding mechanisms to be determined very simply. The method consists essentially of building up the actual collapse mechanism from a certain number of independent components, which are termed the independent partial collapse mechanisms. Corresponding to any mechanism which is being investigated, a value can be found for the applied load by applying the Principle of Virtual Work.[6] It has been shown that the correct collapse mechanism is the one to which there corresponds the smallest possible value of the applied load. The method consists therefore of combining the independent partial collapse mechanisms in a systematic manner in order to reduce the corresponding value of the applied load to its least possible value. In order to explain and justify the method, a simple example will first be discussed. Detailed calculations will then be given for a single-bay pitched-roof portal frame, and the calculations for a three-bay pitched-roof portal frame will also be outlined. Calculations for a two-bay three-storey rectangular frame have been given elsewhere.[7]

SIMPLE ILLUSTRATIVE EXAMPLE

The rectangular portal frame shown in fig. 2 will be used as a basis for the discussion of the method. All the joints of this frame are assumed to be rigid, and the feet of the stanchions are rigidly built in. The dimensions of the frame are as shown, and horizontal and vertical loads W are applied at the positions indicated in the figure. The fully plastic moment of each member is M_p, and the problem is to find the value of W which causes failure by plastic collapse.

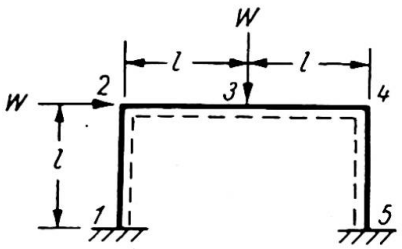

Fig. 2

For this particular type of structure it is known that there are only three possible collapse mechanisms, and these mechanisms are shown in figs. 3(*a*), 3 (*b*) and 3(*c*). In these figures the magnitudes of the plastic hinge rotations are all shown in terms of a single parameter θ. For reference, the signs of the plastic hinge rotations are also given, although in the technique to be described there is no need to take account of these signs. The sign convention adopted is that a hinge rotation is positive if the hinge is opening when viewed from inside the frame.

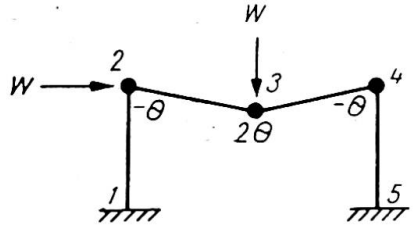

Fig. 3(*a*)

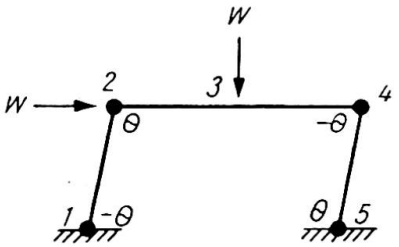

Fig. 3(*b*)

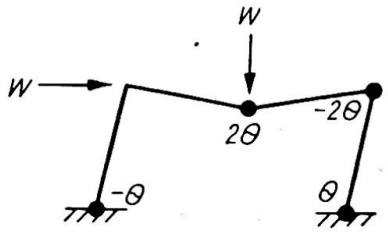

Fig. 3(*c*)

For each mechanism it is possible to calculate a corresponding value of W by applying the principle of virtual work in the special form that the virtual work done by the applied loads during a small displacement of the mechanism is equal to the virtual work absorbed in the plastic hinges. Considering the mechanism of fig. 3(*a*), for example, it is seen that during the small mechanism displacement shown, the horizontal load W does no work and the vertical load W, displaced through a distance $l\theta$, does virtual work $Wl\theta$. To calculate the virtual work absorbed in the plastic hinges, it is noted that the work absorbed in any individual hinge is always positive. Since the fully plastic moment is M_p everywhere in the frame, the virtual work absorbed in the plastic hinges is at once seen to be $4\theta M_p$, since the total rotation of all the plastic hinges is 4θ. Applying the principle of virtual work:

$$Wl\theta = 4\theta M_p, \text{ or } W = 4\frac{M_p}{l} \quad . \quad . \quad . \quad . \quad . \quad . \quad . \quad . \quad (1)$$

Similar calculations for the mechanisms of figs. 3(*b*) and 3(*c*) are readily made. The results of these calculations are:

fig. 3(*b*): $$Wl\theta=4\theta M_p, \text{ or } W=4\frac{M_p}{l} \quad . \ . \ . \ . \ . \ . \ . \ . \quad (2)$$

fig. 3(*c*): $$2Wl\theta=6\theta M_p, \text{ or } W=3\frac{M_p}{l} \quad . \ . \ . \ . \ . \ . \ . \ . \quad (3)$$

The correct collapse mechanism can now be distinguished by applying what has been termed the *kinematic principle* of plastic collapse.[6, 8] This principle states that: " For a given frame and loading, the correct collapse mechanism is the mechanism to which there corresponds the smallest possible value of the applied loads." For the particular problem of fig. 2, it follows that the actual collapse mechanism is the mechanism shown in fig. 3(*c*), which yields the lowest value of W, namely $3M_p/l$.

Examination of figs. 3(*a*), 3(*b*) and 3(*c*) reveals the fact that the mechanism of fig. 3(*c*) is a direct combination of the mechanisms of figs. 3(*a*) and 3(*b*), in the sense that the displacements and plastic hinge rotations of this mechanism are obtained by summing the corresponding quantities for the mechanisms of figs. 3(*a*) and 3(*b*). In fact, as will be seen later, these latter two mechanisms are the independent partial collapse mechanisms for this structure and loading. In general, all possible collapse mechanisms can be formed by combining the independent partial collapse mechanisms. In the simple problem under consideration there is, of course, only one possible combination to be investigated.

The particular feature of the combination of the independent mechanisms of figs. 3(*a*) and 3(*b*) which is of interest is that for both these mechanisms the corresponding value of W was $4M_p/l$, whereas for the mechanism of fig. 3(*c*) which resulted from their combination the value of W was only $3M_p/l$. This reduction of W is due to the cancellation of the plastic hinge at the cross-section 2 which occurs when the mechanisms are combined. When the two mechanisms are superposed, the virtual work done by the loads in each case may be added to obtain the virtual work done in the resulting mechanism. However, to obtain the virtual work absorbed in the plastic hinges in the resulting mechanism, work $2\theta M_p$ must be subtracted from the sum of the virtual work absorbed in the two independent mechanisms. This is to account for the term θM_p which was included in the virtual work absorbed in each of these mechanisms for the plastic hinge at the cross-section 2, which disappears as a result of the superposition. The virtual work equation for the resulting mechanism is thus obtained by adding equations (1) and (2), and subtracting $2\theta M_p$ from the resulting work absorbed in the plastic hinges, giving:

$$Wl\theta+Wl\theta=4\theta M_p+4\theta M_p-2\theta M_p$$

or $$2Wl\theta=6\theta M_p,$$

which was previously obtained as equation (3).

In general, the technique for combining the independent mechanisms thus consists in selecting pairs of independent mechanisms which themselves yield low values of W, and which can be combined so as to cancel a plastic hinge. Such a combination may, as has been seen, result in a value for W which is lower than the value corresponding to either of the mechanisms which were combined. Even in complicated problems, the combinations to be tried are usually small in number, so that a solution can be obtained with great rapidity.

It is, of course, essential to start an analysis with the correct number of independent mechanisms. In fact, the number of independent mechanisms is always equal to the

number of independent equations of equilibrium for the frame. To justify this statement, it is necessary to consider the statics of the illustrative example of fig. 2, although it should be stressed that in actual applications of the technique there is no need to write down the equations of equilibrium. However, it is recommended that solutions should always be checked by statics, making use of the *principle of uniqueness of solution*,[6, 8] which states that: "If a sufficient number of plastic hinges occur in a frame to transform the frame into a mechanism, and if a bending moment diagram can be constructed for the frame in which the fully plastic moment occurs at each plastic hinge position, then the corresponding load is the correct collapse load if the fully plastic moment is not exceeded anywhere in the frame."

Examples of this form of check are given later in the paper.

The equations of equilibrium

The equations of equilibrium for the frame illustrated in fig. 2 are written down most conveniently in terms of the bending moments at the five cross-sections numbered from 1 to 5 in fig. 2. It will be seen from this figure that when these five bending moments are known, the bending moment distribution for the entire frame is determined, for between any adjacent pair of these cross-sections the shear force is constant, so that the bending moment must vary linearly along the length of the member. These five bending moments are denoted by $M_1, M_2, \ldots M_5$, the suffix indicating the relevant cross-section. The sign convention adopted for these bending moments is that a positive bending moment causes tension in the fibres of a member adjacent to the dotted line in fig. 2.

This frame has three redundancies, for if a cut is imagined to be made at section 1, for example, and the values of the shear force, thrust and bending moment at this section are known, the entire frame becomes statically determinate. These three quantities can therefore be regarded as the redundancies of the frame. Since there are five unknown bending moments, it follows that there must be two independent equations of equilibrium.

The first of these equations of equilibrium expresses the fact that the vertical load W is carried by the shear forces in the horizontal member 234. Fig. 4 shows the

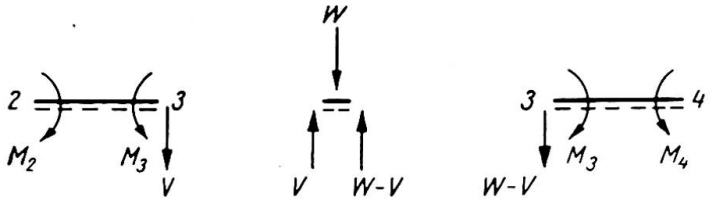

Fig. 4

relevant forces and bending moments, the load W being carried by a shear force V in the member 23 and a shear force $W-V$ in the member 34. Taking moments for the equilibrium of the members 23 and 34, it is found that

$$M_3-M_2=Vl$$

$$M_3-M_4=(W-V)l$$

On adding these equations to eliminate V, it is found that

$$2M_3-M_2-M_4=Wl \quad . \quad . \quad . \quad . \quad . \quad . \quad . \quad . \quad (4)$$

In a similar way, an equation expressing the fact that the horizontal load W is carried

by the shear forces in the vertical members 12 and 45 may be found. This equation is

$$M_2-M_1+M_5-M_4=Wl \quad . \quad . \quad . \quad . \quad . \quad . \quad . \quad . \quad (5)$$

Equations (4) and (5) constitute the two independent equations of equilibrium.

In the mechanism of fig. 3(*a*) plastic hinges have formed at the cross-sections 2, 3 and 4, so that the magnitude of the bending moment at each of these cross-sections is M_p. Having regard to the sign convention, these bending moments are

$$M_2=-M_p, \quad M_3=M_p, \quad M_4=-M_p$$

When these values are substituted in equation (4), a value for W is immediately found, this value being $W=4M_p/l$.

It will be seen that the mechanism of fig. 3(*a*) corresponds to equation (4) in the special sense that in this mechanism each of the bending moments appearing in equation (4) takes on its fully plastic value, and that the sign of each bending moment is such as to give rise to the largest possible value of W. In a similar way, the mechanism of fig. 3(b) may be said to correspond to equation (5). If each of the bending moments appearing in equation (5) is given its fully plastic value, and the sign of each bending moment is such that the largest value of W is obtained, the following values are found:

$$M_1=-M_p, \quad M_2=M_p, \quad M_4=-M_p, \quad M_5=M_p.$$

These are the fully plastic moments appearing in the mechanism of fig. 3(*b*).

To generalise, it may be said that any mechanism corresponds in this special sense to a particular equation of equilibrium. It follows that for any particular frame and loading the number of independent mechanisms will be equal to the number of independent equations of equilibrium. In the particular example under consideration there are only two independent equations of equilibrium, namely equations (4) and (5) and any other equation of equilibrium must be obtainable by combining these two equations. Correspondingly, it follows that any possible mechanism will be found to be a combination of the mechanisms of figs. 3(*a*) and 3(*b*). In this particular example, there is only one possible combination of these mechanisms, which is illustrated in fig. 3(*c*). The equation of equilibrium which corresponds to this mechanism is obtained by adding equations (4) and (5) so as to eliminate M_2, giving

$$2M_3-M_1-2M_4+M_5=2Wl \quad . \quad . \quad . \quad . \quad . \quad . \quad . \quad (6)$$

This addition corresponds to the superposition of the mechanisms of figs. 3(*a*) and 3(*b*). The bending moments at the plastic hinges may be seen from this equation, or from the mechanism of fig. 3(*c*), to be

$$M_1=-M_p, \quad M_3=M_p, \quad M_4=-M_p, \quad M_5=M_p,$$

and the corresponding value of W is $3M_p/l$.

For convenience of discussion, the loads have previously been referred to as the variables, whereas in an actual design the loads will be given quantities and the problem is to find the required fully plastic moments of the members. When viewed in this light, the problem just discussed amounts to determining the *greatest* value of M_p, rather than the least value of W, corresponding to any possible mechanism, for it is the quantity Wl/M_p which is determined for any particular mechanism by a virtual work analysis, and minimising W for given values of M_p and l amounts to maximising M_p for given values of W and l.

To summarise, then, the proposed method is as follows:

(1) Determine the correct number of independent mechanisms by calculating the number of independent equations of equilibrium.
(2) Calculate the required values of the fully plastic moments of the members by virtual work for these independent mechanisms.
(3) Investigate combinations of these mechanisms so as to maximise the required fully plastic moments.
(4) Check the solution by constructing a bending moment diagram.

An application of the method to a single-bay pitched-roof portal frame will now be given in detail, followed by a brief indication of the application of the method to a three-bay pitched-roof portal frame.

PITCHED-ROOF PORTAL DESIGN

As an illustration of the practical application of the proposed method of design, typical calculations for a pitched-roof portal frame will now be given. The dimensions of the frame are as indicated in fig. 5, the roof slope being $22\frac{1}{2}°$. The working loads on the frame are also shown in fig. 5. These working loads, which are given in tons, are assumed to be spread uniformly over the purlins and sheeting rails shown in the figure. Of these loads, the vertical loads of 2·61 tons, acting on each rafter, are due to dead and superimposed (snow) loads, and the remaining loads are wind pressures and suctions. The frame is to be designed to a load factor of 1·75 for the case in which only the dead and superimposed loads are acting, and to a load factor of 1·4 for the case in which the wind loads are also acting. Each member of the frame will be taken to have the same cross-section, with a fully plastic moment M_p.

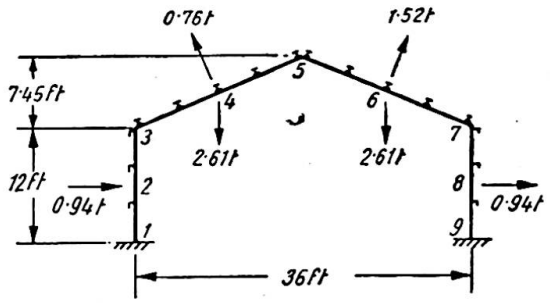

Fig. 5

Design for dead, superimposed and wind loads

The first design case which will be considered is the design to a load factor of 1·4 for the case in which the wind loads are acting in conjunction with the dead and superimposed loads. The first step is to decide how many independent partial collapse mechanisms must be considered. The number of such mechanisms for any given frame and loading has been shown to be equal to the number of independent equations of equilibrium. It is therefore necessary to calculate the number of independent equations of equilibrium, and this is done most conveniently by counting the number of bending moments which are needed to specify the bending moment distribution for the entire frame and subtracting the number of redundancies.

For each of the four members of the frame, the loads will be assumed to be uniformly distributed, so that the distribution of bending moment is parabolic. Each parabola will be completely specified if the values of the bending moment at three sections are known. These three sections are chosen most conveniently for the present purpose as the two end sections and the central section in each member. It follows that the bending moment distribution for the entire frame will be specified completely by the values of the bending moments at the nine cross-sections numbered

from 1 to 9 in fig. 5. This frame has three redundancies, and so there must be six independent equations of equilibrium.

It follows that there must be six independent partial collapse mechanisms. These mechanisms are illustrated in figs. 6–11, inclusive. It will be seen that the mechanisms of figs. 6, 7, 8 and 9 are merely simple beam failure mechanisms, and fig. 10 shows a simple sidesway mechanism. If it were not known that there must be six independent mechanisms, it might be concluded that these five mechanisms constituted the independent partial collapse mechanisms, and thus a calculation of the correct number of independent mechanisms is a vital preliminary operation in the analysis. However, a sixth independent mechanism must be selected, and the most convenient choice is the mechanism shown in fig. 11. In each figure the rotation of each plastic hinge is given in terms of a single variable θ. There is no need to consider the signs of the plastic hinge rotations, since the virtual work absorbed in a plastic hinge is always positive. However, for convenience in the later stages of the calculations when the solution is checked by statics, the signs of the plastic hinge rotations are also given, the sign convention being that a hinge rotation is positive if the joint is opening when viewed from within the portal.

In the simple beam failure mechanisms of figs. 6, 7, 8 and 9, the plastic hinges within the spans are all shown as occurring at mid-span. However, the loads on these spans are all assumed to be uniformly distributed in the first instance, so that these plastic hinges might occur anywhere within the spans. This is because a plastic hinge within a span must occur at a position of maximum bending moment, and the positions at which the maximum bending moments occur are not known until a later stage in the analysis. However, in the preliminary calculations it is convenient to take these plastic hinges as occurring in mid-span.

Now consider the mechanism of fig. 6. For the hinge rotations shown, the plastic hinge at mid-span moves through a distance 6θ ft. The average displacement of the uniformly distributed load of 0·94 tons is therefore 3θ ft., so that the virtual work done by this load, taking into account the load factor of 1·4, is $0{\cdot}94 \cdot 1{\cdot}4 \cdot 3\theta$ tons-ft. The total plastic hinge rotation involved in the mechanism is 4θ, so that the virtual work absorbed in the plastic hinges is $4\theta M_p$. Applying the principle of virtual work, it is found that

$$4\theta M_p = 0{\cdot}94 \cdot 1{\cdot}4 \cdot 3\theta = 3{\cdot}95\theta$$
$$M_p = 0{\cdot}99 \text{ tons-ft.} \quad \ldots\ldots\ldots\ldots \quad (7)$$

The virtual work equation for the mechanism of fig. 7 is precisely the same as

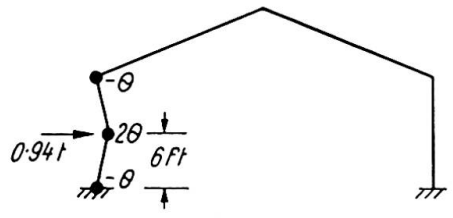

Fig. 6

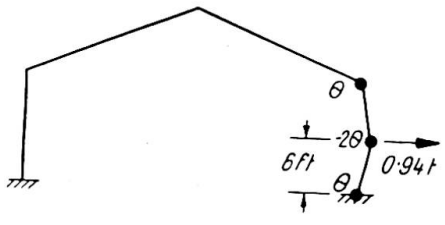

Fig. 7

equation (7). Corresponding virtual work equations may be written down at once for the mechanisms of figs. 8 and 9. These equations are:

fig. 8:
$$4\theta M_p = 1{\cdot}4[2{\cdot}61 \cdot 4{\cdot}5\theta - 0{\cdot}76 \cdot 4{\cdot}87\theta] = 11{\cdot}3\theta$$
$$M_p = 2{\cdot}83 \text{ tons-ft.} \quad \ldots\ldots\ldots\ldots \quad (8)$$

fig. 9:
$$4\theta M_p = 1{\cdot}4[2{\cdot}61 \cdot 4{\cdot}5\theta - 1{\cdot}52 \cdot 4{\cdot}87\theta] = 6{\cdot}08\theta$$
$$M_p = 1{\cdot}52 \text{ tons-ft.} \quad \ldots\ldots\ldots\ldots \quad (9)$$

The geometry of the sidesway mechanism of fig. 10 is also simple. Each side load of 0·94 tons moves through an average distance of 6θ ft., and the entire roof moves laterally through a distance 12θ ft. The virtual work equation is

$$4\theta M_p = 1{\cdot}4[2\,.\,0{\cdot}94\,.\,6\theta + 0{\cdot}76 \sin 22\tfrac{1}{2}^\circ\,.\,12\theta] = 20{\cdot}7\theta$$

$$M_p = 5{\cdot}18 \text{ tons-ft.} \quad . \quad . \quad . \quad . \quad . \quad . \quad . \quad . \quad . \quad . \quad . \quad . \quad (10)$$

The geometry of the mechanism of fig. 11 is a little more complicated. If the hinge at joint 3 rotated through an angle $-\theta$ while the joint 5 remained rigid, joint 7 would

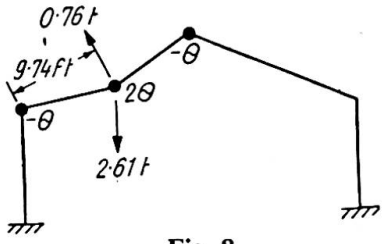

Fig. 8

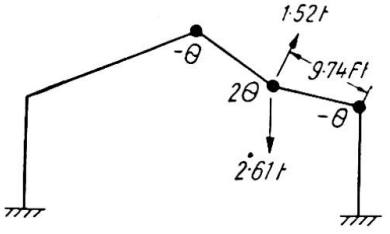

Fig. 9

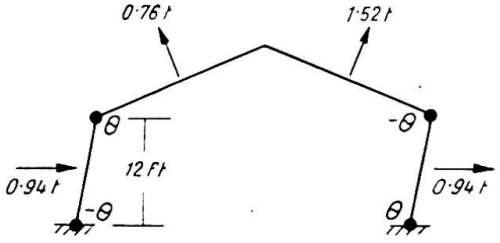

Fig. 10

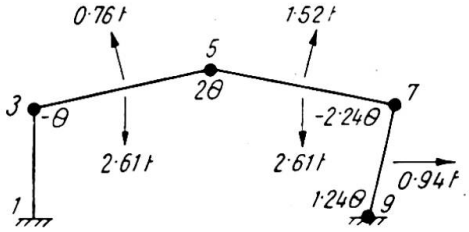

Fig. 11

move downwards through a distance 36θ ft. Since there can be no downwards motion of joint 7 for a small displacement of the mechanism, it follows that the hinge at joint 5 must rotate through an angle $36\theta/18 = 2\theta$ so as to reduce the vertical displacement of joint 7 to zero. This hinge rotation causes a horizontal displacement of joint 7 through a distance $2\theta\,.\,7{\cdot}45 = 14{\cdot}9\theta$ ft., so that the rotation of the hinge at joint 9 is $14{\cdot}9\theta/12 = 1{\cdot}24\theta$. The hinge rotation at joint 7 is then seen to be $-2{\cdot}24\theta$, and it is found that the centre of the member 57 moves $11{\cdot}2\theta$ ft. to the right and 9θ ft. downwards. The virtual work equation for this mechanism may now be written down as follows:

$$6{\cdot}48\theta M_p = 1{\cdot}4[2\,.\,2{\cdot}61\,.\,9\theta - 0{\cdot}76\,.\,9{\cdot}74\theta + 1{\cdot}52 \sin 22\tfrac{1}{2}^\circ\,.\,11{\cdot}2\theta$$
$$- 1{\cdot}52 \cos 22\tfrac{1}{2}^\circ\,.\,9\theta + 0{\cdot}94\,.\,7{\cdot}45\theta]$$
$$= 56{\cdot}6\theta$$
$$M_p = 8{\cdot}73 \text{ tons-ft.} \quad . \quad . \quad . \quad . \quad . \quad . \quad . \quad . \quad . \quad . \quad . \quad . \quad (11)$$

Among the six independent partial collapse mechanisms, the highest values of M_p are thus 5·18 tons-ft. and 8·73 tons-ft. for the mechanisms of figs. 10 and 11, respectively. The next step is thus to investigate the combination of these two mechanisms. It is seen that if the mechanism of fig. 10 is superposed on the mechanism of fig. 11, the rotation of the hinge at joint 3 is cancelled, so that the resulting mechanism is as shown in fig. 12. The virtual work equation for this mechanism is obtained by adding equations (10) and (11), and subtracting $2\theta M_p$ from the resulting virtual work

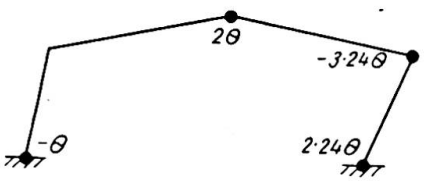

Fig. 12

absorbed in the plastic hinges, since a term θM_p was included in each of these equations for the plastic hinge at joint 3. The virtual work equation is thus:

$$(4+6\cdot48-2)\theta M_p=20\cdot7\theta+56\cdot6\theta$$

$$8\cdot48\theta M_p=77\cdot3\theta$$

$$M_p=9\cdot12 \text{ tons-ft.} \quad . \quad . \quad . \quad . \quad . \quad (12)$$

The highest value of M_p obtained from the other four independent mechanisms of figs. 6, 7, 8 and 9 was 2·83 tons-ft. for the mechanism of fig. 8, and it is readily seen that there is no possible combination of these mechanisms with the mechanism of fig. 12 which will result in a further increase in the value of M_p. It is therefore concluded that the mechanism of fig. 12 is the actual collapse mechanism, subject to the proviso that no consideration has yet been given to the possibility of the occurrence of plastic hinges at positions other than those numbered from 1 to 9 in fig. 5. When this solution is checked by statics it will, in fact, be found that the plastic hinge shown at the apex of the roof in fig. 12 should be located somewhat to the left of the apex.

Check by statics

The solution can be checked by constructing a bending moment diagram for the frame. If the fully plastic moment is not exceeded at any cross-section, the solution is correct. The actual bending moment at a cross-section may be regarded as the sum of the "free bending moment," produced in the frame by the applied loads when a cut has been made at some cross-section so as to render the frame statically determinate, and the "redundant bending moment" produced in the frame by the three redundancies. For convenience, the form of the redundant bending moment diagram will be considered first.

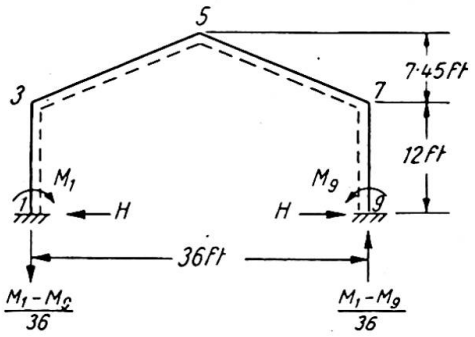

Fig. 13

The three redundancies may be taken as the bending moments, M_1 and M_9, at the feet of the vertical members, and the horizontal thrust H, as in fig. 13. With no external loads acting on the structure, the vertical reactions at the feet of the vertical members would be equal and opposite, and of magnitude $(M_1-M_9)/36$ as shown in the figure. In drawing the bending moment diagrams, the sign convention will be that a positive bending moment will cause a member to sag inwards, and thus to produce tension in the flange of the member which is adjacent to the dotted line in fig. 13. With the redundancies as shown in this figure, the redundant bending moment diagram is thus of the form indicated in fig. 14, in which the members of the frame have been redrawn to a horizontal base, and positive bending moments are plotted as ordinates below this base. In fig. 14 the dotted line

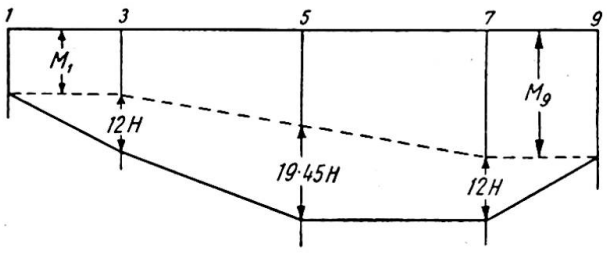

Fig. 14

indicates the form of the redundant bending moment diagram for the case in which H is zero, and the full line indicates the effect of superposing the bending moment diagram for the case in which H acts alone.

The free bending moment diagram refers to the bending moments produced in the frame by the applied loads when a cut is made at any arbitrary cross-section. The most convenient choice of cross-section for this purpose is the roof apex. Fig. 15 shows the free bending moment diagram, consisting of three parabolas, which is obtained in this way, the loads having been multiplied by the load factor of 1·4.

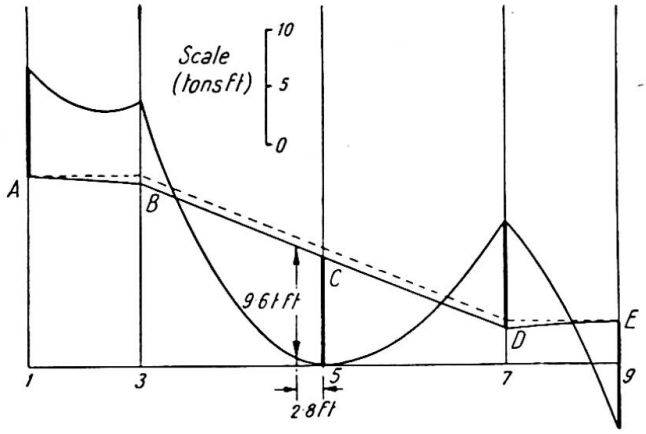

Fig. 15

The collapse mechanism of fig. 12 has four plastic hinges at the cross-sections 1, 5, 7 and 9, so that at these cross-sections the bending moment has its fully plastic value, which was found to be 9·1 tons-ft. To check the solution, it must be verified that a diagram of actual bending moments can be constructed in which the bending moment has the value 9·1 tons-ft. at these four cross-sections, and does not exceed this value at any other cross-section in the frame. Now the actual bending moment is equal to the sum of the free and redundant bending moments, so that if a redundant bending moment diagram is drawn in fig. 15 with the signs of the bending moments changed, the actual bending moment will be represented by the difference in ordinate between this diagram and the free bending moment diagram. The appropriate diagram is shown in fig. 15 as ABCDE.

The construction for this diagram is to lay off from the free bending moment diagram the calculated fully plastic moment of 9·1 tons-ft., with appropriate sign, at the four cross-sections 1, 5, 7 and 9. This gives the four points A, C, D and E on the redundant bending moment diagram. Referring to fig. 14, it is seen that the point B may then be plotted by making the slope of AB equal in magnitude to the slope of DE, but of opposite sign. A check can then be made by observing that the vertical intercept between C and the dotted line in fig. 15 is 19·45 H, whereas the corresponding intercept at D is 12 H. These intercepts both correspond to a value of H of 0·05 tons, thus checking the solution. However, it will be seen that although the bending moment at the cross-section 3 is less than the calculated fully plastic moment of 9·1 tons ft., a higher value of the bending moment occurs at a distance of 2·8 ft. along the left-hand rafter member from the apex joint, this value being 9·6 tons-ft. This does not imply an error in the virtual work calculations, for in those calculations the choice of plastic hinge positions was restricted to the ends and centres of the members. The calculation of the required fully plastic moment could be refined by carrying out

a fresh virtual work calculation in which the plastic hinge at the apex joint 5 was moved to the new position 2·8 ft. along the left-hand rafter member. However, it is unnecessary to perform this calculation, for it will be seen that the design is, in fact, not governed by this loading case but by the dead and superimposed loading case. It is therefore noted that a value of M_p between 9·1 and 9·6 tons-ft. would be adequate for dead, superimposed and wind loads in conjunction.

Design for dead and superimposed loads

The design for dead and superimposed loads to a load factor of 1·75 will now be considered. The relevant working loads are merely loads of 2·61 tons uniformly distributed over the two rafters, as shown in fig. 16. Since this loading is symmetrical, the bending moment distribution for the frame is also symmetrical, and so only four bending moments are needed to specify the bending moment distribution. These may be taken as the bending moments at the cross-sections 1, 3, 4 and 5 in fig. 16. Due to symmetry, the frame has only two redundancies, for the bending moments at the cross-sections 1 and 9 are equal. The bending moment at cross-section 1 and the horizontal thrust can thus be regarded as the two redundancies. It follows that there are only two equations of equilibrium, and therefore two independent mechanisms. Both of these mechanisms must be symmetrical.

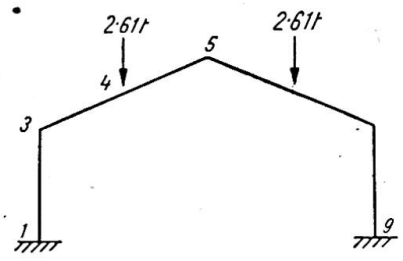

Fig. 16

The two independent mechanisms are illustrated in figs. 17 and 18. Fig. 17 merely represents failure of the two rafters as beamS, and the equation of virtual work is

$$8\theta M_p = 2 \,.\, 2{\cdot}61 \,.\, 1{\cdot}75 \,.\, 4{\cdot}5\theta = 41{\cdot}1\theta$$

$$M_p = 5{\cdot}14 \text{ tons-ft.} \quad . \quad . \quad . \quad . \quad . \quad . \quad . \quad . \quad . \quad . \quad . \quad (13)$$

In the mechanism of fig. 18, the hinge rotation θ at cross-section 1 would produce a horizontal movement of $19{\cdot}45\theta$ at the roof apex if there were no hinge rotation

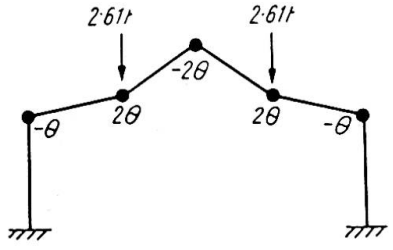

Fig. 17

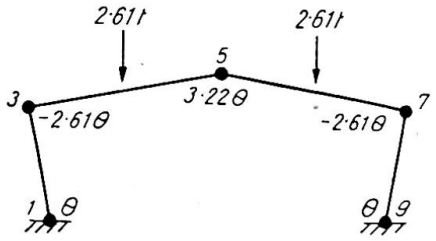

Fig. 18

at cross-section 3. The hinge rotation at cross-section 3 must therefore be $-19{\cdot}45\theta/7{\cdot}45 = -2{\cdot}61\theta$ in order that there should be no horizontal movement at the apex. The downwards vertical displacement at the apex is thus $18 \,.\, 1{\cdot}61\theta = 29{\cdot}0\theta$ ft. The virtual work equation is:

$$10{\cdot}44\theta M_p = 2 \,.\, 2{\cdot}61 \,.\, 1{\cdot}75 \,.\, 14{\cdot}5\theta = 132{\cdot}5\theta$$

$$M_p = 12{\cdot}7 \text{ tons-ft.} \quad . \quad . \quad . \quad . \quad . \quad . \quad . \quad . \quad . \quad . \quad . \quad (14)$$

It will be noted that this value of M_p exceeds the value found for the case in which the wind loads act in conjunction with the dead and superimposed loads. It follows

that the design must be governed by the present case in which only the dead and superimposed loads are acting.

Considering now the combination of the independent mechanisms, it will be seen that cancellation of the plastic hinge rotation at the roof apex can be achieved by superposing the mechanism of fig. 17, with all the hinge rotations and displacements increased by a factor of $3{\cdot}22/2=1{\cdot}61$, on the mechanism of fig. 18. The mechanism thus obtained is illustrated in fig. 19. The virtual work equation for this mechanism is obtained by adding equation (13), multiplied by 1·61, to equation (14), and subtracting $6{\cdot}44\theta M_p$ from the resulting virtual work absorbed in the plastic hinges, since a plastic hinge rotation of $3{\cdot}22\theta$ in each of the mechanisms at the roof apex has been cancelled. The resulting equation is:

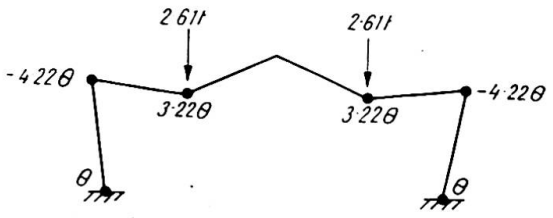

Fig. 19

$$(8\ .\ 1{\cdot}61+10{\cdot}44-6{\cdot}44)\ \theta M_p=41{\cdot}1\ .\ 1{\cdot}61\theta+132{\cdot}5\theta$$

$$16{\cdot}88\theta M_p=198{\cdot}7\theta$$

$$M_p=11{\cdot}8 \text{ tons-ft.} \quad . \quad . \quad . \quad . \quad . \quad . \quad (15)$$

The highest value of M_p obtained from these mechanisms is thus 12·7 tons-ft. for the mechanism of fig. 18. This is therefore the actual collapse mechanism, subject to possible alterations due to the occurrence of plastic hinges within the spans of the members rather than at the joints. A statical check will reveal, in fact, that the plastic hinge at the roof apex should be replaced by one plastic hinge in each rafter member.

Check by statics

The free bending moment diagram for the frame, cut at the roof apex, when subjected to the factored loads, is shown in fig. 20, together with the redundant bending moment diagram. This latter diagram is constructed by setting off the calculated fully plastic moment of 12·7 tons-ft. from the free bending moment diagram at the

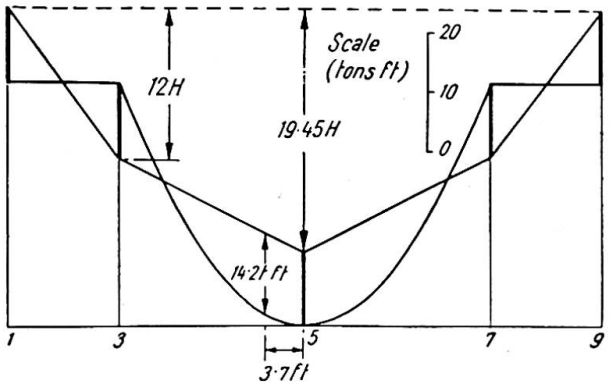

Fig. 20

cross-sections 1, 3, 5, 7 and 9. The value of the horizontal thrust can be calculated from the intercepts between the redundant bending moment line and the dotted line in fig. 20 at both the cross-sections 3 and 5. The value obtained in each case is 2·1 tons, thus checking the virtual work calculation. It will be seen that the greatest bending moment which occurs with this bending moment distribution is 14·2 tons-ft. at a distance of 3·7 ft. from the roof apex. Thus in the correct collapse mechanism

there should be plastic hinges in each rafter at a distance of about 3·7 ft. from the roof apex in place of the single plastic hinge shown at the apex in fig. 18. A fresh calculation for these new plastic hinge positions is readily made, either by virtual work or by adjusting the redundant bending moment line on the bending moment diagram, and the resulting value of M_p is found to be 13·2 tons-ft. A final refinement is to take account of the fact that the loads are not, in fact, uniformly distributed over the rafters, but are carried by five uniformly spaced purlins, as shown in fig. 5. The plastic hinges in the rafters will be located beneath the purlins which are adjacent to the roof apex, and the corresponding value of M_p is found to be 13·0 tons-ft. or 156 tons-in.

A choice of section can now be made. The fully plastic moment for a rolled steel joist is known to exceed the moment at which the yield stress is just reached in the outermost fibres by a factor termed the shape factor, which is about 1·15 for most sections.[4] Taking a yield stress of 15·25 tons/in.^{2}, the fully plastic moment M_p is thus:

$$M_p = 1{\cdot}15 \,.\, 15{\cdot}25 \,.\, Z = 17{\cdot}5\, Z \text{ tons-in.}$$

where Z in.^{3} is the section modulus. The required value of Z in the present case is:

$$Z = 156/17{\cdot}5 = 8{\cdot}91 \text{ in.}^3$$

The nearest available British Standard beam section is a 7×4×16 lb., with a section modulus of 11·29 in.^{3} This is therefore the required section. From the point of view of stability, the purlins and sheeting rails, together with some cross-bracing, would provide adequate stiffening for this section over the given spans.

THREE-BAY PITCHED-ROOF PORTAL FRAME

To illustrate the scope of the technique which has been described in detail, calculations for the three-bay frame whose dimensions and loads are as shown in fig. 21 will now be outlined briefly. As before, all the loads are assumed to be uniformly

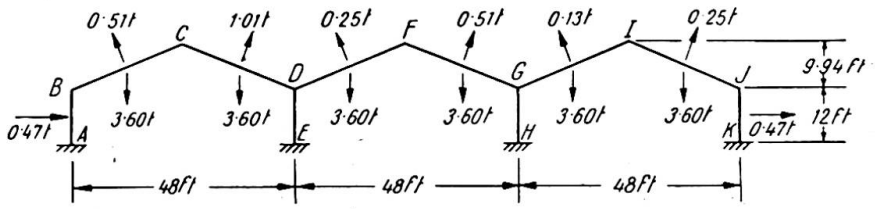

Fig. 21

distributed, and the vertical loads of 3·60 tons on each rafter member are due to dead and superimposed loads, the remaining loads being wind loads. In the first instance, it will be assumed that all the members of the frame are of the same cross-section, with a fully plastic moment M_p.

Design for dead, superimposed and wind loads

For this loading case, a load factor of 1·4 will be used. Examination of fig. 21 shows that twenty-three bending moments are needed to specify the bending moment distribution for the entire frame, which has nine redundancies. There must therefore be fourteen independent mechanisms. Eight of these mechanisms are accounted for by the simple beam type of failure mechanism (as in figs. 6, 7, 8 and 9, for example) occurring in the members AB, BC, CD, DF, FG, GI, IJ and JK. For these mechanisms, the highest value of M_p is obtained for the member GI, this value of M_p being

7·28 tons-ft. Two mechanisms must be counted for rotations of the joints D and G in fig. 21, for it will be realised that for each of these joints there will be an equation of rotational equilibrium between the three bending moments acting on the joint. There will also be one sidesway mechanism, with plastic hinges in the vertical members at A, B, D, E, G, H, J and K, for which the corresponding value of M_p is 1·69 tons-ft. The remaining three independent mechanisms may be chosen in a variety of ways, but the three mechanisms illustrated in figs. 22, 23 and 24 are probably the most convenient for the present purpose. It will be seen that each of these mechanisms is basically of the same type, with the rafters collapsing in one bay and thus causing sidesway of those parts of the frame lying to the right of the collapsing bay. For reference, the plastic hinge rotations are shown in these figures in magnitude only. It will be noted that the joints D and G remain unrotated in each of these mechanisms, since in each case any rotation of these joints would increase the work absorbed in the plastic hinges and so reduce the value of M_p.

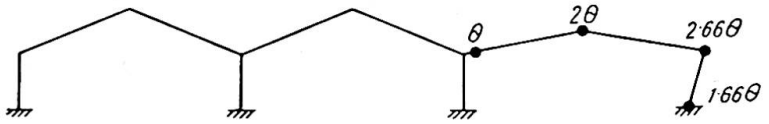

Fig. 22

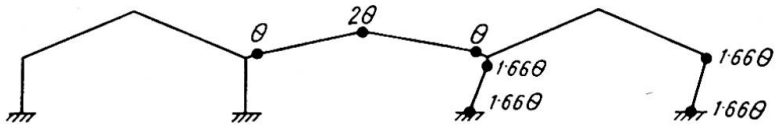

Fig. 23

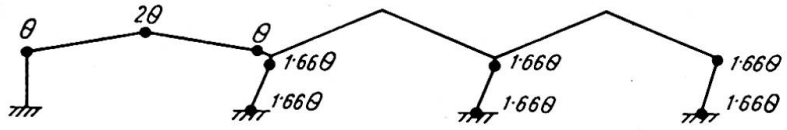

Fig. 24

The virtual work equations for these three mechanisms are found to be:

fig. 22: $7{\cdot}32\theta M_p = 123{\cdot}5\theta$, $M_p = 16{\cdot}9$ tons-ft. . . . . (16)

fig. 23: $10{\cdot}64\theta M_p = 120{\cdot}4\theta$, $M_p = 11{\cdot}3$ tons-ft. . . . . (17)

fig. 24: $13{\cdot}96\theta M_p = 115{\cdot}1\theta$, $M_p = 8{\cdot}25$ tons-ft. . . . . (18)

The highest value of M_p obtained from the independent mechanisms is thus 16·9 tons-ft. for the mechanism of fig. 22. It is easily seen that this value of M_p will not be increased by combination with any of the simple beam mechanisms, for which the highest value of M_p was found to be 7·28 tons-ft. It is also clear that the sidesway mechanism, for which M_p was found to be only 1·69 tons-ft., cannot be combined with advantage. It remains to investigate possible combinations of the three mechanisms of figs. 22, 23 and 24.

The mechanisms of figs. 22 and 23 can be combined if the hinge rotations and displacements in the mechanism of fig. 22 are all multiplied by a factor of 1·66, and

then superposed on the mechanism of fig. 23. This enables a clockwise rotation, of magnitude $1{\cdot}66\theta$, to be given to joint G, which cancels plastic hinge rotations of $1{\cdot}66\theta$ in the members GI and GH at this joint, while increasing the plastic hinge rotation in the member GF by $1{\cdot}66\theta$. This produces a net reduction in the virtual work absorbed of $1{\cdot}66\theta M_p$. The resulting virtual work equation for this combination is then seen from equations (16) and (17) to be:

$$1{\cdot}66 \,.\, 7{\cdot}32 \,.\, \theta M_p + 10{\cdot}64\theta M_p - 1{\cdot}66\theta M_p = 1{\cdot}66 \,.\, 123{\cdot}5\theta + 120{\cdot}4\theta$$

$$21{\cdot}1\theta M_p = 325\theta$$

$$M_p = 15{\cdot}4 \text{ tons-ft.} \quad . \quad . \quad . \quad . \quad (19)$$

This value of M_p is smaller than the value of 16·9 tons-ft. obtained for the mechanism of fig. 22, and it is clear that no other possible combination of the three mechanisms of figs. 22, 23 and 24 will yield a larger value of M_p. It is therefore concluded that the mechanism of fig. 22 is the actual collapse mechanism. This solution will not be adjusted to allow for the possible occurrence of plastic hinges at cross-sections other than the ends and centres of the members, for when the dead plus superimposed loading case is considered, it will be found that the wind loading case does not govern the design.

An interesting feature brought out by this analysis is that there are only four plastic hinges in the collapse mechanism, whereas the frame has nine redundancies. At collapse, therefore, only the right-hand bay of the frame is statically determinate, and in carrying out a statical check the bending moment diagram for the other two bays could not be constructed directly. Instead, it would be necessary to carry out a trial and error investigation to show that the six redundancies of these two bays could be chosen in at least one way so as to produce a resultant bending moment diagram in which the fully plastic moment was not exceeded anywhere in the frame. This would be a tedious process, and in view of the fact that this is not the loading case which governs the design, the check is probably not worth performing.

Design for dead and superimposed loads

A load factor of 1·75 will be used for this loading case. The loading, consisting merely of the vertical loads of 3·60 tons on each rafter, is symmetrical, so that the collapse mechanism and the bending moment distribution at collapse must also be symmetrical. It will be seen that the values of eleven bending moments will specify the bending moment distribution for the entire frame, and that owing to symmetry there are only five redundancies. There are thus six independent mechanisms, which must all be symmetrical. Three of these mechanisms are the simple beam type of failure mechanism in the *pairs* of rafters BC and IJ, CD and GI, and DF and FG. For each of these mechanisms, the corresponding value of M_p is 9·45 tons-ft. One mechanism must be counted for rotation of the joints D and G. The remaining two mechanisms are most conveniently chosen as the mechanisms shown in figs. 25 and 26.

The virtual work equations for these two mechanisms are:

fig. 25: $14{\cdot}64\theta M_p = 302{\cdot}4\theta, \quad M_p = 20{\cdot}6$ tons-ft. . . . . (20)

fig. 26: $10{\cdot}64\theta M_p = 151{\cdot}2\theta, \quad M_p = 14{\cdot}2$ tons-ft. . . . . (21)

The only possible combination of these mechanisms is obtained if the hinge rotations and displacements in the mechanism of fig. 25 are all multiplied by a factor of 0·83, and then superposed on the mechanism of fig. 26. This enables a counter-clockwise rotation of the joint D, of magnitude $0{\cdot}83\theta$, to be made, thus cancelling plastic rotations of $0{\cdot}83\theta$ in the members DC and DE at this joint, while increasing

the plastic hinge rotation in the member DF by $0{\cdot}83\theta$. This produces a net reduction in the virtual work absorbed of $0{\cdot}83\theta M_p$, and a similar reduction can be achieved by a clockwise rotation of the joint G. The resulting virtual work equation is then seen from equations (20) and (21) to be:

$$0{\cdot}83\,.\,14{\cdot}64\theta M_p+10{\cdot}64\theta M_p-1{\cdot}66\theta M_p=0{\cdot}83\,.\,302{\cdot}4\theta+151{\cdot}2\theta$$

$$21{\cdot}1\theta M_p=402\theta$$

$$M_p=19{\cdot}1 \text{ tons-ft.} \quad . \quad . \quad . \quad . \quad (22)$$

This value of M_p is less than the value of 20·6 tons ft. which was found to correspond to the mechanism of fig. 25. It may also be checked that the beam collapse mechanisms for the rafters cannot be combined with any of these mechanisms to produce a value

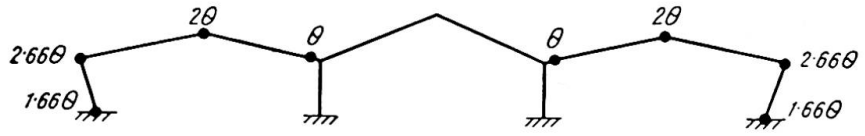

Fig. 25

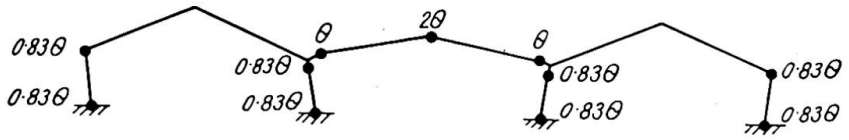

Fig. 26

of M_p greater than 20·6 tons-ft. The mechanism of fig. 25 is thus the actual collapse mechanism, subject to alterations due to the occurrence of plastic hinges at positions other than at the ends and centres of the members. A statical check will now be made which will also serve to indicate such alterations in the position of the plastic hinges.

Check by statics

Because of symmetry, the statical check need only be made for one half of the frame, say the left-hand half. For this portion of the frame, the free bending moment diagram is constructed by imagining cuts to be made at the apices C and F. The resulting diagram is given in fig. 27, for the case in which the loads have been multiplied by the load factor of 1·75. It will be seen that there is no free bending moment in the vertical member DE, and the diagram for this member has not been drawn.

For the members AB, BC and CD the redundant bending moment diagram may be constructed directly, since the bending moment has its fully plastic value at A, B, C and D. The horizontal thrust H in this bay can be calculated from the vertical intercept between the redundant bending moment diagram and the dotted line in fig. 27. In each case a value of 3·44 tons is obtained, thus checking the solution. Since the centre bay of the frame is not statically determinate at collapse, the redundant bending moment diagram for the member DF cannot be constructed directly. However, it is clear from the symmetry of the diagram about D that one possible redundant bending moment line for DF is the dotted line df shown in fig. 27, where fF represents the calculated fully plastic moment of 20·6 tons-ft. This line has a slope equal in magnitude to the line cd in fig. 27, and this corresponds to the same value of the

horizontal thrust of 3·44 tons which was found for the left-hand bay of the frame. If this were the actual redundant moment line for the member DF at collapse, it follows that there would be no resultant horizontal thrust on the vertical member DE, which would thus have zero bending moment throughout its length. It is therefore possible to construct a bending moment diagram for the entire frame in which the fully plastic moment is not exceeded at any cross-section, except within the spans of

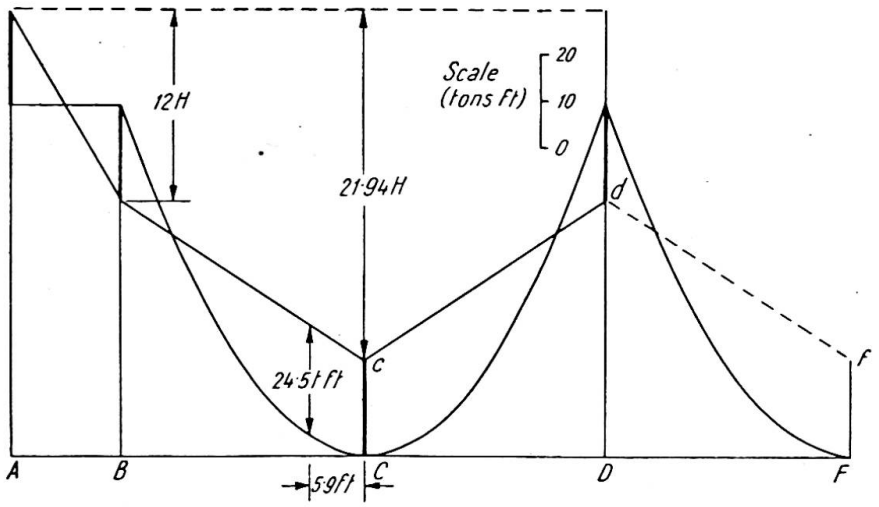

Fig. 27

the rafter members. This confirms that the correct solution was found by the virtual work analysis.

It will be seen from fig. 27 that plastic hinges will actually occur in the rafter members at distances of 5·9 ft. from the apices C and G, rather than at these apices. When this is taken into account, the value of M_p is found to be 21·9 tons-ft.

The statical check reveals the fact that the internal stanchions DE and GH need not be called upon to participate in the collapse mechanism, for it is possible to construct a resultant bending moment diagram in which these members are free from bending moment. These members, which were assumed in the first instance to possess a fully plastic moment M_p, thus function merely as props which hold up the rafter members. They could therefore be designed simply as compression members, and made of hollow tubing.

Conclusions

The merits of the method of design described in this paper can really be appreciated only by applying the method to practical examples. However, the foregoing examples serve to illustrate some of its advantages. The outstanding feature of the method is, of course, its rapidity. This is mainly due to the ease with which corresponding values of M_p can be obtained by the principle of virtual work, and this in turn is due largely to the fact that there is no need to establish sign conventions when applying this principle, since the virtual work absorbed in a plastic hinge must always be positive. A further important advantage of the method is that it enables solutions to be found without difficulty for those cases in which the entire frame is not statically determinate at collapse. Such cases have hitherto been somewhat intractable.

REFERENCES

(1) BAKER, J. F., "A Review of Recent Investigation into the Behaviour of Steel Frames in the Plastic Range," *J. Inst. Civ. Engrs.*, **31**, 188, 1949.
(2) BAKER, J. F., and HEYMAN, J, "Tests on Miniature Portal Frames," *The Structural Engineer*, **28**, 139, 1950.
(3) MAIER-LEIBNITZ, H. "Die Bedeutung der Zähigkeit des Stahles," *Prelim. Publ. 2nd Congress Intl. Assoc. Bridge and Structural Eng. Berlin*, 1936, p. 103.
(4) BAKER, J. F., "The Design of Steel Frames," *The Structural Engineer*, **27**, 397, 1949.
(5) NEAL, B. G., and SYMONDS, P. S., "The Calculation of Collapse Loads for Framed Structures," *J. Inst. Civ. Engrs.*, **35**, 20, 1950.
(6) GREENBERG, H. J., and PRAGER, W., "On Limit Design of Beams and Frames," *Proc. A.S.C.E.* **77**, *Separate* No. 59, 1951.
(7) NEAL, B. G., and SYMONDS, P. S., "The Rapid Calculation of the Plastic Collapse Load for a Framed Structure" (to be published in *Proc. Inst. Civ. Engrs. Part III*, **1**).
(8) HORNE, M. R., "Fundamental Propositions in the Plastic Theory of Structures," *J. Inst. Civ. Engrs.*, **34**, 174, 1950.

Summary

In suitable instances the application of plastic design methods to plane frames of ductile material, such as mild steel, leads to more rational and economical designs. These design methods are based on the calculation of the loads at which a structure collapses owing to excessive plastic deformation. Such collapses occur when a sufficient number of plastic hinges have formed to transform the structure into a mechanism, so that deflections can continue to grow, due to rotations of the plastic hinges, while the loads remain constant.

It is known that among all possible collapse mechanisms for a given frame and loading, the actual collapse mechanism is the one to which there corresponds the smallest possible value of the load. Recently, it has been pointed out that all the possible collapse mechanisms for a frame can be regarded as built up from a certain number of simple mechanisms. This has led to the development of a new technique for determining plastic collapse loads, in which these simple mechanisms are combined in a systematic manner so as to reduce the corresponding value of the load to its least possible value. For each mechanism which is investigated, the corresponding value of the load is determined very quickly by applying the Principle of Virtual Work.

In the present paper, the theoretical basis of this new technique is discussed, and typical calculations for a pitched-roof portal frame are given.

Résumé

Dans différents cas, l'application de la théorie de la plasticité au calcul des cadres plans en matériaux forgeables, comme l'acier fondu, conduit à des solutions rationnelles économiques. Cette méthode de calcul repose sur la détermination des charges sous lesquelles un ouvrage cède à la suite de déformations plastiques infiniment grandes. La rupture se produit à la suite de la formation d'articulations plastiques en nombre suffisant pour transformer l'élément porteur en un "mécanisme"; à la suite du processus de rotation des articulations plastiques, les déformations prennent des amplitudes de plus en plus grandes, tandis que la charge reste constante.

On sait que parmi tous les processus possibles de rupture d'un cadre donné sous l'action de conditions de mise en charge données, le processus décisif est celui qui correspond à la plus petite valeur possible de la charge. On a montré récemment que tous les processus possibles de rupture d'un cadre peuvent être considérés comme composés d'un certain nombre de processus habituels. Ceci a conduit à la mise au

point d'un nouveau procédé pour la détermination de la charge plastique de rupture, procédé dans lequel les processus simples sont combinés d'une manière systématique en vue de réduire la charge correspondante à sa plus petite valeur possible. Les valeurs de la charge peuvent être déterminées très rapidement pour chaque processus ainsi introduit, par l'application du principe des travaux virtuels.

Les auteurs discutent dans le présent rapport les bases théoriques du nouveau procédé et exposent les modes de calcul caractéristiques pour un cadre-portique avec toit incliné.

Zusammenfassung

In verschiedenen Fällen führt die Anwendung der Plastizitätstheorie bei der Berechnung ebener Rahmen aus schmiedbarem Material, wie z.B. Flusstahl, zu rationellen und wirtschaftlichen Lösungen. Diese Berechnungsmethode beruht auf der Bestimmung derjenigen Lasten, unter welchen ein Bauwerk infolge unendlich grossen plastischen Verformungen versagt. Das Versagen tritt ein, wenn sich plastische Gelenke in genügender Zahl ausgebildet haben, um das Tragwerk in einen Mechanismus umzuwandeln; als Folge der Drehungen der plastischen Gelenke vergrössern sich dann die Formänderungen weiter, während die Belastung konstant bleibt.

Es ist bekannt, dass unter allen möglichen Bruchmechanismen eines gegebenen Rahmens mit gegebener Belastungsanordnung derjenige massgebend ist, dem der kleinstmögliche Wert der Belastung entspricht. Unlängst wurde gezeigt, dass alle möglichen Bruchmechanismen eines Rahmens als aus einer gewissen Zahl von gewöhnlichen Mechanismen zusammengesetzt betrachtet werden können. Dies hat zur Entwicklung eines neuen Verfahrens zur Bestimmung der plastischen Bruchlast geführt, bei welchem die einfachen Mechanismen systematisch kombiniert werden, um so den entsprechenden Wert der Last zu seiner kleinstmöglichen Grösse zu reduzieren. Die Werte der Last können für jeden eingeführten Mechanismus sehr schnell durch Anwendung des Prinzips der virtuellen Arbeit bestimmt werden.

Im vorliegenden Aufsatz wird die theoretische Grundlage des neuen Verfahrens diskutiert, und es werden die typischen Berechnungen für einen Portalrahmen mit geneigtem Dach gegeben.

AI 3

Plastic analysis and design of steel-framed structures

Analyse plastique et calcul des ouvrages métalliques en cadres

Plastizitäts-Untersuchung und -Berechnung von Rahmenkonstruktionen aus Stahl

JACQUES HEYMAN, M.A., Ph.D.
Cambridge University

Introduction

The methods presented in this paper for the analysis and design of rigid structures are purely mathematical in character; that is, techniques are formulated on the basis of certain fundamental assumptions. These assumptions may or may not be true for any particular structure; for example, the instability of axially loaded stanchions is ignored, as is the lateral instability of beams subjected to terminal bending moments. While for some simple structures under particular conditions of loading these effects may be relatively unimportant, recent work by Neal (1950a) and Horne (1950) has shown that the problem may in fact be critical. In addition, it will be seen below that an "ideal" plastic material is assumed. Structural mild steel approximates to such an ideal material, but a highly redundant frame will experience strain-hardening which may invalidate the calculations. The techniques presented here, in short, in no sense form a practical design method; however, it is felt that they are of sufficient interest to warrant a description of some of the more important results.

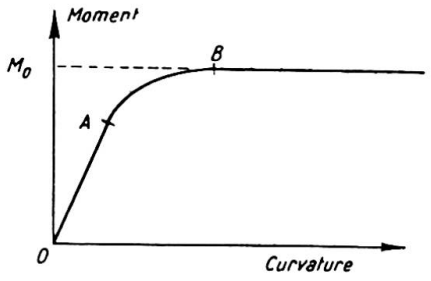

Fig. 1

The characteristic ideally plastic behaviour of a beam in pure bending is shown in fig. 1. From O to A increase of bending moment is accompanied by purely elastic (linear) increase of curvature. Between A and B, increase of bending moment is accompanied by a greater increase of curvature, until at the point B the full plastic moment M_0 is attained. At this moment the curvature can increase indefinitely, and "collapse" occurs.

In a general plane structural frame, a section at which the bending moment has the value M_0 is called a plastic hinge, and has the property that rotation at the hinge can occur freely under constant bending moment. From the definition of the full plastic moment, the moments in the frame can nowhere exceed M_0; if the component members of a frame have different sizes, it must be understood of course that M_0 refers to the particular member under consideration.

Collapse of a frame is said to occur when a sufficient number of plastic hinges are formed to turn whole or part of the frame into a mechanism of one degree of freedom; in general, the number of hinges exceeds by one the number of redundancies of that part of the frame concerned in the collapse. For example, the simple rectangular portal frame, of constant section throughout, subjected to loads V and H as shown in fig. 2(*a*), may fail in any one of the three basic modes shown in figs. 2(*b*), (*c*) and (*d*). The actual mode is determined by the values of the two loads.

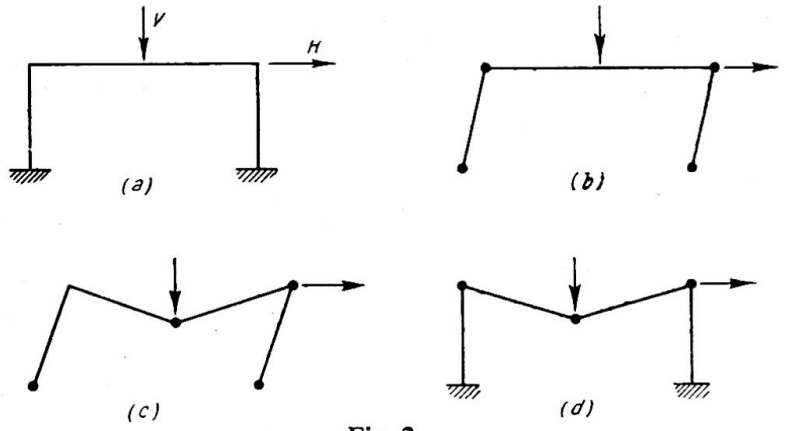

Fig. 2

The first part of this paper deals with methods for the exact determination of the quantities required (location of the hinges, values of collapse loads, etc.); the second part presents methods for determining upper and lower bounds on the loads, it being possible to make these bounds as close as is considered necessary. The third part applies the ideas to space frames, where hinges are formed under the combined action of bending and torsion.

Exact methods

The use of inequalities in the solution of structural problems was first introduced by Neal and Symonds (1950), who used a method due to Dines (1918). The very simple example shown in fig. 3 will be used to illustrate the solution of linear sets of inequalities.

(a) *Collapse analysis under fixed loads*

Suppose in fig. 3 that the two spans of the continuous beam are of length l, and that the fixed loads P_1 and P_2 act at the centres of the spans. The full plastic moment of the beam will be taken as M_0, and it is required to find the minimum value of M_0 in order that collapse shall just occur. (P_1 and P_2 may be taken to incorporate a suitable load factor.)

The general equilibrium state of a frame of n redundancies can be expressed as the sum of one arbitrary equilibrium state and n arbitrary independent residual states.

By a "state" is meant some bending moment distribution, so that a state in equilibrium with the applied loads is *any* bending moment distribution such that equilibrium is attained. A residual state is a bending moment distribution that satisfies equilibrium conditions when no external loads are applied to the frame. Thus, confining attention to any one cross-section in the frame, the bending moment there may be expressed as

$$M^*+M_1'+M_2'+\ldots+M_n' \qquad \ldots\ldots\ldots \quad (1)$$

where M^* is the equilibrium bending moment at the section and M_1', M_2', . . . M_n' are the bending moments, at the section considered, corresponding to n arbitrary residual states. Suppose that the full plastic moment at the section (as yet undetermined) is M_0. Then

$$-M_0 \leqslant M^*+M_1'+M_2'+\ldots+M_n' \leqslant M_0 \qquad \ldots\ldots \quad (2)$$

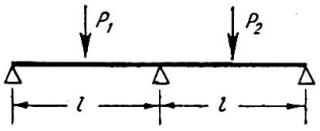

Fig. 3

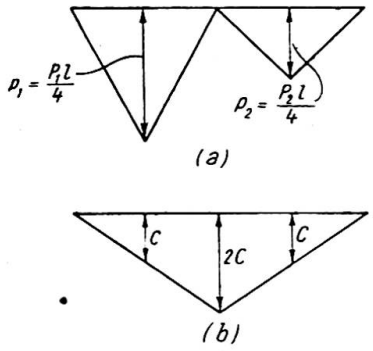

Fig. 4

Since the continuous beam system under consideration has one redundancy, the plastic behaviour can be represented as the sum of an equilibrium state and one residual state, which may be taken as the two bending moment distributions in fig. 4. The continued inequality (2) may be written for the three critical sections:

$$\left.\begin{array}{r} \text{Under the load } P_1,\ -M_0 \leqslant p_1+c \leqslant M_0 \\ \text{At the central support},\ -M_0 \leqslant\ \ 2c \leqslant M_0 \\ \text{Under the load } P_2,\ -M_0 \leqslant p_2+c \leqslant M_0 \end{array}\right\} \qquad \ldots\ldots \quad (3)$$

The set (3) may be rewritten as simple inequalities:

$$\left.\begin{array}{rl} c+p_1+ & M_0 \geqslant 0 \\ c\ \ \ \ +\tfrac{1}{2} & M_0 \geqslant 0 \\ c+p_2+ & M_0 \geqslant 0 \\ -c-p_1+ & M_0 \geqslant 0 \\ -c\ \ \ \ +\tfrac{1}{2} & M_0 \geqslant 0 \\ -c-p_2+ & M_0 \geqslant 0 \end{array}\right\} \qquad \ldots\ldots\ldots \quad (4)$$

If now every inequality in set (4) which has a coefficient of $+1$ for c is added to every inequality which has a coefficient -1 for c, c will be eliminated, and Dines has shown that the resultant set of inequalities (nine in number in this example) gives necessary and sufficient conditions for the existence of a value of c in order that the original set should be satisfied. This is exactly what is required for the present purposes; the actual value of c is of no interest so long as it is known that a c exists such that at each critical section of the frame the bending moment is less than the full plastic value.

In eliminating c from the set (4), it is found that a large number of the resulting inequalities are redundant, and if it is assumed that $P_1 \geqslant P_2$, the single inequality

$$-p_1+\tfrac{3}{2}M_0 \geqslant 0 \qquad \ldots\ldots\ldots \quad (5)$$

is found to be critical. As long as this inequality is satisfied, all the moments in the beam will be less than M_0. For collapse just to occur, the equality sign should be taken in (5), giving $M_0=\frac{2}{3}p_1$. Now inequality (5) was derived by adding the second and fourth of set (4); substituting this value of M_0 into these two inequalities gives

$$\left.\begin{aligned} c+\tfrac{1}{3}p_1 &\geqslant 0 \\ -c-\tfrac{1}{3}p_1 &\geqslant 0 \end{aligned}\right\} \qquad \ldots\ldots\ldots \quad (6)$$

i.e.

$$-\tfrac{1}{3}p_1 \geqslant c \geqslant -\tfrac{1}{3}p_1 \qquad \ldots\ldots\ldots \quad (7)$$

that is, a unique value of c has been derived. Using this value of c, the bending moment distribution shown in fig. 5 has been derived from the analysis; it will be seen that hinges ($M_0=\frac{2}{3}p_1$) are formed under the load P_1, and at the central support, forming a mechanism of one degree of freedom for small (really, infinitesimal) displacements.

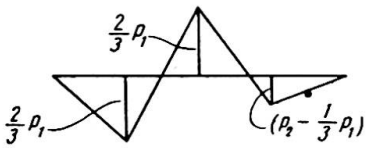

Fig. 5

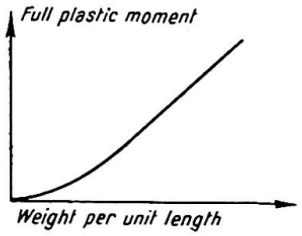

Fig. 6

The type of result obtained in this problem will in general be derived for any more complicated example. For more residual states defined by c_1, c_2, . . . c_n, each parameter c is eliminated successively from the inequalities, and the final inequality, if just satisfied, will generate a unique set of residual states completely defining the collapse configuration.

The method given above may be applied to the analysis of frames collapsing under variable loads; however, this problem will be treated with reference to the slightly more complex condition of minimum weight design.

(b) *Minimum weight design under fixed loads*

The parameters used in order to determine the minimum weight of a structure will be the values of the full plastic moments. If a plot is made for typical structural sections of full plastic moment against weight per unit length, and the points joined by a smooth curve, a non-linear relationship of the type shown in fig. 6 will be obtained. (Owing to the methods used in this paper, the actual relationship is immaterial, but it is of interest to note that a curve given in a British Welding Research Association report (1947) for British structural sections can be approximated by $w=2{\cdot}7M^{0{\cdot}6}$, where w is the weight in lb./ft. of a beam of full plastic moment M tons ft.) In order to develop suitable methods for design, it will be assumed that a continuous range of sections is available so that a section can be used with any specified full plastic moment.

The assumption is made that the moment–weight curve can be replaced in the region which is significant for any particular problem by a straight line. For a frame built up of N members, each of constant section, the total material consumption will be given by the proportionality

$$W \approx \sum_{i=1}^{N} M_i l_i \qquad \ldots\ldots\ldots\ldots \quad (8)$$

where M_i is the full plastic moment of the ith member of the frame, and l_i is its length.

Considering again the two-span beam shown in fig. 3, suppose that the left-hand span has a full plastic moment M_1, that of the right-hand span being M_2. Since the two spans are of equal length, proportionality (8) may be replaced by the weight parameter

$$X = M_1 + M_2 \qquad \ldots\ldots\ldots\ldots \quad (9)$$

The problem of minimum weight design for this problem is then reduced to choosing values of M_1 and M_2 such that X is made a minimum. The work starts in the same manner as for the collapse analysis given above; set (3) is replaced by

$$\left.\begin{aligned} -M_1 &\leqslant p_1 + c \leqslant M_1 \\ -M_1 &\leqslant 2c \leqslant M_1 \\ -M_2 &\leqslant 2c \leqslant M_2 \\ -M_2 &\leqslant p_2 + c \leqslant M_2 \end{aligned}\right\} \qquad \ldots\ldots\ldots\ldots \quad (10)$$

The two continued inequalities are necessary for the central support since it is not known *a priori* whether $M_1 \gtrless M_2$.

Of the sixteen possible inequalities obtained by the elimination of c from set (3), only five are found to be non-redundant if it be assumed that $P_1 \geqslant P_2$. These are

$$\left.\begin{aligned} -p_1 \qquad\quad + \tfrac{3}{2}M_1 \qquad\quad &\geqslant 0 \\ -p_1 \qquad\quad + M_1 + \tfrac{1}{2}M_2 &\geqslant 0 \\ -p_1 + p_2 + M_1 + M_2 &\geqslant 0 \\ -p_2 + \tfrac{1}{2}M_1 + M_2 &\geqslant 0 \\ -p_2 \qquad\quad + \tfrac{3}{2}M_2 &\geqslant 0 \end{aligned}\right\} \qquad \ldots\ldots\ldots\ldots \quad (11)$$

The material consumption parameter X will now be introduced into set (10) by the replacement of M_1 by $(X - M_2)$ from equation (9). Upon slight rearrangement,

$$\left.\begin{aligned} -M_2 + X \quad -\tfrac{2}{3}p_1 &\geqslant 0 \\ -M_2 + 2X - 2p_1 &\geqslant 0 \\ M_2 + X \quad -2p_2 &\geqslant 0 \\ M_2 \qquad -\tfrac{2}{3}p_2 &\geqslant 0 \end{aligned}\right\} \qquad \ldots\ldots\ldots\ldots \quad (12)$$

together with

$$X \geqslant (p_1 - p_2) \qquad \ldots\ldots\ldots\ldots \quad (13)$$

Now for the problem of determining the minimum value of X, the value of M_2 is not required, and Dines' method may be employed again on set (12) to eliminate M_2. On performing this operation, inequality (13) becomes redundant, and the only significant inequality resulting is

$$X \geqslant p_1 + \tfrac{1}{3}p_2 \qquad \ldots\ldots\ldots\ldots \quad (14)$$

It should be repeated that this single inequality is a necessary and completely sufficient condition that values of M_1, M_2 and c can be found to satisfy the original set (10). Since it is required that X should be as small as possible, the equality sign will be taken in (14), so that

$$X = p_1 + \tfrac{1}{3}p_2 \qquad \ldots\ldots\ldots\ldots \quad (15)$$

Substitution of this value of X back into the previous sets gives the unique values

$$\left.\begin{aligned} M_1 &= p_1 - \tfrac{1}{3}p_2 \\ M_2 &= \tfrac{2}{3}p_2 \\ 2c &= -\tfrac{2}{3}p_2 = -M_2 \end{aligned}\right\} \quad \ldots\ldots\ldots \quad (16)$$

The bending moment distribution resulting from the analysis is shown in fig. 7, plastic hinges being formed at all three of the critical points.

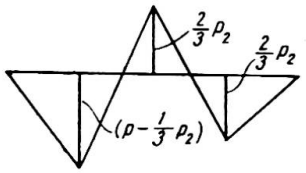

Fig. 7

The method given above for minimum weight design against collapse under fixed loads has been applied by the Author (1950a, 1950b) to the solution of a rectangular portal frame (cf. fig. 2), and also to derive a design method for continuous beams of any number of spans under either concentrated or distributed loads.

(c) *Minimum weight design against collapse under variable loads*

Consider the same beam in fig. 3, but with the loads varying arbitrarily between the limits

$$\left.\begin{aligned} -Q_1 \leqslant P_1 \leqslant Q_1 \\ -Q_2 \leqslant P_2 \leqslant Q_2 \\ Q_1 \geqslant Q_2 \end{aligned}\right\} \quad \ldots\ldots\ldots \quad (17)$$

The work proceeds as before up to the derivation of set (11). Now, in this set, the worst values of p_1 and p_2 (i.e. $\pm q_1$, $\pm q_2$) must be inserted in each inequality, giving

$$\left.\begin{aligned} -q_1 \quad\quad +\tfrac{3}{2}M_1 \quad\quad\quad &\geqslant 0 \\ -q_1 \quad\quad + M_1 + \tfrac{1}{2}M_2 &\geqslant 0 \\ -q_1 - q_2 + M_1 + M_2 &\geqslant 0 \\ -q_2 + \tfrac{1}{2}M_1 + M_2 &\geqslant 0 \\ -q_2 \quad\quad\quad +\tfrac{3}{2}M_2 &\geqslant 0 \end{aligned}\right\} \quad \ldots\ldots\ldots \quad (18)$$

Operating on set (18) as before to find the minimum value of X, it is found that

$$\left.\begin{aligned} M_1 + M_2 = X &= q_1 + q_2 \\ (q_1 + \tfrac{1}{3}q_2) &\geqslant M_1 \geqslant \tfrac{2}{3}q_1 \\ 2q_2 &\geqslant M_2 \geqslant \tfrac{2}{3}q_2 \\ (\tfrac{1}{3}q_1 + q_2) &\geqslant M_2 \end{aligned}\right\} \quad \ldots\ldots\ldots \quad (19)$$

As a specific example, suppose $q_1 = q_2 = q$. Then

$$\left.\begin{aligned} M_1 + M_2 &= 2q \\ \tfrac{4}{3}q &\geqslant M_1 \geqslant \tfrac{2}{3}q \\ \tfrac{4}{3}q &\geqslant M_2 \geqslant \tfrac{2}{3}q \end{aligned}\right\} \quad \ldots\ldots\ldots \quad (20)$$

and any values of M_1 and M_2 satisfying (20) will give a constant material consumption. (It is perhaps of interest to note that for $X = \Sigma(M)^n l$, where $n < 1$, the minimum material consumption is given by $M_1 = 2M_2 = \frac{4}{3}q$ (or *vice versa*), the worst case occurring for $M_1 = M_2 = q$. An asymmetrical solution is obtained for what appears to be a completely symmetrical problem. For $n = 0{\cdot}6$, the symmetrical solution gives an increase of less than 2% in material consumption compared with the asymmetrical solution.)

Inexact methods

The theorems concerning the existence of upper and lower bounds on the collapse load of a structure were first proved rigorously by Greenberg and Prager (1950). It

is assumed that the loads on a structure are all specified in terms of one load, so that when the collapse load is mentioned, this implies the whole system of loads.

An upper bound on the collapse load

Suppose that enough hinges are inserted into a redundant structure in order to turn it into a mechanism of one degree of freedom. Hill (1948) has shown that the stress system is constant during collapse of an ideally plastic body, so that for the frame with one degree of freedom, the equation of virtual work may be written, equating the work done in the hinges to the work done by the external load during a small displacement in the equilibrium state. The work done in a hinge is equal to the full plastic moment multiplied by the absolute value of the change in angle at that hinge (i.e. plastic rotation) and the work done by the load simply the load multiplied by its displacement. There will, of course, be elastic displacements obtaining in the frame, but these do not appear in the equations provided it is assumed that they are small so that the overall geometry of the frame is not disturbed.

For any arrangement of hinges in the frame producing a mechanism of one degree of freedom, the load given by the virtual work equation is either greater than or equal to the true collapse load.

A lower bound on the collapse load

If a state can be found for the structure which nowhere violates the yield condition, and which is an equilibrium state for a given value of the load, then that value is either less than or equal to the value of the true collapse load.

In practice, Greenberg and Prager found it useful to derive a lower bound from the mechanism giving the upper bound. The example will make the ideas clear.

Suppose the values of the loads in fig. 3 are

$$P_1=2P_2=2P \quad . \quad . \quad . \quad . \quad . \quad . \quad . \quad . \quad . \quad (21)$$

and that as a first trial the mechanism in fig. 8 is assumed for failure. The rotation at the central hinge is θ, and at the hinge under the load P, 2θ. Hence, by virtual work,

$$P \cdot \frac{l}{2}\theta = M_0(2\theta)+M_0(\theta) \quad . \quad . \quad . \quad . \quad . \quad . \quad . \quad . \quad (22)$$

i.e.

$$p=\tfrac{3}{2}M_0 \quad . \quad . \quad . \quad . \quad . \quad . \quad . \quad . \quad . \quad . \quad (23)$$

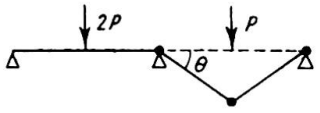

Fig. 8

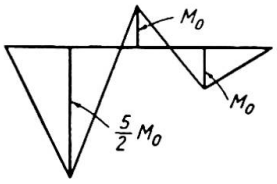

Fig. 9

(It is taken that the beam has the same full plastic moment M_0 in both spans.) By the upper bound theorem, the true value of the collapse load (p_c) is less than $\frac{3}{2}M_0$. The bending moment distribution corresponding to the assumed mechanism and this value of p given in equation (23) is shown in fig. 9, from which it will be seen that the yield condition is exceeded under the load $2P$ in the ratio 5/2. Suppose now that the loads are reduced in the ratio 2/5. Then if the values in fig. 9 are multiplied by 2/5,

an equilibrium bending moment distribution is obtained which nowhere violates the yield condition. Hence the load of $\frac{3}{5}M_0$ is a lower bound on the collapse load, i.e.

$$\tfrac{3}{5}M_0 \leqslant p_c \leqslant \tfrac{3}{2}M_0 \quad . \quad . \quad . \quad . \quad . \quad . \quad . \quad . \quad (24)$$

It can be shown that removing one of the assumed hinges to the point of maximum moment will improve the bounds on the collapse load; in this example, shifting the hinge from under the load P to under the load $2P$, while retaining the central hinge, immediately gives the correct solution $p_c=\frac{3}{4}M_0$. There is, however, no means at present of choosing which hinge to remove, and in any case the bounds cannot be narrowed indefinitely; either they are separated by a finite amount, which may be quite large for even a relatively redundant frame, or the exact solution will be obtained. Accordingly, Nachbar and the Author (1950) have developed more general methods for obtaining both upper and lower bounds which may be made as close to the true collapse value as is considered necessary.

A general method for the upper bound

Suppose yield hinges are inserted into the frame at any suspected critical sections. In general a frame of N degrees of freedom will result, specified in terms of N deflection parameters. If the equation of virtual work is written, then the corresponding value of the load is an upper bound on the true collapse load. In fact, the virtual work equation is inapplicable, since the system is not an equilibrium system, but it may be shown that the value of the load resulting from this equation is in fact a true upper bound, providing that the mechanism is such that the work done by the loads is positive.

For the general mechanism in fig. 10,

$$2P \cdot \frac{l}{2}\theta_1 + P \cdot \frac{l}{2}\theta_2 = M_0(|2\theta_1| + |\theta_1+\theta_2| + |2\theta_2|)$$

i.e.

$$p = M_0\left(\frac{|2\theta_1| + |\theta_1+\theta_2| + |2\theta_2|}{4\theta_1+2\theta_2}\right) \quad . \quad . \quad . \quad . \quad (25)$$

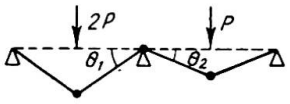

Fig. 10

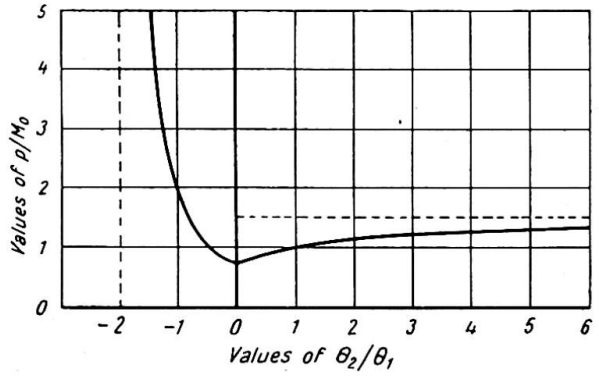

Fig. 11

In equation (25), values of θ_1 and θ_2 must be chosen to give the minimum value of p; since p is always an upper bound on p_c, the minimum value will be equal to p_c. A plot of equation (25) is given in fig. 11, from which it will be seen that $p_c=\frac{3}{4}M_0$ corresponds to $\theta_2=0$. The minimum is not a stationary value, since equation (25) is a ratio of two linear expressions. Nachbar has shown that equations of this type containing absolute values can be reduced by rational successive steps, and the method has been applied to mechanisms with a large number of parameters necessary for their specification.

A general method for the lower bound

Suppose the members of a redundant structure are cut in such a way that a number of separate redundant or statically determinate structures are formed. If the collapse loads are calculated for each of these resulting structures, then the lowest value of these loads is less than the collapse load of the structure as a whole. The proof of this theorem follows immediately from the special lower bound theorem above. An immediate corollary is that if a cut portion of the structure carries no load, then that portion can be ignored in the derivation of the lower bound. In order to make the theorem of practical use, an additional lemma is needed. The collapse load of a structure is unaffected by any initial system of residual stresses (moments, shear forces). That is, at a cut, equal and opposite longitudinal forces, shear forces, and moments may be introduced in an attempt to raise the lower bound.

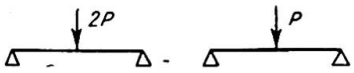

Fig. 12

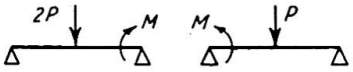

Fig. 13

Suppose the beam in the previous example is cut at the central support; then the two separate beams shown in fig. 12 will be obtained. The collapse loads of the right- and left-hand halves are respectively $p=M_0$ and $p=\frac{1}{2}M_0$, i.e.

$$p_c \geqslant \tfrac{1}{2}M_0 \quad . \quad . \quad . \quad . \quad . \quad . \quad . \quad . \quad . \quad . \quad (26)$$

Now if a central moment is introduced (fig. 13), it is easy to show that the collapse loads are respectively

$$p=\frac{M+2M_0}{2} \quad \text{and} \quad p=\frac{M+2M_0}{4} \quad . \quad . \quad . \quad . \quad . \quad (27)$$

The maximum value which M can take is, of course, M_0, and hence from (27)

$$p_c \geqslant \tfrac{3}{4}M_0 \quad . \quad . \quad . \quad . \quad . \quad . \quad . \quad . \quad . \quad . \quad (28)$$

and the problem has been completed. For other more complicated examples (a two-storey, two-bay portal frame has been solved under both concentrated and distributed loads), it is found that shear and longitudinal forces as well as bending moments must be introduced at the cuts.

SPACE FRAMES

The type of space frame considered has members which lie all in the same plane, all loads acting perpendicularly to this plane. Thus bending moments whose axes lie perpendicular to the plane and shear forces in the plane are zero. Any member of the frame is then acted upon by shear forces parallel to the applied loads and by two moments whose axes lie in the plane, that is, a bending moment (M) and a torque (T). For ideal plasticity, hinges will be formed in exactly the same way as for plane frames; the breakdown criterion will be some such expression as

$$g(M, T)=g(M_0, 0)=\text{const.} \quad . \quad . \quad . \quad . \quad . \quad . \quad . \quad . \quad (29)$$

where M_0 is the full plastic moment in pure bending, as before. At any one hinge, the maximum work principle of Hill (1948) shows that the moment and torque will be constant during collapse, and that the rate at which work is done at a hinge will be a maximum. If β and θ are the incremental changes in angle in bending and twisting

respectively during a displacement in the equilibrium collapse configuration, then the rate at which work is done is

$$M\beta+T\theta \quad . \quad . \quad . \quad . \quad . \quad . \quad . \quad . \quad . \quad . \quad (30)$$

For a maximum,

$$\beta \,.\, \delta M+\theta \,.\, \delta T=0 \quad . \quad . \quad . \quad . \quad . \quad . \quad . \quad . \quad . \quad (31)$$

Now the breakdown criterion, equation (29), gives

$$\frac{\partial g}{\partial M} \,.\, \delta M+\frac{\partial g}{\partial T} \,.\, \delta T=0 \quad . \quad . \quad . \quad . \quad . \quad . \quad . \quad . \quad . \quad (32)$$

that is,

$$\frac{\beta}{\theta}=\frac{\dfrac{\partial g}{\partial M}}{\dfrac{\partial g}{\partial T}} \quad . \quad . \quad . \quad . \quad . \quad . \quad . \quad . \quad . \quad . \quad (33)$$

This flow relationship may be solved simultaneously with the breakdown criterion to give the moment and torque acting at a hinge during any collapse displacement.

The author (1951) has shown that for a box section, equation (29) becomes

$$M^2+\tfrac{3}{4}T^2=M_0^2 \quad . \quad . \quad . \quad . \quad . \quad . \quad . \quad . \quad . \quad (34)$$

For the present purposes, the circular breakdown criterion

$$M^2+T^2=M_0^2 \quad . \quad . \quad . \quad . \quad . \quad . \quad . \quad . \quad . \quad (35)$$

will be used for the sake of simplicity. The restriction in no way affects the generality of the methods proposed for the solution of space frames.

Equation (33) becomes

$$\frac{\beta}{\theta}=\frac{M}{T} \quad . \quad . \quad . \quad . \quad . \quad . \quad . \quad . \quad . \quad . \quad (36)$$

which, taken with equation (35), gives

$$\left.\begin{aligned} M&=\frac{\beta}{\sqrt{\beta^2+\theta^2}}M_0 \\ T&=\frac{\theta}{\sqrt{\beta^2+\theta^2}}M_0 \end{aligned}\right\} \quad . \quad . \quad . \quad . \quad . \quad . \quad . \quad . \quad (37)$$

together with the expression for the work done at the hinge (expression (30))

$$\text{Plastic work}=M_0\sqrt{\beta^2+\theta^2} \quad . \quad . \quad . \quad . \quad . \quad . \quad . \quad (38)$$

Owing to the non-linearity of the breakdown criterion, it is not possible to set up exact systems of linear inequalities to be solved by the Dines' method. However, approximations may be made to the breakdown criterion itself; for example, equation (35) could be replaced by the circumscribed octagon

$$\left.\begin{aligned} M&=\pm M_0 \\ T&=\pm M_0 \\ M\pm T&=\pm\sqrt{2}M_0 \end{aligned}\right\} \quad . \quad . \quad . \quad . \quad . \quad . \quad . \quad . \quad (39)$$

and the moment M and torque T at any section constrained to lie within this yield domain.

As will be shown, simple problems are best solved by a direct method; and the systems of linear inequalities corresponding to equations (39) become too complicated

for practical use in the solution of highly redundant structures. For the latter, the determination of bounds on the collapse load seems to give the quickest results.

Direct solution

As an example of the direct method, consider the symmetrical two-leg right-angle bent shown in fig. 14. The ends A and D are *encastré* against both torque and moment, and the load P acts at the midpoint B of the leg AC. Suppose failure occurs by the formation of symmetrical hinges at A and D, so that the point C moves vertically downward for a small displacement. It is easy to see that $\beta_A=\beta_D=\theta_A=\theta_D=\theta$, say, so that, from equation (38), the work done in the two hinges is

$$2M_0\sqrt{2}\theta^2 \quad . \quad . \quad . \quad . \quad . \quad . \quad . \quad . \quad . \quad . \quad (40)$$

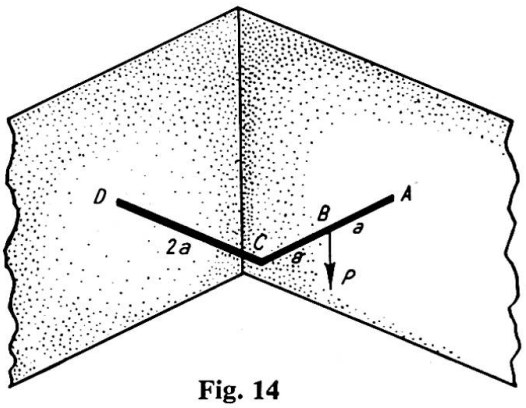

Fig. 14

while the work done by the load P is

$$Pa\theta \quad . \quad . \quad . \quad . \quad . \quad . \quad . \quad . \quad . \quad . \quad (41)$$

Equating these two expressions, and using the upper bound theorem given above,

$$P_c \leqslant P=2\frac{\sqrt{2}M_0}{a} \quad . \quad . \quad . \quad . \quad . \quad . \quad . \quad . \quad (42)$$

The frame is, of course, statically determinate in this collapse configuration, and, by using equations (37) to determine the conditions at the hinges, the forces and moments shown in fig. 15 are obtained. The yield criterion is exceeded by the greatest amount at B, where the moment and torque are $\sqrt{2}M_0$ and $\frac{1}{\sqrt{2}}M_0$ respectively, i.e.

$$M_B^2+T_B^2=\tfrac{5}{2}M_0^2 \quad . \quad . \quad . \quad . \quad . \quad . \quad . \quad . \quad (43)$$

Hence if the load is reduced by a factor $\sqrt{2/5}$, a lower bound will be obtained,

$$\frac{4}{\sqrt{5}}\frac{M_0}{a} \leqslant P_c \leqslant \frac{4}{\sqrt{2}}\frac{M_0}{a} \quad . \quad . \quad . \quad . \quad . \quad . \quad . \quad (44)$$

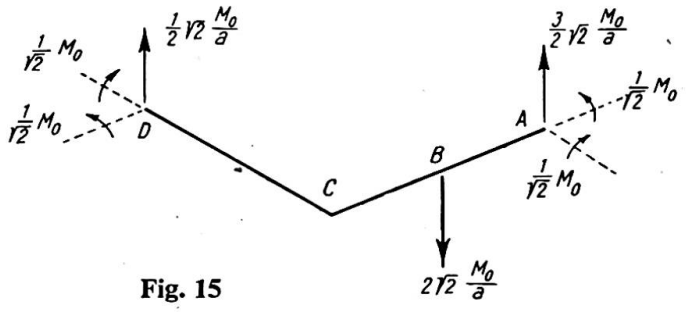

Fig. 15

In order to improve these bounds, a hinge must be inserted at B; but collapse actually occurs with hinges at all three points A, B and D. At first sight this would appear to be a mechanism of three independent degrees of freedom. In fact, owing to the simultaneity of the breakdown and flow criterions (equations (35) and (36)), each hinge as a whole has only one degree of freedom; since a continuity condition is required at each hinge, a space frame of the type considered here may collapse with any number of hinges formed in its members, and an extra hinge may be inserted without actually increasing the number of degrees of freedom.

The general method for the exact solution of a structure with R redundancies may be tabulated as follows:

(1) Construct a mechanism with N hinges.
(2) Specify the mechanism in terms of an arbitrary displacement (one degree of freedom) and $[2N-(R+1)]$ deflection parameters α_j.
(3) $(2N-R)$ equilibrium equations may be formulated in terms of the moments (M_i) and torques (T_i) at the hinges and the applied load.
(4) M_i and T_i at each hinge may be calculated in terms of the α_j from the breakdown and flow criteria.
(5) The load may be eliminated from the $(2N-R)$ equilibrium equations, leaving a set of $(2N-\{R+1\})$ simultaneous equations for the determination of the α_j.
(6) Having determined the α_j, the moments and torques at each hinge may be calculated, and hence the value of the load. This value is an upper bound on the collapse load.
(7) If the yield criterion is violated at any point in the structure, a lower bound may be determined.
(8) If hinges are moved or added to the points where the yield criterion is violated, the whole process can be repeated.

Following these rules, and inserting hinges at A, B and D, the final exact solution is found to be

$$P_c=\frac{8}{\sqrt{10}}\frac{M_0}{a}=2{\cdot}53\frac{M_0}{a} \qquad \ldots\ldots\ldots \quad (45)$$

which as a check lies between the previous limits (44).

Bounds on the collapse load

In the method outlined above, it has been tacitly assumed that the theorems on upper and lower bounds may be extended from plane to space frames; this is in fact the case, and indeed Drucker, Greenberg and Prager (1950) have shown that the special theorems may be applied to the problem of the continuum. The general theorem of an upper bound determined from a non-equilibrium mechanism is also valid for space frames, and this gives the quickest method for the solution of such problems.

The advantage of the kinematic method of determining an upper bound on the collapse load is that no reference is made to equilibrium conditions. Suppose, for

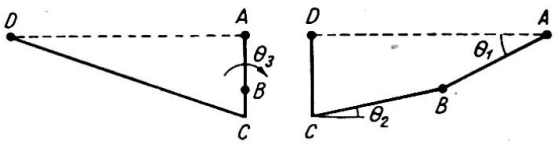

Fig. 16

example, the mechanism in fig. 16 (horizontal projection of frame in fig. 14) is specified by assigning arbitrary deflections to the joints B and C, with hinges occurring at A, B and D. Then an upper bound may be determined simply by equating the work done in the hinges to the work done by the load. By trial of various mechanisms, this bound may be lowered. Alternatively, if, after a trial, the frame is examined statically, it will be found that it is impossible to satisfy equilibrium conditions, the total load at B being either lower or in excess of the value of P determined from the work equation. This implies that an extra (positive or negative) force is required at B in order to produce the originally assumed collapse configuration. The significance of this force is best appreciated by an example.

In fig. 16, take $\delta_B=\delta_C=2a$, say, since the mechanism may be specified in terms of one unknown degree of freedom. The following table gives the conditions at the hinges.

TABLE I

Hinge	β	θ	$\sqrt{\theta^2+\beta^2}$	Moment ($\times M_0$)	Torque ($\times M_0$)
A . . .	2	0·5*	2·062	0·97	0·24
B . . .	2	0·5*	2·062	0·97	0·24
D . . .	1	0	1·000	1·00	0

The asterisked values were chosen to make the torques equal at A and B, as they should be; this is an unnecessary restriction, and improves only slightly the value of the upper bound, and any values of the twist totalling 1·0 could have been used. The work equation gives

$$P\,.\,2a=5{\cdot}124M_0$$

i.e.
$$P_c\leqslant P=2{\cdot}56\frac{M_0}{a} \quad . \quad . \quad . \quad . \quad . \quad . \quad . \quad . \quad . \quad (46)$$

The statical analysis of the frame is shown in fig. 17. The number in a circle at the joint B gives the actual load required to maintain equilibrium, and it appears that a load of $2{\cdot}91M_0/a$ is required as against the calculated value $2{\cdot}56M_0/a$. Since the equilibrium load is greater than it should be, it is indicated that the assumed deflection of the point B was too large; if this deflection is reduced slightly, a better bound should result. Similarly, a negative load is required at C; the deflection should be increased.

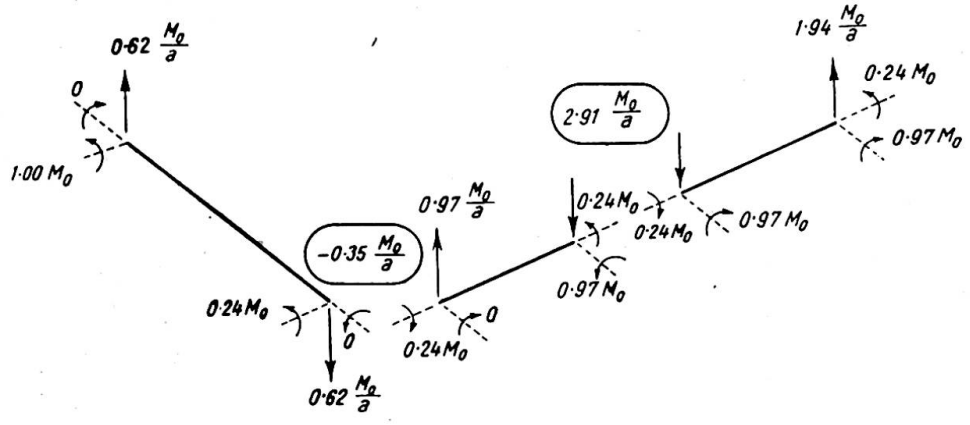

Fig. 17

In working more complicated examples, it is found that the process of adjusting deflections at neighbouring joints bears a marked resemblance to a relaxation process, and that a reduction in the out-of-balance forces at one joint induces increased errors at the ones adjacent. However, the technique is soon mastered, and the Author (1950c) solved, with very little labour, a rectangular grid formed by a set of parallel beams intersecting at right angles another set of 9 beams, loaded transversely at each of the 81 joints, and requiring 108 hinges in the collapse mechanism.

When it is suspected that the upper bound is fairly good, small adjustments in the statical analysis will produce an equilibrium system. For example, in fig. 17, if the torque in CD is increased from 0 to $0{\cdot}35M_0$, the other values remaining unchanged, an equilibrium system results which, however, violates the yield condition at the hinge D in the ratio 1·06. Hence, using the value in equation (46)

$$2{\cdot}41\frac{M_0}{a} \leqslant P_c \leqslant 2{\cdot}56\frac{M_0}{a} \qquad \ldots\ldots\ldots \quad (47)$$

The general procedure for the solution of space frames may be tabulated as follows:

(1) Insert yield hinges at a large number of points in the frame, producing a mechanism of many degrees of freedom. The hinges should be placed at all the sections at which it is suspected actual hinges might occur in the collapse.

(2) Assign arbitrary (reasonable) deflections to the joints of the grid, and determine the corresponding changes in angle at each hinge. Equating the work dissipated in the hinges to the work done by the external loads gives a value of the load which is in excess of the true collapse load.

(3) Calculate the out-of-balance forces at each joint that are necessary to produce the assumed deflections. If the out-of-balance force acts in the same direction as the actual load at a joint, the deflection of that joint was estimated as too large, and *vice versa*.

(4) Adjust the deflections, and repeat the whole process.

(5) At any stage, if the out-of-balance forces are small, and it is suspected that the upper bound is a good estimate of the collapse load, a statical analysis may be made. Small adjustments are made in the values of the various shear forces and moments in order to produce an equilibrium system, from which a lower bound may be determined.

The Author wishes to thank Professors Prager and Drucker of Brown University for their criticism and encouragement of the work reported in this paper.

References

British Welding Research Association. 1947. Report FE1/2.

Dines, L. L. 1918. *Ann. Math.*, **20**, 191.

Drucker, D. C., Greenberg, H. J., and Prager, W. 1950. Technical Report A18-3 from the Graduate Division of Applied Mathematics, Brown University, to the Office of Naval Research, U.S.

Greenberg, H. J., and Prager, W. 1950. To be published in *Proc. A.S.C.E.*

Heyman, J. 1950a. Technical Report A11–45 from the Graduate Division of Applied Mathematics, Brown University, to the Office of Naval Research, U.S.

1950b. *Quart. J. Appl. Math.*, **8**, No. 4, January 1951.

1950c. Technical Report A11–52 from the Graduate Division of Applied Mathematics, Brown University, to the Office of Naval Research, U.S. To be published in *J. Appl. Mech.*

1951. *J. Appl. Mech.*, **18**, No. 2, June 1951.

HILL, R. 1948. *Quart. J. Mech. and Appl. Math.*, **1**.

HORNE, M. R. 1950. Unpublished.

NACHBAR, W., and HEYMAN, J. 1950. Technical Report A11–54 from the Graduate Division of Applied Mathematics, Brown University, to the Office of Naval Research, U.S. To be published in *J. Appl. Mech.*

NEAL, B. G. 1950a. *Phil. Trans. Roy. Soc. A.*, **846**, 197–242.

NEAL, B. G., and SYMONDS, P. S. 1950. *J. Inst. Civ. Engrs.*, **35**, 20.

Summary

The preparation of this paper forms part of a general investigation into the behaviour of rigid frame structures being carried out at the Cambridge Engineering Laboratory under the direction of Professor J. F. Baker. The paper deals with the mathematical analysis and design of both plane and space frames, and the ideas are presented with reference to very simple examples in order to illustrate the techniques developed. The first part considers methods for the exact determination of conditions at collapse of rigid ideally plastic plane structures. In the second part it is shown that inexact methods lead to upper and lower bounds on the collapse loads, and that these bounds may be made as close as is considered necessary. The various theorems are applied in the third part to the solution of space frames.

Résumé

Le présent mémoire rentre dans le cadre d'une investigation générale portant sur le comportement d'ouvrages en cadres rigides, investigation actuellement en cours au Cambridge Engineering Laboratory, sous la direction du Professeur J. F. Baker. L'auteur traite de l'analyse mathématique et du calcul des cadres, tant en plan que dans l'espace, et son exposé est accompagné d'exemples très simples, qui illustrent les procédés adoptés.

La première partie se rapporte aux méthodes de détermination exacte des conditions qui se manifestent au rupture des ouvrages plans rigides idéalement plastiques. Dans la deuxième partie, l'auteur montre que des méthodes non rigoureuses permettent de fixer des limites supérieures et inférieures aux charges sous lesquelles les ouvrages cèdent; ces limites peuvent d'ailleurs recevoir des valeurs aussi étroites qu'il est jugé nécessaire. Les différents théorèmes sont appliqués, dans la troisième partie, au calcul de cadres à trois dimensions.

Zusammenfassung

Die Arbeiten zum vorliegenden Aufsatz stellen einen Teil der umfassenden Untersuchungen über das Verhalten steifer Rahmenkonstruktionen dar, die am Cambridge Engineering Laboratory unter der Leitung von Professor J. F. Baker durchgeführt werden. Der Verfasser behandelt die mathematische Untersuchung und Bemessung ebener und auch räumlicher Rahmen und entwickelt seine Ueberlegungen an Hand sehr einfacher Beispiele, an denen er die gewählten Verfahren darlegt. Der erste Teil behandelt Methoden zur genauen Bestimmung der Bruch-Verhältnisse steifer, ideal-plastischer ebener Tragwerke. Im zweiten Teil wird gezeigt, dass durch Näherungsmethoden eine obere und untere Grenze der Bruchlast ermittelt werden kann und dass diese Grenzwerte so nahe zusammengebracht werden können, wie es für notwendig erachtet wird. Die verschiedenen Theorien werden im dritten Teil zur Berechnung räumlicher Rahmenwerke angewandt.

Leere Seite
Blank page
Page vide

AI 3

Determination of the shape of fixed-ended beams for maximum economy according to the plastic theory

Détermination de la forme à donner aux poutres encastrées d'après la théorie de la plasticité en vue du maximum d'économie

Bestimmung der wirtschaftlichsten Querschnittsform eingespannter Balken nach der Plastizitätstheorie

M. R. HORNE, M.A., Ph.D., A.M.I.C.E.
Cambridge University

1. Introduction

In the design of structures according to the plastic theory, the members are so proportioned that collapse would not occur at a load less than the working load multiplied by a "load factor." The plastic theory provides a means of estimating the collapse loads of ductile structures by considering their behaviour beyond the elastic limit. It has been shown[1] that, in the absence of instability, these collapse loads may be calculated simply by reference to the conditions of equilibrium, without considering the equations of flexure. Hence the design process is essentially reduced to the selection of members with plastic moments of resistance sufficient to withstand the bending moments imposed by the "factored loads"—that is, by the working loads multiplied by the load factor.

The direct nature of the design of structures by the plastic theory facilitates the relative proportioning of the members such that the total weight is an absolute minimum. A method of proportioning simple structures composed of prismatic members for minimum weight has already been presented.[2] Further economy of material can, however, be achieved by using members of varying cross-section, and may be sufficient to compensate for the increased cost of fabrication. It is thus worth while investigating the maximum saving in material theoretically attainable by this means. No consideration will be given to the increased cost of manufacture of such members compared with those of uniform section, since this must depend primarily on the quantities required; for this reason, it is impossible to arrive at any conclusions regarding possible overall economies.

[1] For references see end of paper.

The relationship to be assumed between weight per unit length and full plastic moment of resistance is discussed in 2 below; 3 contains a discussion of a member of continuously varying section fixed at the ends and supporting a uniformly distributed load; while the case of a similarly loaded member in which the cross-section is only to be varied by one or two discrete intervals is discussed in 4.

The term "fixed at the ends" is not here intended to imply complete flexural rigidity at the supports, but rather that the members to which the beam under consideration is attached are together capable of resisting the full plastic moment of the end sections of that beam.

2. The relationship between full plastic moment and weight per unit length

The full plastic moment of a member (denoted by M_p) is the moment of resistance when the whole section is undergoing plastic deformation. If f_y is the yield stress, at which pure plastic deformation can occur, then for a beam of rectangular cross-section, of width b and depth $2d$ (see fig. 1),

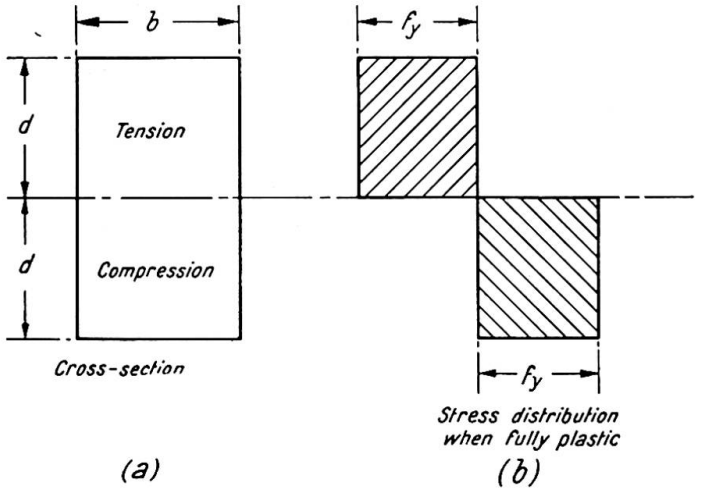

Fig. 1. Fully plastic stress distribution for a rectangular beam

$$M_p = bd^2 f_y \quad . . . . . (1)$$

Let the weight per unit length of the beam be w, and let the density of the material be ρ. Then

$$w = 2bd\rho \quad . . . . . (2)$$

If b is constant and d varies, then

$$w \propto M_p^{\frac{1}{2}} \quad . . . . . (3)$$

If d is constant and b varies,

$$w \propto M_p \quad . . . . . (4)$$

while if b and d both vary such that b/d remains constant

$$w \propto M_p^{\frac{3}{2}} \quad . . . . . (5)$$

Hence, however the section is varied,

$$w = kM_p^n \quad . . . . . (6)$$

where k is a constant and $\frac{1}{2} < n < 1$.

Arguments similar to the above may be applied to sections other than rectangular, and thus equation (6) gives a general relationship between M_p and w. This formula

isfactory in that it takes no account of the effect of shear forces. hear forces have little effect on the value of the full plastic moment,[3] esisting shear forces will prevent the section of a beam being allowed the applied bending moment at collapse is zero. Hence it will in ned that

$$w=w_0+kM_p^n \quad . \quad . \quad . \quad . \quad . \quad . \quad . \quad . \quad . \quad (7)$$

constant.

ENDED BEAM OF CONTINUOUSLY VARYING SECTION

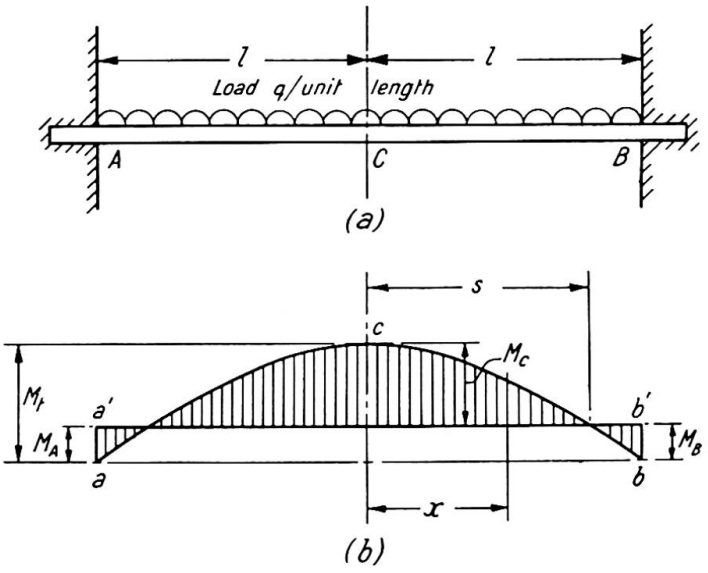

Fig. 2. Bending moment distribution for a beam of continuously varying section (uniformly distributed load)

The beam AB (see fig. 2(*a*)), of length $2l$, is fixed at the ends and carries a uniformly distributed load at collapse of q per unit length. Let the hogging bending moments at the ends (M_A and M_B) be assumed equal at collapse, and let M_C denote the sagging bending moment at the centre. Let M_t be the central bending moment which would be induced in a similar simply supported beam. The bending moment distribution at collapse in the fixed-ended beam may be obtained by superimposing on a parabolic bending moment diagram acb of height M_t (fig. 2(*b*)) the bending moment distribution aa′b′a due to the terminal moments M_A and M , giving the resultant shaded area. Let s denote the distance of the points of contraflexure from the centre of length of the beam.

Then

$$\left.\begin{aligned} M_t &= \frac{ql^2}{2} \\ M_A=M_B &= \frac{l^2-s^2}{l^2}M_t \\ M_C &= \frac{s^2}{l^2}M_t \end{aligned}\right\} \quad . \quad . \quad . \quad . \quad . \quad . \quad . \quad . \quad (8)$$

If x denotes the distance of any section from the centre of length of
then the minimum full plastic moment at that section becomes

when $0<x<s$, $M_p=\frac{s^2-x^2}{l^2}M_t$

when $s<x<l$, $M_p=\frac{x^2-s^2}{l^2}M_t$ . . . . . .

Hence if W denotes the weight of the beam,

$$W=2w_0l+2k\frac{M_t^n}{l^{2n}}\left[\int_o^s(s^2-x^2)^n dx+\int_s^l(x^2-s^2)^n dx\right] \quad . .$$

The most economical design will be obtained with that value of s for which W
minimum, i.e. putting $dW/ds=0$, when

$$\int_o^s(s^2-x^2)^{n-1}dx=\int_s^l(x^2-s^2)^{n-1}dx \quad . . . . . (11)$$

If M_p' and W' denote the full plastic moment and weight respectively of the least prismatic beam sufficient to carry the load, then

$$M_p'=\frac{M_t}{2} \quad . . . . . (12)$$

$$W'=2w_0l+2k\left(\frac{M_t}{2}\right)^n l \quad . . . . . (13)$$

When $n=0{\cdot}5$, the most economical value of s is given by

$$\frac{s}{l}=\operatorname{sech}\frac{\pi}{2}=0{\cdot}3986$$

The corresponding minimum weight is

$$W=2w_0l+0{\cdot}9172kM_t^{\frac{1}{2}}l$$

while $$W'=2w_0l+1{\cdot}4142kM_t^{\frac{1}{2}}l$$

The percentage saving of material depends on the ratio of w_0 to $kM_t^{\frac{1}{2}}$. If the requirements of resistance to shear are ignored ($w_0=0$), an economy of up to 35·1% of the weight of the uniform beam can be achieved. When the effect of shear is allowed for, the percentage economy will become less.

When $n=1{\cdot}0$, the economical value of s is $s/l=0{\cdot}5$,

whence $$W=2w_0l+0{\cdot}5kM_tl$$

while $$W'=2w_0l+kM_tl$$

In this case therefore a maximum economy (ignoring shear) of 50% is possible.

When $\frac{1}{2}<n<1$, it may be shown from equation (11) that the most economical value of s is given approximately by the formula

$$\frac{l}{s}=2+1{\cdot}2467\left(\frac{3}{2}\right)^{1-n}\left(\frac{1-n}{1+n}\right) \quad . . . . . (14)$$

Values of s/l for various values of n are given in Table I.

TABLE I

n	s/l
1·0	0·5000
0·9	0·4835
0·8	0·4651
0·7	0·4447
0·6	0·4226
0·5	0·3986

Points of contraflexure for beam of continuously varying section carrying a uniform load (see fig. 2)

Although for any given value of n the maximum economy is only achieved for some definite value of s, the loss in economy is negligible if $s/l=0{\cdot}45$. This is demonstrated in fig. 3, which shows the percentage economies achieved (assuming $w_0=0$) with various values of s/l for $n=0{\cdot}5$ and $n=1{\cdot}0$.

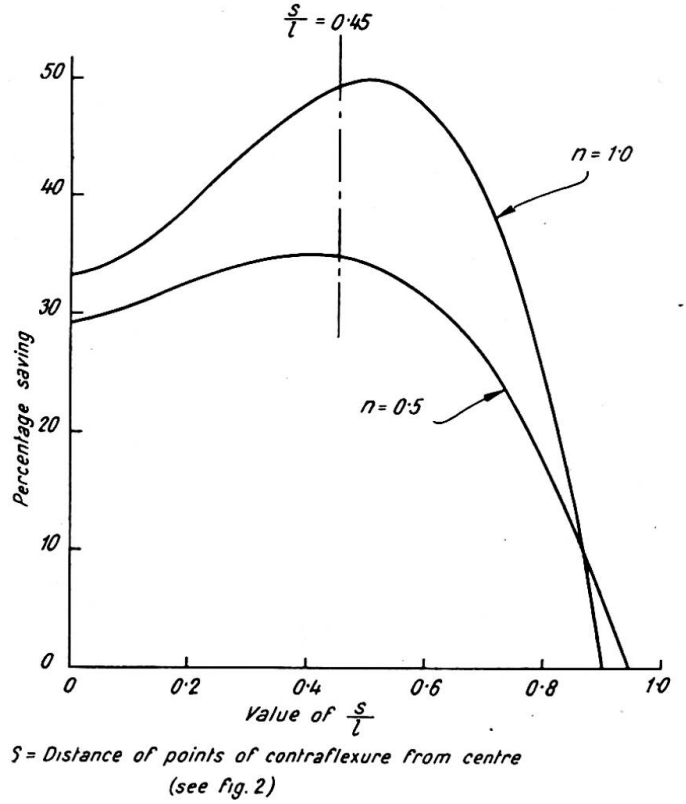

Fig. 3. Economies achieved by continuously varying the section of a fixed-ended beam (uniformly distributed load)

4. FIXED-ENDED BEAM WITH DISCRETE VARIATIONS IN SECTION

Due to the practical difficulties of varying the section of a beam continuously as envisaged above, it is worth while investigating the economies which can be achieved when the full plastic moment is increased by discrete amounts (a) at the centre only, (b) at the ends only and (c) at both centre and ends.

Since the full plastic moment of resistance is nowhere reduced to zero, there will in general be no need to allow for the effects of shear on the relationship between w and M_p (equation (7)). In the following analysis it is therefore assumed that $w_0=0$.

(a) *Section increased over a central length only*

Let the beam previously considered have a uniform value of M_p denoted by M_1, except over a central length $2a$, where it is reinforced so that $M_p=M_2$ where $M_2>M_1$ (see fig. 4(*a*)). The bending moments at collapse are shown by the shaded area in

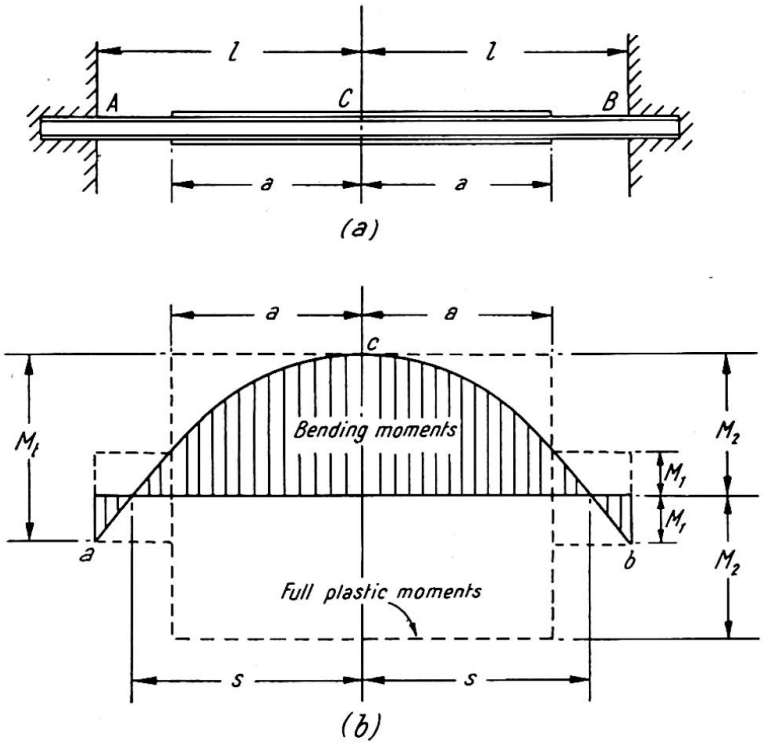

Fig. 4. Bending moment distribution for a beam reinforced at centre only (uniformly distributed load)

fig. 4(*b*), while the moments of resistance M_1 and M_2 are indicated by dotted lines, which must completely enclose the bending moment diagram. Hence

$$M_1=M_A=M_B=\frac{l^2-s^2}{l^2}M_t \quad . \quad . \quad . \quad . \quad . \quad . \quad . \quad . \quad (15)$$

$$M_2=M_C=\frac{s^2}{l^2}M_t \quad . \quad . \quad . \quad . \quad . \quad . \quad . \quad . \quad . \quad . \quad . \quad (16)$$

The value of a is obtained by noting that where the beam changes section, the sagging moment is equal to M_1, and hence

$$M_1=\frac{s^2-a^2}{l^2}M_t \quad . \quad . \quad . \quad . \quad . \quad . \quad . \quad . \quad (17)$$

It follows from equations (15) and (16) that

$$M_1+M_2=M_t \quad . \quad . \quad . \quad . \quad . \quad . \quad . \quad . \quad . \quad (18)$$

while from equations (15) and (17), putting $M_1/M_t=r$,

$$\frac{a}{l}=\sqrt{1-2r} \quad . \quad . \quad . \quad . \quad . \quad . \quad . \quad . \quad . \quad (19)$$

The total weight W of the beam is given by

$$W=2kM_1{}^n(l-a)+2kM_2{}^n a \quad . \quad . \quad . \quad . \quad . \quad . \quad . \quad (20)$$

It may be shown from equations (18), (19) and (20) that

$$W=2kM_t{}^n l[r^n(1-\sqrt{1-2r})+(1-r)^n\sqrt{1-2r}] \quad . \; . \; . \quad (21)$$

When W has its minimum value,

$$\left(\frac{r}{1-r}\right)^{1-n}=\frac{n\sqrt{1-2r}+(2nr-n+r)}{1-(2nr-n+r)} \quad . \; . \; . \; . \; . \quad (22)$$

TABLE II

n	$r=M_1/M_t$	a/l
1·0	0·4444	0·3333
0·9	0·4432	0·3371
0·8	0·4418	0·3412
0·7	0·4403	0·3456
0·6	0·4388	0·3500
0·5	0·4370	0·3550

Plastic moment ratio and proportion of beam to be reinforced for beam reinforced at centre only (see fig. 4)

The most economical values of r and a/l are given in Table II for values of n between 0·5 and 1·0. It may be noted that r represents the ratio of M_1, the full plastic moment of the unreinforced part of the beam, to M_t, the full plastic moment of the uniform simply supported beam which would just carry the same load. Hence r will be termed the "plastic moment ratio." It will be seen that r and a/l (the proportion of the beam to be reinforced) are almost constant, r varying from 0·4444 to 0·4370 and a/l from 0·3333 to 0·3550. As a working rule therefore the beam should be reinforced for about one-third of its length, the reinforced section having a full plastic moment some 25% or 30% greater than the unreinforced section.

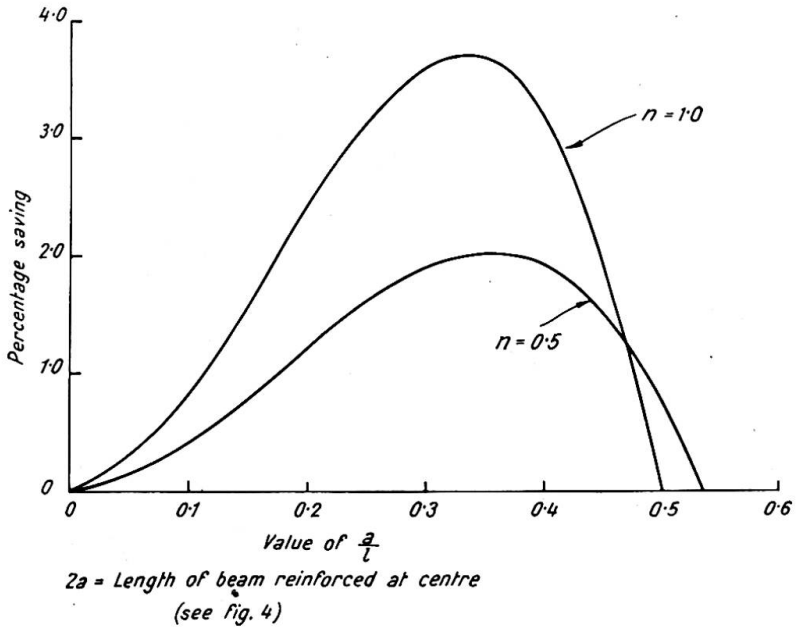

Fig. 5. Economies achieved by reinforcing the centre of a fixed-ended beam (uniformly distributed load)

The variation of the percentage saving (as compared with a beam of uniform section throughout) with a/l for $n=0{\cdot}5$ and $n=1{\cdot}0$ is shown in fig. 5. It will be observed that if more than about half of the beam is reinforced, there is no saving in material. When $n=0{\cdot}5$, the maximum saving possible is $2{\cdot}03\,\%$ as compared with a saving of $35{\cdot}1\,\%$ when the section is varied continuously in an ideal manner. When $n=1{\cdot}0$, the corresponding figures are $3{\cdot}70\,\%$ and $50{\cdot}0\,\%$ respectively. It is therefore apparent that no great advantage accrues by increasing the section only at the centre.

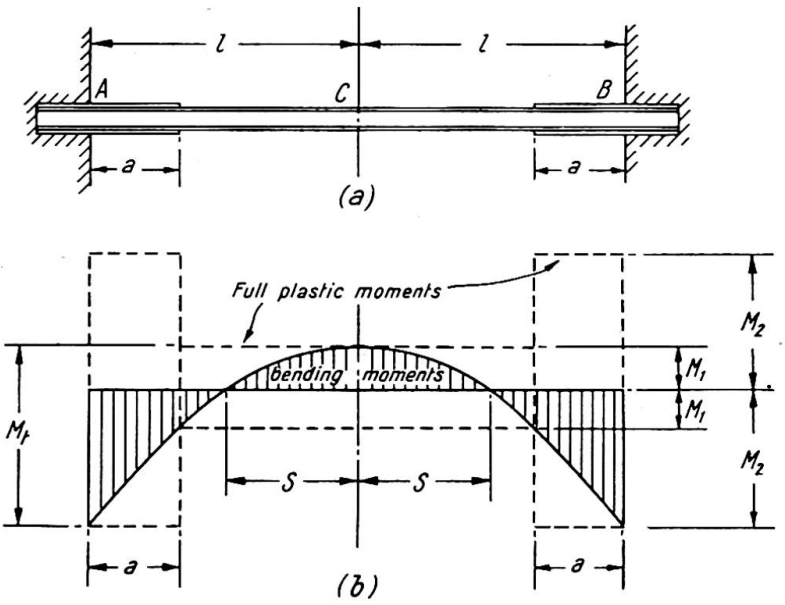

Fig. 6. Bending moment distribution for a beam reinforced at ends only (uniformly distributed load)

(b) *Section increased at ends only*

A beam of uniform plastic moment of resistance M_1 is reinforced for a distance a from either end so that its plastic moment of resistance becomes M_2 (see fig. 6(*a*)). The bending moment distribution at collapse is shown by the shaded area in fig. 6(*b*), while the moments of resistance are superimposed as dotted lines. If full plastic moments are just sufficient to withstand the applied moments, then

$$M_1=M_C=\frac{s^2}{l^2}M_t \quad . \quad . \quad . \quad . \quad . \quad . \quad . \quad . \quad . \quad . \quad . \quad (23)$$

$$M_2=M_A=M_B=\frac{l^2-s^2}{l^2}M_t \quad . \quad . \quad . \quad . \quad . \quad . \quad . \quad . \quad . \quad (24)$$

Since where the beam changes section the hogging moment has the value M_1,

$$M_1=\frac{(l-a)^2-s^2}{l^2}M_t \quad . \quad . \quad . \quad . \quad . \quad . \quad . \quad . \quad . \quad . \quad (25)$$

From equations (23) and (24),

$$M_1+M_2=M_t \quad . \quad . \quad . \quad . \quad . \quad . \quad . \quad . \quad . \quad . \quad . \quad . \quad . \quad (26)$$

while from equations (23) and (25), if $M_1/M_t=r$,

$$\frac{a}{l}=1-\sqrt{2r} \quad . \quad . \quad . \quad . \quad . \quad . \quad . \quad . \quad . \quad . \quad (27)$$

The total weight W of the beam is given by

$$W=2kM_1{}^n(l-a)+2kM_2{}^n a \quad . \quad . \quad . \quad . \quad . \quad . \quad (28)$$

which, by virtue of equations (26) and (27) becomes

$$W=2kM_t{}^n l[r^n\sqrt{2r}+(1-r)^n(1-\sqrt{2r})] \quad . \quad . \quad . \quad . \quad (29)$$

At minimum W,

$$\left(\frac{r}{1-r}\right)^{1-n}=\frac{(2n+1)r}{(1-2nr-r+n\sqrt{2r})} \quad . \quad . \quad . \quad . \quad . \quad . \quad . \quad . \quad . \quad (30)$$

TABLE III

n	$r=M_1/M_t$	a/l
1·0	0·2946	0·2324
0·9	0·2866	0·2429
0·8	0·2777	0·2548
0·7	0·2680	0·2679
0·6	0·2571	0·2829
0·5	0·2449	0·3001

Plastic moment ratio and proportion of beam to be reinforced for beam reinforced at ends only (see fig. 6)

The most economical values of r and a/l are given in Table III for values of n from 0·5 to 1·0. The value of $r(=M_1/(M_1+M_2))$ varies from 0·2946 to 0·2449, and hence the reinforced section has a full plastic moment from 140% to 208% greater than the unreinforced section. The value of a/l varies from 0·2324 to 0·3001. A satisfactory working rule would therefore be to reinforce an eighth of the length of the beam at either end.

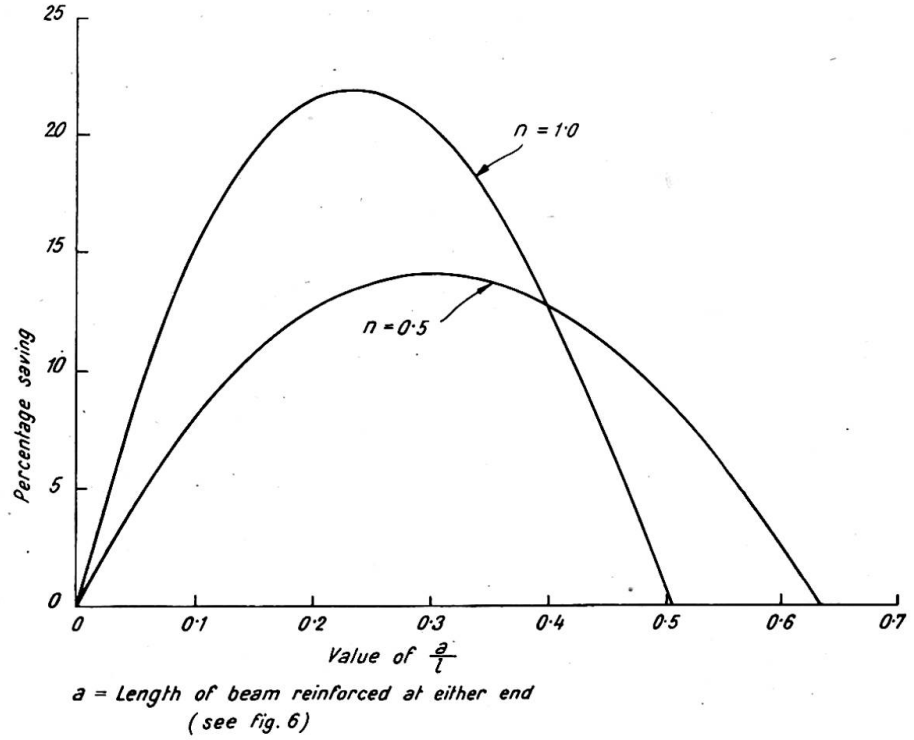

Fig. 7. Economies achieved by reinforcing the ends of a fixed-ended beam (uniformly distributed load)

The variation of the percentage saving (compared with a uniform beam) as a/l is altered is shown in fig. 7 for $n=0{\cdot}5$ and $n=1{\cdot}0$. It will be seen that by taking $a/l=0{\cdot}25$ there is very little loss in economy in either case. When $n=0{\cdot}5$ the maximum saving possible is 14·1 % and for $n=1{\cdot}0$ it is 22·0 %. These figures compare with the ideally attainable economies of 35·1 % and 50·0 % respectively.

The economy practically attainable by reinforcing the ends alone is therefore quite appreciable. It should be noted, however, that the surrounding members must provide a total moment of resistance equal to the full plastic moment of the reinforced part of the beam, and this may sometimes be a serious disadvantage.

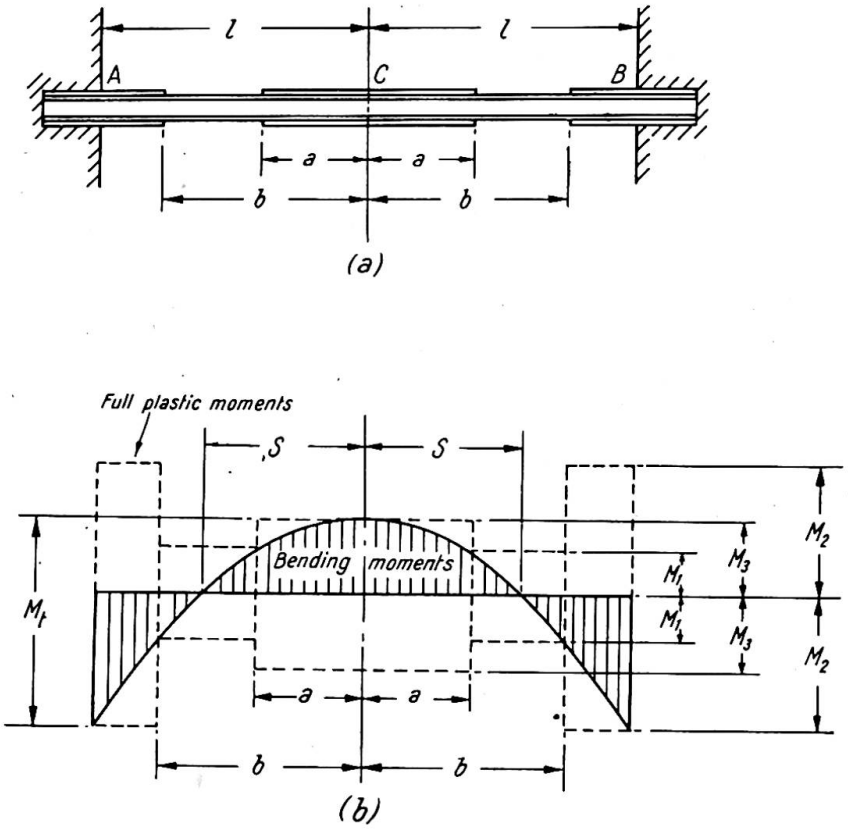

Fig. 8. Bending moment distribution for a beam reinforced at both centre and ends (uniformly distributed load)

(c) *Section increased at both centre and ends*

The advantage obtained by reinforcing both centre and ends may be estimated by considering the beam shown in fig. 8(*a*). This is reinforced for a distance a either side of the centre and at each end for a distance $(l-b)$. The bending moment diagram, shown shaded in fig. 8(*b*), is completely enclosed by the graph of the full plastic moments (shown dotted). The unreinforced section has a moment of resistance M_1, the ends a moment of resistance M_2 and the centre a moment of resistance M_3.

Hence

$$M_3-M_1=\frac{a^2}{l^2}M_t \quad . \quad . \quad . \quad . \quad . \quad . \quad . \quad . \quad . \quad . \quad (31)$$

$$M_3+M_1=\frac{b^2}{l^2}M_t \quad . \quad . \quad . \quad . \quad . \quad . \quad . \quad . \quad . \quad . \quad (32)$$

$$M_2+M_3=M_t \quad . \quad . \quad . \quad . \quad . \quad . \quad . \quad . \quad . \quad . \quad . \quad (33)$$

Solving for M_1, M_2 and M_3,

$$M_1=\frac{b^2-a^2}{2l^2}M_t \quad . \quad . \quad . \quad . \quad . \quad . \quad . \quad . \quad . \quad . \quad (34)$$

$$M_2=\frac{2l^2-a^2-b^2}{2l^2}M_t \quad . \quad . \quad . \quad . \quad . \quad . \quad . \quad . \quad . \quad (35)$$

$$M_3=\frac{a^2+b^2}{2l^2}M_t \quad . \quad . \quad . \quad . \quad . \quad . \quad . \quad . \quad . \quad . \quad (36)$$

The total mass of the beam thus becomes

$$W=2^{1-n}k\frac{M_t^n}{l^{2n}}[a(a^2+b^2)^n+(b-a)(b^2-a^2)^n+(l-b)(2l^2-a^2-b^2)^n] \quad . \quad (37)$$

When W has its minimum value, $\partial W/\partial a=0$ and $\partial W/\partial b=0$.

When $n=1{\cdot}0$ the above conditions give $3a^2-al=0$ and $3b^2-bl-l^2=0$,

whence
$$\frac{a}{l}=\tfrac{1}{3}=0{\cdot}3333$$

$$\frac{b}{l}=\frac{1+\sqrt{13}}{6}=0{\cdot}7676$$

The moment of resistance is 171·8% greater than that of the unreinforced beam at the ends, and 46·5% greater at the centre. The saving is 25·7%, compared with 22·0% with end reinforcement only and 3·7% with central reinforcement only.

When $n=0{\cdot}5$, it is found that

$$\frac{ab}{\sqrt{a^2+b^2}}+\frac{(b-a)(a+2b)}{\sqrt{b^2-a^2}}-\frac{2l^2+lb-a^2-2b^2}{\sqrt{2l^2-a^2-b^2}}=0$$

$$\frac{2a^2+b^2}{\sqrt{a^2+b^2}}-\frac{(b-a)(2a+b)}{\sqrt{b^2-a^2}}-\frac{a(l-b)}{\sqrt{2l^2-a^2-b^2}}=0$$

These equations give $a/l=0{\cdot}3185$ and $b/l=0{\cdot}7074$. The moments of resistance at the ends and centre are respectively 250·5% and 50·9% greater than that of the unreinforced beam. The saving is 16·1%, compared with 14·1% with end reinforcement only and 2·0% with central reinforcement only.

Hence the percentage saving with both central and end reinforcement is very little greater than the saving with end reinforcement only.

5. Conclusions

It has been shown that the adoption of beams of varying cross-section can lead to considerable economies in total material consumption when the basis of design is the ultimate load which the beam will carry as calculated by the simple plastic theory. The best shape for the beams has been calculated for the case of a fixed-ended beam carrying a uniformly distributed load, the minimum cross-sections occurring at about one-fifth the length of the beam from the centre. The maximum theoretical economies are of the order 35–50%.

Since the construction of a beam of continuously varying cross-section may have considerable practical disadvantages, an investigation has been made into the effect of reinforcing either the centre or the ends of the beam, or both centre and ends simultaneously. It has been shown that there is only a negligible advantage in reinforcing the centre, but that reinforcing the ends does lead to appreciable

economies. The economy achieved by reinforcing both centre and ends is virtually no greater than that achieved by reinforcing the ends alone.

REFERENCES

(1) HORNE, M. R. "Fundamental Propositions in the Plastic Theory of Structures," *J. Inst. Civ. Engrs.*, **34**, 174, 1950.

(2) HEYMAN, J. "Plastic Design of Beams and Plane Frames for Minimum Material Consumption," *Quart. J. Appl. Math.*, **8**, 373, 1951.

(3) HORNE, M. R. "The Plastic Theory of Bending of Mild Steel Beams, with Particular Reference to the Effect of Shear Forces," *Proc. Roy. Soc. A.*, Series A, **207**, 216, 1951.

Summary

The simple plastic theory gives a direct means of determining the form of a fixed-ended beam of varying cross-section such that the total weight of material shall be an absolute minimum. The paper shows how this form may be deduced for a uniformly distributed load, both when the cross-section of the beam can be varied continuously, and when the size of the beam can only be adjusted in discrete intervals. The maximum theoretically attainable economies of material are discussed.

Résumé

La théorie simple de la plasticité fournit un moyen direct pour déterminer la forme à donner à une poutre encastrée à ses extrémités et présentant une section non uniforme, pour que le poids total de métal employé constitue un minimum absolu. L'auteur montre comment l'on peut déterminer une telle forme dans le cas d'une charge uniformément répartie, aussi bien lorsque la section de la poutre peut varier d'une manière continue que lorsque ses dimensions effectives ne peuvent être choisies que dans des intervalles déterminés. Il discute l'économie maximum de métal que l'on peut réaliser du point de vue théorique.

Zusammenfassung

Die einfache Plastizitätstheorie erlaubt uns die direkte Bestimmung derjenigen Form eines eingespannten Balkens mit veränderlichem Querschnitt, bei der das Gesamtgewicht des Materials ein absolutes Minimum sein soll. Der Aufsatz zeigt die Ermittlung dieser Form bei gleichmässig verteilter Belastung, einerseits, wenn der Querschnitt des Balkens stetig veränderlich ausgeführt werden kann und andererseits, wenn seine Abmessungen nur in bestimmten Abstufungen verändert werden können. Die höchste theoretisch mögliche Ausnützung des Materials wird untersucht.

AI 3

Sur la plastification de flexion des poutres à âme pleine en acier doux

(Récents essais français—Examen critique des essais antérieurs—Questions restant à résoudre)

Plastification of bending plate-web girders in mild steel

(Recent French tests—Critical study of previous tests—Problems still to be solved)

Plastifizierung der Vollwand-Biegeträger aus Flusstahl

(Neue französische Versuche—Kritische Betrachtung der früheren Versuche—Noch zu lösende Aufgaben)

A. LAZARD

Ingénieur en Chef des Ponts et Chaussées

Chef des Divisions Centrales des Ouvrages d'Art et des Études d'Aménagements de la S.N.C.F.

Introduction

Les recherches sur la plastification de flexion des poutres à âme pleine en acier doux de construction doivent conduire à une économie de métal et à une économie d'argent. Cela s'obtiendra par relèvement des contraintes maxima autorisées par les règlements officiels, basés presque tous sur l'ancienne conception de l'élasticité, en sollicitant soit certaines dérogations, soit des modifications permanentes à ces règlements. Il n'y a espoir d'aboutir que si le dossier présenté aux Organismes responsables des Grandes Administrations est basé sur des faits indiscutables, résultats d'expériences nombreuses et probantes, et si les limites d'utilisation des dérogations sollicitées ou des nouvelles prescriptions proposées sont bien précisées.

Or à la suite d'importantes expériences de flexion effectuées sur poutrelles Grey de 1 mètre de hauteur (c'est-à-dire sur les plus grands laminés du monde) qui nous a permis d'entrevoir quantité de phénomènes de plastification peu ou mal connus, il nous est apparu, en procédant à un examen critique général des théories et des expériences existantes, que les généralisations étaient souvent hâtives, qu'il existait un nombre considérable de questions non posées ou restées sans réponse, que, malgré des tentatives isolées dans ce sens, les limites d'utilisation des nouvelles méthodes n'étaient pas suffisamment précisées, et, qu'en définitive, il fallait procéder à un nouvel examen du problème en opérant avec beaucoup d'ordre.

Pour notre part nous avons mis en train, avec la collaboration de la Chambre Syndicale des Constructeurs Métalliques Français, des séries d'expériences dans le domaine fort vaste, quoique très restrictif, des

laminés I ou H
bruts*
de longueur dépassant 6 fois la hauteur
sollicités à la flexion
statiquement
et isostatiquement
jusqu'à ruine.

Le chapitre I de la présente communication est consacré à une description rapide des expériences déjà réalisées et au développement des conclusions auxquelles on est conduit, en insistant sur les points qui appellent des expériences de contrôle par d'autres chercheurs.

Compte tenu de ces conclusions, les autres essais connus de nous† sont examinés et discutés au chapitre II, en suivant la classification qui a paru la plus adéquate. Chaque fois nous nous sommes basés sur la description détaillée des circonstances expérimentales: malheureusement les détails font souvent défaut.

Les conclusions d'ensemble sont développées au chapitre III. On insiste sur les lacunes des recherches actuelles. On propose d'établir un programme général des expériences à reprendre ou restant à faire, dont on souhaite un partage entre les membres de l'Association.

Chapitre I—Les récents essais français sur la plastification en flexion statique et isostatique de laminés I ou H bruts

On décrira quatre séries d'essais qui tous ont été poussés jusqu'à la ruine.

1*ère Série: Poutrelles H de* 1 *mètre de hauteur*

Ces essais, exécutés pour le compte de la S.N.C.F. en 1948–49, ont été décrits en détail par nous, dans le Xème Volume des Mémoires de l'A.I.P.C., et ont fait l'objet d'un léger complément théorique dans *Travaux*, numéro de mai 1950. Ils sont schématisés figs. 1 et 2.

Ils ont clairement mis en évidence les faits suivants:

(*a*) Les premiers signes de plastification sont apparus bien avant que les contraintes à la Navier (quotient du Moment M par le module de résistance de la section I/v ou W), aient atteint la limite élastique conventionnelle du métal (à $2\,‰$) déterminée sur une éprouvette prélevée dans une semelle d'un about. L'apparition de la plastification dépend essentiellement des appareils de mesure utilisés pour la déceler et du critère choisi pour la définir. Elle semble débuter dans la semelle tendue.

Il apparaît que la notion de "Moment Elastique" (ou produit de la limite élastique par le module de résistance), souvent utilisée par les théoriciens, ne correspond à

* C'est-à-dire sans trous. Nous mettons en route, à l'époque à laquelle nous rédigeons la présente communication—juin 1951—une nouvelle série, avec trous cette fois. Nous espérons pouvoir en rendre compte à l'époque du Congrès.

† Il ne nous a pas toujours été possible de nous procurer tous les articles originaux. Compte tenu du nombre limité de pages dont nous pouvions disposer dans la présente communication, nous ne donnons qu'un aperçu des expériences. Un texte détaillé paraîtra dans *Travaux*, numéros de novembre et décembre 1951.

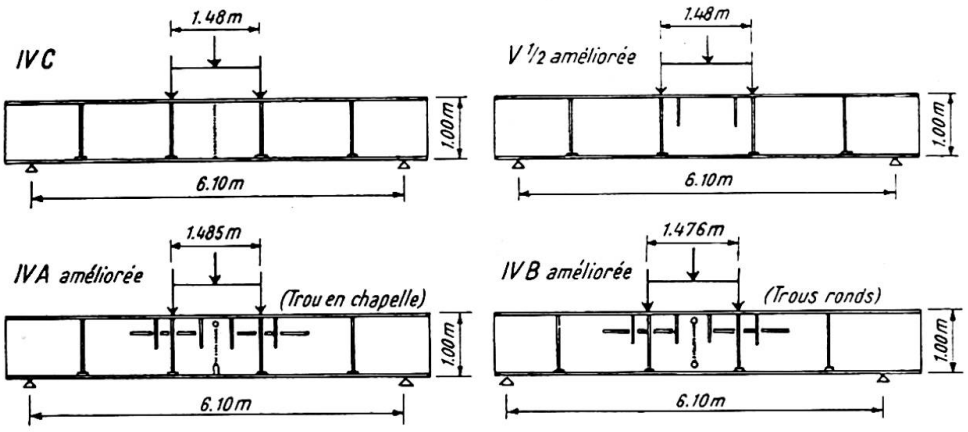

Fig. 1

Fig. 2

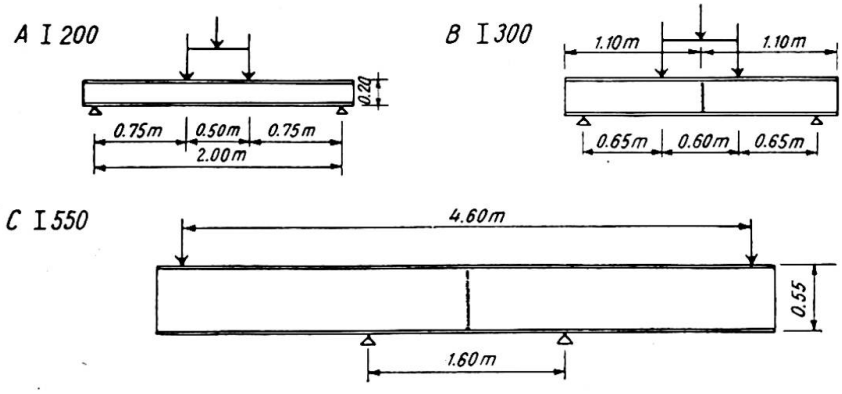

Fig. 3

aucun phénomène physique réel.* Pour cette valeur la poutrelle est déjà partiellement plastifiée. Cela paraît être sous la dépendance des contraintes préalables, enfermées dans la poutre par les traitements: chimique, physique, mécanique, subis antérieurement (et que le prélèvement de l'éprouvette libère partiellement).

(*b*) La plastification est un phénomène essentiellement discontinu. Elle se produit en des points très variables et diversement localisés. Ces points se mettent brusquement à fluer, la limite d'écoulement ayant été localement atteinte; les points voisins

* En réalité c'est la limite du domaine de proportionnalité de la poutrelle qu'on a déterminé. Il faudrait donc la comparer à la limite de proportionnalité du métal. A supposer que cette limite ait un sens pour le métal *in situ* (état contraint) et soit une constante en tous les points.

modifient leur progression de déformation, dans des proportions fort variables, allant d'un simple ralentissement à une régression.*

Les charges augmentant, la plastification se propage graduellement, par à coups, en intéressant des zones de plus en plus considérables. Il ne se passe rien de spécial dans les zones tendues; au contraire dans les zones comprimées on finit par parvenir à des flambements locaux *âme ou semelle* qui entraînent la ruine de la poutrelle.

(*c*) L'hypothèse de Bernoulli sur la conservation des sections planes (ou sur la proportionnalité des déformations aux distances de la fibre neutre) devient de plus en plus inexacte, au fur et à mesure que la plastification progresse.

(*d*) Dans les zones tendues apparaissent des lignes de glissement, dans les zones comprimées des rides de glissement, selon la terminologie du professeur Baes (voir fig. 2).† Lignes et rides n'apparaissent que dans des zones fortement plastifiées. Leur progression permet d'évaluer grossièrement, et probablement avec un certain retard, la progression de la plastification.

(*e*) On est amené à en déduire l'existence de contraintes de compression agissant sur les facettes longitudinales.

Dans l'âme c'est une conséquence de l'effet de courbure de la poutre. Dans les semelles on voit mal à quoi cela correspond.

(*f*) Les dispositions ayant été prises pour empêcher l'apparition de tous les phénomènes d'instabilité élastiques (déversement, flambements élastiques locaux) et dans une certaine mesure les flambements plastiques locaux la ruine des poutrelles est intervenue par plastification quasi totale. La "contrainte à la Navier" lors de la ruine plastique a certainement dépassé 30 kg./mm.^{2}

2ème Série: IPN de 200 *et* 300 *et HPN de* 550

Ces essais, exécutés pour le compte de la Chambre Syndicale des Constructeurs Métalliques en septembre–octobre 1949, ont été décrits, en détails par M. Dawance‡ lors d'une conférence faite à Paris le 13 décembre 1949, suivie d'une intéressante discussion (voir fig. 3).

Les prélèvements d'éprouvettes ont montré que les limites élastiques dans les âmes sont plus élevées que celles des semelles. C'est là d'ailleurs un phénomène tout à fait général.

Les essais ont sensiblement confirmé les conclusions de nos propres essais.

3ème Série: Mâts encastrés en poutrelles HN de 180 *et* 260

Ces essais ont été exécutés en 1950, sur des chantiers de la S.N.C.F., à l'occasion de recherches sur les poteaux supports de caténaires des futures électrifications.

Les essais de Marolles (5 septembre 1950) où des poutrelles HN de 180 étaient profondément encastrées dans un important massif de béton sont représentés à la fig. 4.

3 poutrelles ont été essayées avec efforts dans le plan de l'âme seule (fig. 4(*b*)). Toutes trois ont été ruinées pour une contrainte à la Navier de 35,2 kg./mm.^{2} calculée à la base de l'encastrement.

* Cette régression (à laquelle nous avons donné le nom de "bec d'oiseau" quand elle apparaît similairement dans le béton tendu au moment de la fissuration) a été également observé par M. Soete, professeur à Gand, dans des essais de traction sur éprouvettes soudées. Elle semble correspondre aux phénomènes observés, en rayons X, par les Allemands. Toutefois Schleicher (par exemple Bauingenieur, juillet 1950) prétend qu'on mesure par ce procédé les contraintes vraies.

† Ces phénomènes ont déjà été notés, mais avec beaucoup de prudence, par le prof. Kayser. Congrès de Berlin, Rapport final, 1938, p. 557, et *Stahlbau*, 26.2.1937.

‡ *Annales de l'Institut du Bâtiment et Travaux Publics*, mai 1950. Construction Métallique No. 6: "Nouvelles recherches expérimentales sur la plasticité des éléments de construction métallique."

Nous avons pu suivre avec précision le phénomène de ruine plastique sur l'une d'elles. Malgré les précautions prises l'effort n'était pas rigoureusement exercé dans le plan de l'âme et la poutrelle avait un aspect légèrement vrillé. Brusquement, au moment où l'effort de traction dans le câble atteignait 1 300 kg. (mesuré au dynamomètre), correspondant à un moment à l'encastrement de 14 940 kgm. et une contrainte à la Navier de 35,15 kg./mm.^{2}, nous avons vu sur une des ailes de la semelle tendue se propager vers le bas, et à partir d'une hauteur d'environ 60 cm. au-dessus du sol, comme une sorte de vibration de plastification; le vrillage a disparu et la poutrelle est alors venue, sans résistance, à la demande du câble. Compte tenu de la rapide décroissance du moment en fonction de la hauteur, la contrainte à la Navier, dans la zone d'où est parti l'ébranlement plastique de ruine, atteignait environ 32 kg./mm.^{2}

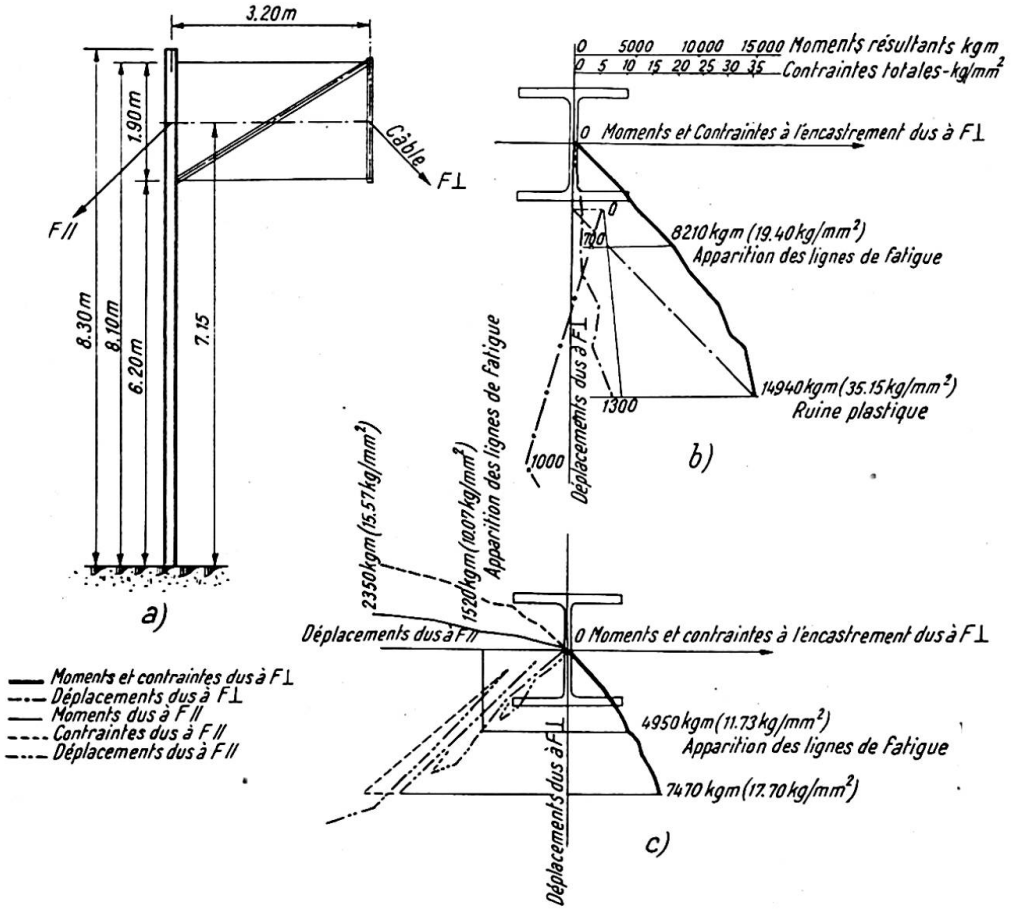

Fig. 4

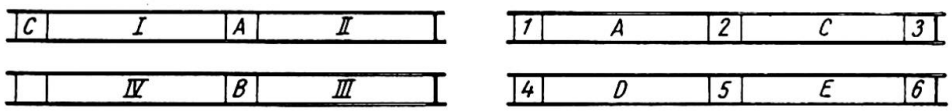

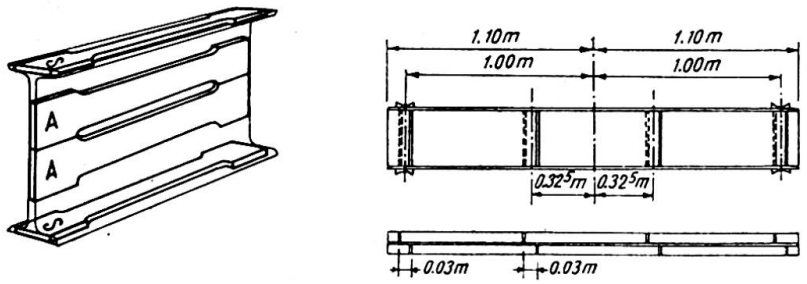

Fig. 5

Dès qu'on arrêtait l'enroulement du câble sur le treuil, les poutrelles cessaient de se déformer. Nous avons alors déchargé complètement (les poutrelles gardant une déformation importante) puis rechargé. A partir de cette déformation résiduelle, les poutrelles se sont comportées sensiblement comme des poutrelles neuves et élastiques tant que la charge n'a pas atteint une valeur très peu inférieure à celle ayant provoqué la ruine plastique; la poutrelle s'est remise alors à se déformer exagérément au simple appel du câble.

Ces essais complémentaires ont donc montré clairement (contrairement à une opinion répandue) qu'une poutrelle peut avoir été amenée à la plastification totale et être réutilisée dans certaines limites à partir de la déformation permanente acquise. Il n'y a ruine définitive que si la sollicitation est maintenue en permanence: si la sollicitation cesse la poutrelle peut être récupérée dans une certaine mesure.*

Une autre poutrelle a été essayée à la flexion déviée (fig. 4(*c*)). La ruine plastique est intervenue pour une valeur des efforts correspondant à une contrainte à la Navier à l'encastrement de l'aile de la membrure la plus comprimée égale à 33,3 kg./mm.^{2}

D'autres essais ont eu lieu à Vigneux avec des HN de 260 enfoncées de 3 m. dans un massif de béton de 55 cm. de diamètre et de 3 m. de profondeur.

Ils ont manifesté des phénomènes d'instabilité élastique qui sont susceptibles de se produire chaque fois qu'on ne prend pas les précautions nécessaires pour les rendre impossibles.

4ème Série: IPN de 200*: Sollicitations cycliques*

Ces essais ont été exécutés, conjointement par la S.N.C.F. et la Chambre Syndicale des Constructeurs Métalliques en 1950 et 1951, par M. Dawance et son équipe de collaborateurs habituels.

Les tronçons de 2,20 m. des poutrelles IPN 200 ont été extraits dans des barres de 7 m. provenant des parcs de la S.N.C.F. Les éprouvettes ont été prélevées dans des sections d'essai repérées en bout de chaque tronçon: deux dans les âmes, une dans chaque semelle (voir fig. 5). Le tableau suivant donne les limites élastiques conventionnelles (en kg./mm.^{2}) des sections d'essai.

Poutrelles des:	1ère sous-série			2ème sous-série			3ème sous-série		
Sections d'essais:	A	C	B	1	2	3	4	5	6
Semelles hautes	24,7	29	28,3	26,9	26,1	26,7	26,6	26,9	27,7
Semelles basses	27	28,3	28,3	26,6	25,4	24,9	26	25,9	24,2
Âmes hautes	29,2	33,8	29,6	26,8	27,9	27,8	28	28,2	29
Âmes basses	30	34,8	32,0	27,8	28,4	29,9	30,2	29,4	28,8

On notera *une très notable dispersion des résultats le long d'une même fibre du métal* ainsi que des valeurs plus élevées dans les âmes que dans les semelles.

Ces essais ont eu pour but de rechercher l'influence de la répétition de cycles de sollicitations sur les phénomènes de plastification et notamment de déterminer la valeur des cycles à partir desquels les déformations permanentes ne se stabiliseraient plus.

On craignait, en particulier, que la ruine plastique intervint, dans ces conditions,

* Dix ans plus tôt nous avions reçu l'ordre de mettre à la ferraille la charpente d'un pont détruit par faits de guerre, dont nous avions proposé la réutilisation partielle. C'est la raison qui nous a poussé à procéder à cette contre épreuve.

bien avant celle qui aurait été observée en suivant le processus des trois premières séries d'essais.

Première sous-série: Sollicitations ondulées—Cycles* 4 *à* $+n$ *kg./mm.*^{2} (*fig.* 6) (*Poutres I et II, III*)—*essais des* 17 *et* 23 *mai, du* 21 *juin et du* 7 *juillet* 1950

Les contraintes à la Navier variaient, dans chaque cycle, entre 4 et $+n$ kg./mm.^{2} La valeur supérieure n du cycle n'était augmentée que lorsque la stabilisation des flèches était obtenue. Deux poutrelles (I et II de la fig. 5) ont été essayées dans ces conditions.

On a pu tirer les conclusions suivantes:

1° *La répétition de cycles de sollicitations ondulées ne modifie pas la valeur du moment entraînant la ruine plastique.* La ruine plastique correspond pour une poutrelle sollicitée statiquement, dans des conditions de flexion déterminées, à un phénomène bien caractérisé qui est indépendant du processus d'application des charges.

2° On peut "accommoder élastiquement" une poutrelle, une fois la déformation permanente acquise. On peut, ce faisant, dépasser, en contrainte à la Navier, la limite élastique conventionnelle.

Nous en avons conçu la possibilité d'utiliser en flexion des poutrelles brutes bien au delà des limites actuellement tolérées par les règlements, *en procédant à une prédéformation volontaire des poutrelles*, sous une contrainte légèrement supérieure aux contraintes maxima d'utilisation.

Mais avant de mettre en application un tel procédé qui peut, naturellement, être conjugué avec un enrobement par du béton de la semelle tendue et déformée, en vue de précontraindre ce béton lorsqu'on retire les charges (les déformations sont, en particulier, très réduites et ne limitent plus l'utilisation des hautes contraintes), *il faut s'assurer que l'accommodation élastique, ainsi acquise, se conserve dans le temps.*

Des essais sont nécessaires pour le vérifier.

Deuxième sous-série: Sollicitations alternées—Cycles 10 *kg./mm.*^{2} *à* $+n$ *kg./mm.*^{2} (*fig.* 7(*a*)), 20 *kg./mm.*^{2} *à* $+n$ *kg./mm.*^{2} (*fig.* 7(*b*))

Les résultats confirment sensiblement les conclusions de la première sous-série; la ruine n'a pas été avancée par les sollicitations alternées et elle est intervenue pratiquement pour les mêmes valeurs de la contrainte à la Navier que dans les essais sans répétitions cycliques.

Troisième sous-série: Sollicitations oscillantes—Cycles entre plus et moins n kg./mm.^{2} (*fig.* 8)

L'essai a montré:

(*a*) que la stabilisation était assez rapidement acquise;†

* Nous adoptons ici la Terminologie que met au point actuellement une sous-commission de l'A.F.N.O.R., présidée par M. Prot:

Une sollicitation périodique est ondulée lorsque les forces varient entre deux limites de même signe.

Une sollicitation périodique est alternée lorsque les forces varient entre deux limites ayant des signes opposés.

Une sollicitation périodique est oscillante lorsque les forces varient entre deux limites ayant des signes opposés et une même valeur absolue.

Une sollicitation périodique est répétée lorsque les forces varient entre zéro et une limite.

† Toutefois le nombre de répétitions (20) n'a peut-être pas toujours été suffisant. La flèche pouvait paraître stabilisée puis brusquement, par exemple à la quinzième répétition, s'accroître à nouveau.

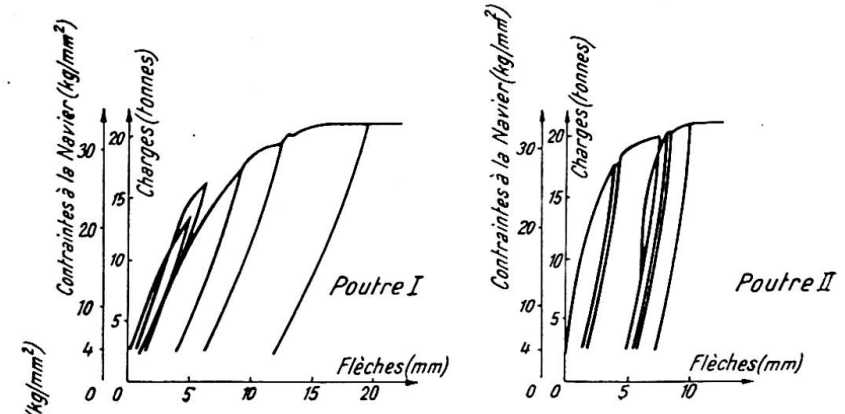

Fig. 6

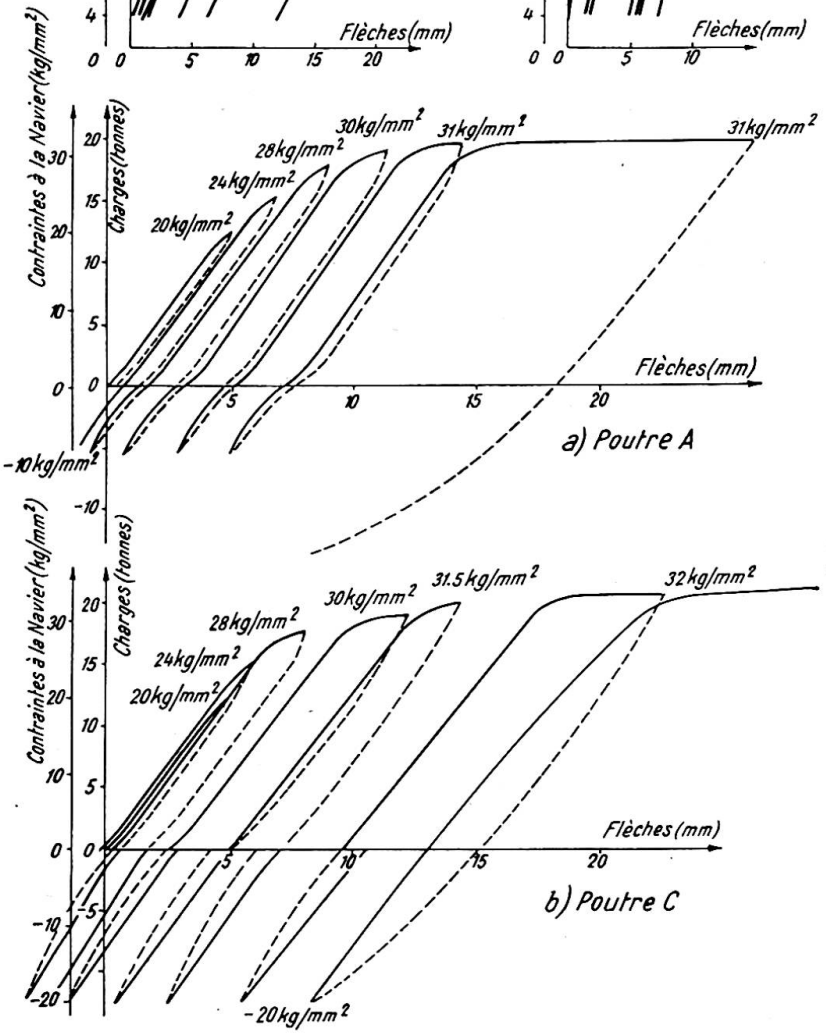

Fig. 7

(*b*) que les cycles d'hystérésis devenaient de plus en plus marqués, la diagonale s'inclinant de plus en plus sur l'horizontale;

(*c*) que l'effet Bauschinger jouait à plein, c'est-à-dire que les déchargements étaient à peu près linéaires, mais que les rechargements (dans un sens ou dans l'autre) montraient au contraire une courbure prononcée;

(*d*) qu'enfin la ruine est intervenue sensiblement pour la même contrainte à la Navier que dans les essais précédents.

Quatrième sous-série: Poutrelles A et D—Essais des 9 *et* 11 *mai* 1951 (*fig.* 9)

Nous nous sommes posé la question suivante: reste-t-il quelques traces, décelables, d'une plastification plus ou moins totale d'une poutrelle? Il est bien certain, en effet,

que lorsqu'une poutrelle est livrée par les forges elle a subi, au cours de son élaboration tant chimique que thermique que mécanique, d'innombrables plastifications. Or le contrôle consiste à mesurer les caractéristiques mécaniques d'une éprouvette prélevée dans le métal; si elles sont satisfaisantes on utilise la poutrelle dans les limites réglementaires. Comment distinguera-t-on une poutrelle "vierge" d'une poutrelle plus ou moins "outrageusement plastifiée" qui, après redressement, aura été remise sur parc.

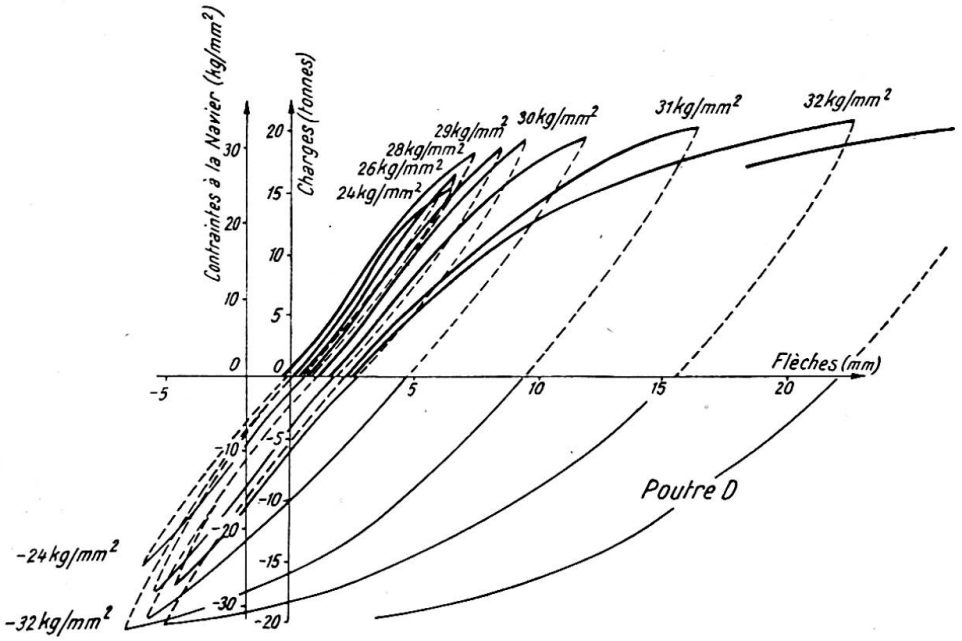

Fig. 8

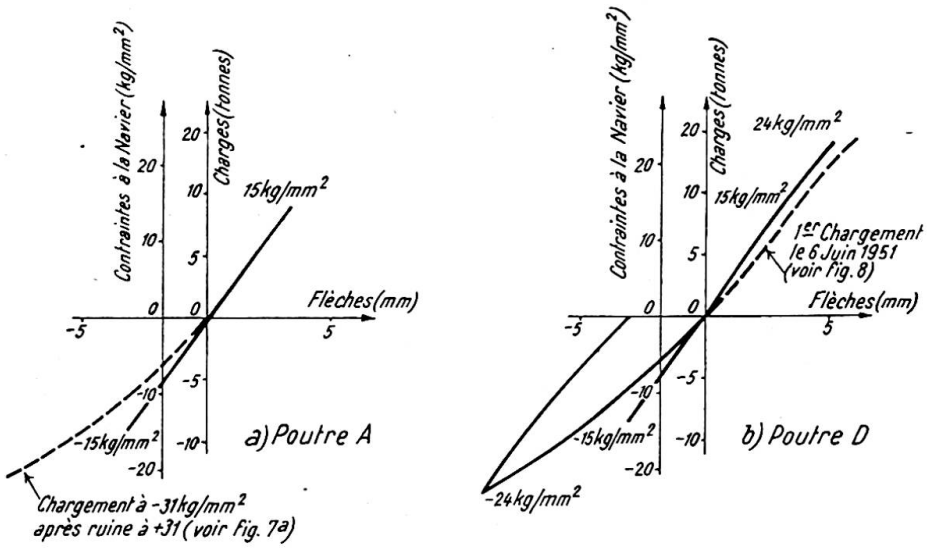

Fig. 9

A cet effet nous avons demandé qu'on soumette à nouveau à des essais de flexion, jusqu'à des contraintes de 15 kg./mm.², la poutrelle A de la 2ème sous-série et la poutrelle D de la 3ème sous-série qui toutes deux avaient été plastifiées jusqu'à la ruine dans des cycles Bauschinger (contraintes positives et négatives).

Selon le sens dans lequel l'effort serait appliqué on pouvait penser que ces poutrelles se comporteraient élastiquement ou manifesteraient la courbure caractérisque de l'effet Bauschinger, sous réserve que le temps n'ait pas modifié les propriétées acquises.

Les essais ont eu lieu le 9 mai 1951. Les poutrelles étaient au repos depuis 2 mois ½ pour A et 1 mois 2 jours pour D. Ils sont schématisés par les fig. 9(*a*) pour des essais sous + ou −15 kg./mm.² et fig. 9(*b*) pour des essais sous + ou −24 kg./mm.²

Il semble qu'on puisse conclure de ces deux essais (qui méritent d'être renouvelés):

1° qu'*après un repos de plusieurs semaines* des poutrelles* même sévèrement plastifiées (et tordues) *ont récupéré leurs qualités élastiques* (fig. 9(*a*)): les phénomènes de plastification ne se manifestent à nouveau que sous des sollicitations importantes voisines de la limite élastique (fig. 9(*b*)).

2° il n'existe pas de moyen de déterminer les plastifications antérieures†: au vrai cela devient sans intérêt à cause du 1° ci-dessus.

Tous ces essais nous conduisent à conclure comme suit:

Conclusions du chapitre I

(1) A la précision des essais et compte tenu de l'extrême dispersion des caractéristiques mécaniques du métal on peut dire que le moment produisant la ruine plastique d'une poutrelle brute sollicitée statiquement et isostatiquement est une donnée physique indépendante du processus de chargement (chargement continu, chargement par paliers avec déchargements, sollicitations cycliques: ondulées, répétées, alternées ou oscillantes).

(2) Si l'on supprime l'application des charges dès que se produit la ruine, la poutrelle est encore réutilisable élastiquement dans un domaine fort étendu qui paraît dépasser largement le domaine des contraintes réglementaires généralement admises. Le temps semble jouer, à ce sujet, un rôle très important, et encore mal défini.

(3) Le moment de ruine plastique est plus élevé, de plusieurs pour cent, que celui qui est déterminé par l'hypothèse du matériau idéalement plastique, la limite élastique étant déterminée sur une éprouvette de traction prélevée dans une semelle.

(4) Les contraintes préalables ne jouent aucun rôle dans la valeur du moment de ruine, car leur moment est nul (système en équilibre). Par contre elles interviennent certainement dans le déclanchement local des premières déformations plastiques. A ce sujet la considération du "moment élastique" est pratiquement dénuée de sens.

(5) Il semble qu'on puisse utiliser les poutrelles brutes à des contraintes très élevées, si l'on prend bien soin d'éviter les phénomènes de déversement et de flambement locaux des zones comprimées (âme et semelle). Les dispositions à prendre doivent varier d'ailleurs avec le profil des laminés; ces phénomènes perturbateurs sont d'autant plus à craindre que le laminé est plus haut ou plus grêle.

(6) La prédéformation volontaire en vue d'obtenir l'accommodation élastique, permet le relèvement des contraintes.

La question n'est, toutefois, pas encore complètement résolue.

Chapitre II—Autres essais sur la plastification en flexion des poutres à âme pleine

Nous distinguerons les essais statiques et de fatigue; dans chaque sous-chapitre les essais isostatiques et hyperstatiques: d'où quatre paragraphes.

On traitera d'abord des laminés bruts, puis percés, ensuite des poutres composées et enfin des poutres dissymétriques. On décrira d'abord les essais où le moment fléchissant joue le rôle principal, ensuite ceux où intervient l'effort tranchant, enfin

* Il pourrait être intéressant de préciser ce délai.

† Il serait intéressant de vérifier si l'approvisionnement des laminés sur parcs améliore leurs qualités élastiques.

on s'attachera aux phénomènes d'instabilité. On insistera sur le processus de chargement.

Ces considérations ont amené à prévoir systématiquement dix sections dans chacun des quatre paragraphes envisagés, avec pour les systèmes hyperstatiques une subdivision supplémentaire des sections en quatre sous-sections, afin de bien mettre en évidence les conditions d'appui. De nombreuses réponses "Néant" font mieux ressortir les lacunes des recherches actuelles, ainsi qu'il ressort du tableau schématique ci-joint.

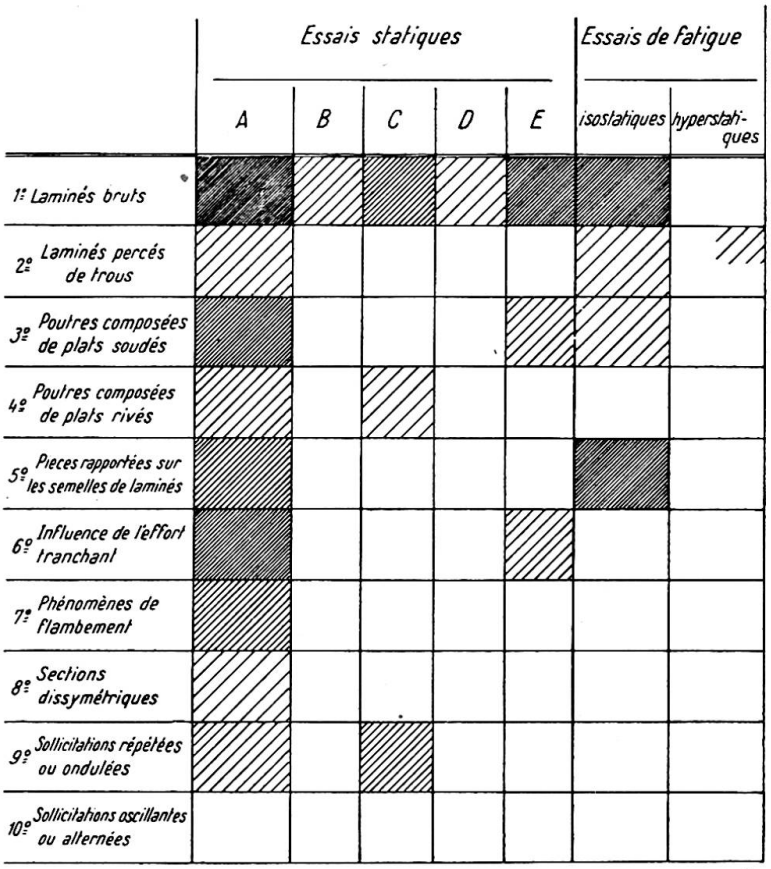

Tableau Schématique

Suivant Dutheil* nous distinguerons *l'adaptation dans la section* en comparant le moment de plastification vrai au moment calculé d'après la théorie élémentaire du matériau idéalement plastique que nous désignerons comme moment plastique théorique, de *l'adaptation entre sections* dans les systèmes hyperstatiques, en comparant les résultats à la théorie de l'égalisation des moments.

La quasi totalité des essais ont porté sur des laminés ou des poutres de petites dimensions. La prudence s'imposera quand on voudra généraliser aux poutres de grandes dimensions.

* *Annales de l'Institut Technique du Bâtiment et des Travaux Publics*—Théories et Méthodes de Calcul No. 2, janvier 1948: "L'exploitation du phénomène d'adaptation dans les ossatures en acier doux"; et *Ossature Métallique*, 3, 1949, p. 143.

SOUS-CHAPITRE I—ESSAIS STATIQUES

PARAGRAPHE 1: ESSAIS ISOSTATIQUES

1ère Section: Laminés bruts

On a étudié divers essais de Maier-Leibnitz; d'autres de Stüssi et Kollbrunner, Kazinczy, Hendry, Wilson, et Graf (aciers mi-durs) qui n'ont pas été tous poussés jusqu'à la ruine, chargements croissants ou par paliers et déchargements. A l'exception de l'essai de Wilson où la contrainte à la Navier a à peine dépassé la limite élastique, les autres montrent, comme nous l'avons trouvé au chapitre 1er, que le moment de ruine *dépasse nettement le moment plastique théorique*: un essai de Kollbrunner donne un dépassement de 32%.

2ème Section: Laminés percés de trous

On cite deux essais de la Chambre Syndicale des Constructeurs Métalliques Français où la section médiane était affaiblie par deux trous dans chaque semelle. Dans l'un les trous étaient *forés*; il y eut ruine plastique et peu de différence avec un laminé sans trou. Dans l'autre les trous étaient *poinçonnés sans alésage*. Il y eut cette fois *rupture, brutale*, dans la semelle tendue à partir d'un trou, avec cassure brillante; l'essai est donc plus défavorable.

Les contraintes à la Navier, calculées en section brute et en section nette sont données dans le tableau ci-après en kg./mm.^{2} où elles sont comparées aux limites de rupture R de l'acier des semelles tendues.

Trous	Section	1er I (très doux)	2ème I (assez dur)	Ruine
forés	brute nette	28,8 ou 0,90R 41,2 ou 1,29R	35,8 ou 0,90R 51,2 ou 1,28R	Plastique
poinçonnés sans alésage	brute nette	28,0 ou 0,84R 40,0 ou 1,20R	31,5 ou 0,79R 45 ou 1,12R	Rupture brutale

3ème Section: Poutres composées de plats soudés

On a étudié: un essai de Kayser où la poutre a péri par voilement de l'âme et pour une contrainte à la Navier supérieure à la limite de rupture de l'acier des semelles (mais l'acier de l'âme était beaucoup plus dur); des essais de Hendry et des essais remarquables de Patton et Gorbunow sous chargements répétés cycliquement, avec ou non introduction de contraintes préalables.

Ces essais montrent que ces poutres se comportent aussi bien, sinon mieux, que des laminés bruts de même section et de même acier. Les contraintes préalables sont sans influence sur la valeur de ruine.

4ème Section: Poutres composées de plats rivés

On a noté un essai peu concluant de Kazinczy et un essai de la Chambre Syndicale des Constructeurs Métalliques Français sur deux poutres où les trous étaient *poinçonnés sans alésage* et où il y a eu *rupture, brutale*, de la semelle tendue à partir d'un trou de rivet.

Les contraintes à la Navier, en kg./mm.^{2}, calculées en section brute et en section nette, sont données dans le tableau ci-après et comparées aux limites de rupture R de l'acier des semelles tendues.

Section	1ère poutre	2ème poutre	Ruine
brute nette	28,8 ou 0,61R 39,2 ou 0,83R	30,8 ou 0,67R 42,0 ou 0,91R	Rupture brutale

Ces résultats paraissent inférieurs à ceux de poutres soudées ou d'I bruts.

5ème Section: Pièces rapportées sur des semelles de laminés

On cite quelques essais comparatifs de Bryla et Chmieloviec et un ensemble très remarquable d'essais de Wilson qui semblent marquer *l'influence défavorable de semelles additionnelles partielles* soudées et au contraire la supériorité des semelles additionnelles soudées de toute la longueur du profilé, les semelles rivées s'inscrivant entre les deux.

6ème Section: Influence de l'effort tranchant ou d'une petite portée ($L<6h$)

On cite deux essais de Kayser où la ruine est intervenue par *voilement de l'âme* sans que puisse intervenir une semelle additionnelle soudée, deux essais d'Albers sur poutre de 1,86 m. de haut où la ruine est également intervenue par *voilement de l'âme* malgré un délardage très important des semelles tendues, qui ont ainsi supporté des contraintes à la Navier considérables, un essai de Wilson et une série d'essais très intéressants d'Hendry à la suite desquels cet auteur a essayé de fixer des règles pratiques pour savoir quand faire intervenir l'effort tranchant; malheureusement il s'agissait de très petits laminés. Son étude pourrait servir utilement de base à des essais systématiques.

7ème Section: Phénomènes de flambement

On cite des essais systématiques, un peu spéciaux, d'Hendry, sur des cadres en forme de L à deux branches égales. L'auteur donne, dans la limite de ses essais, des règles pratiques intéressantes.

8ème Section: Sections dissymétriques

Patton et Gorbunow ont montré que la théorie habituelle de l'adaptation dans la section s'appliquait parfaitement aux sections dissymétriques en essayant des profilés en Π composés de plats soudés ou des profils en caissons avec appendices longitudinaux soudés. Sollicitations ondulées.

La ruine, plastique, intervient pour des contraintes à la Navier dépassant largement la limite élastique (1,81 et 1,54 fois).

Cependant Patton et Gorbunow, en vue d'éviter l'apparition de déformations élastiques trop importantes ou de déformations permanentes, prescrivent de vérifier que la contrainte à la Navier ne dépasse pas la limite élastique.

On pourrait sans doute aller plus loin, grâce à l'accommodation en utilisant la prédéformation.

Il semble qu'il y ait le plus grand intérêt, contrairement aux idées héritées des leçons de Navier, à utiliser en flexion des pièces dissymétriques. En théorie, à quantité de matière donnée, il serait préférable d'utiliser des pièces rectangulaires car les centres de gravité des sections comprimées et tendues sont alors les plus éloignées possible (bras de levier maximum); mais, pratiquement, compte tenu des phénomènes d'instabilité en compression, il faut s'orienter vers des sections dissymétriques en forme de T ou Π.

D'autant plus qu'à l'avenir la Construction Métallique va devoir utiliser largement les tôles minces et abandonner de nombreux laminés symétriques.

En particulier on pourrait renforcer commodément des ouvrages par des *appendices soudés* s'écartant le plus rapidement possible de la fibre neutre.

Il est *regrettable que ces expériences n'aient pas connu le retentissement qu'elles méritaient* et qu'elles n'aient pas été systématiquement poursuivies.

9ème Section: Sollicitation ondulées ou répétées

On a déjà mentionné, à diverses reprises, les essais de Patton et Gorbunow.

10ème Section: Sollicitations alternées ou oscillantes. Néant.

PARAGRAPHE 2: ESSAIS HYPERSTATIQUES

C'est ici qu'il a paru nécessaire de subdiviser chaque section en quatre sous-sections pour tenir compte des conditions spéciales d'hyperstaticité et étudier si la plastification débutait sous les points d'application des charges ou sur les appuis et comment se faisait l'égalisation des moments que postule la théorie élémentaire.

11ème Section: Laminés bruts

1ère sous-section—Poutres continues sur quatre appuis

L'analyse d'un essai bien connu de Maier-Leibnitz nous a conduit aux conclusions suivantes (voir fig. 10):

Dans une 1ère phase les phénomènes sont purement élastiques (jusqu'à $10T$; contrainte à la Navier en travée, 26,2 kg./mm.^{2}).

Une 2ème phase—de transition—de $10T$ à $11{,}2T$ correspond au début de la plastification de la section médiane (contrainte croissant de 26,2 à 29 kg./mm.^{2}). Elle est caractérisée par la formation d'un jarret permanent sous la charge.

Une 3ème phase—de $11{,}2T$ à $17T$, qui correspond à l'accroissement linéaire du moment sur appuis, est marquée par la tendance, conforme à l'hypothèse classique, vers l'égalisation des moments en travée et sur appui. Cette égalisation se produirait pour la valeur du moment plastique *vrai.*

Mais cette égalisation ne peut se produire. Elle est entravée par l'apparition (à partir de $17T$) des phénomènes de plastification dans la section sur appui: contrainte à la Navier sur appui 23,3 kg./mm.^{2} pour une limite élastique des semelles voisine de 24–25 kg./mm.^{2} Cette plastification de la section sur appui, avec jarret, se poursuit difficilement; la section médiane est alors obligée de se plastifier à nouveau avec entrée dans le domaine de raffermissement de l'acier.* C'est la 4ème phase, qui s'achève par la ruine de la poutre à $20{,}7T$, caractérisée par l'apparition de nouveaux jarrets dans la travée médiane et même dans les travées extrêmes.

On note par rapport aux essais isostatiques les trois différences essentielles suivantes:

(*a*) il se forme *un jarret sous la charge* dès le début de la plastification de la section médiane;

(*b*) les sections sur appuis *éprouvent de la difficulté à se plastifier* complètement† il se forme également un jarret;

* C'est le seul cas, à notre connaissance, où le raffermissement ait été indubitablement observé.

† Il est probable que la surplastification de la section médiane, avec raffermissement, est plus facile que la plastification des sections sur appui. Il n'est pas exclu que le contraire se produise dans d'autres conditions d'essai.

(*c*) la section médiane est contrainte d'entrer *dans le domaine de raffermissement.**

L'essai, bien connu lui-aussi, de Stüssi et Kollbrunner, confirme cette analyse. Nous pensons toutefois que la charge de ruine est supérieure à celle que propose Stüssi à cause du dépassement de fait du moment plastique théorique dans la section.

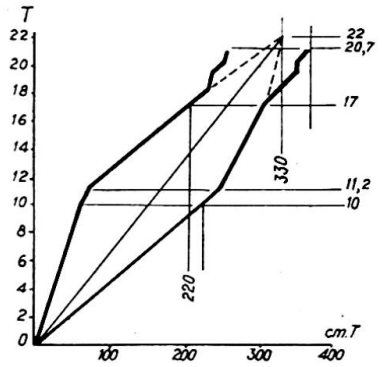

Fig. 10

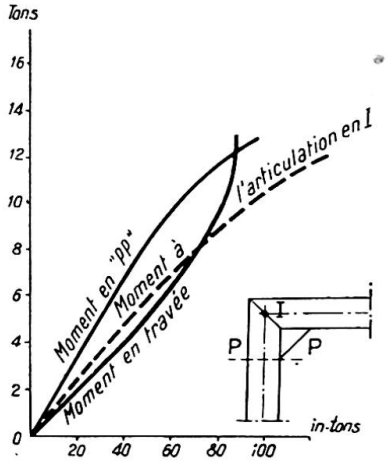

Fig. 11 (Portique A2)

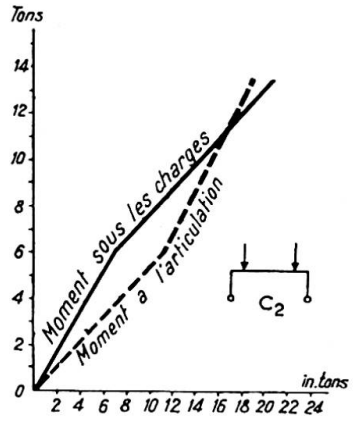

Fig. 12

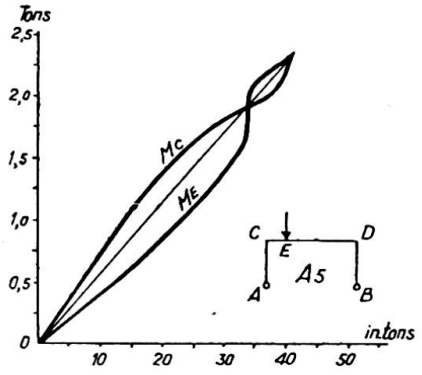

Fig. 13

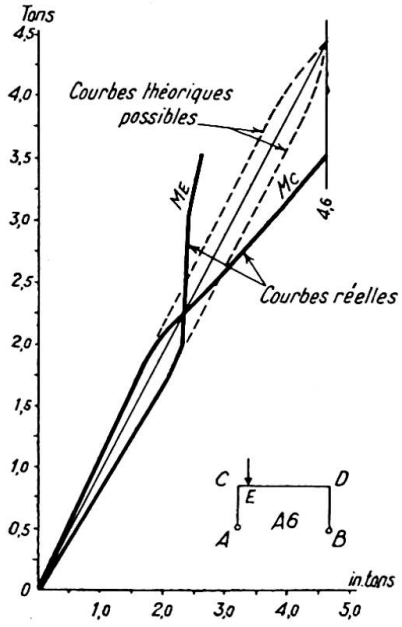

Fig. 14

* Il est probable que la surplastification de la section médiane, avec raffermissement, est plus facile que la plastification des sections sur appui. Il n'est pas exclu que le contraire se produise dans d'autres conditions d'essai.

2ème sous-section—Poutres continues sur trois appuis

On cite des essais de Maier-Leibnitz, Hartmann et Patton et Gorbunow qui systématiquement montrent un dépassement de la charge calculée (à cause, semble-t-il, d'une mauvaise estimation du moment plastique vrai dans la section) et la non influence sur la ruine d'une quelconque dénivellation d'appui. Par contre la succession des plastifications a rarement suivi la théorie élémentaire.

3ème sous-section—Poutres encastrées

On ne cite qu'un essai de Maier-Leibnitz pour lequel on peut répéter sensiblement ce qui a été dit à la 1ère sous-section quoique l'égalisation ait failli ici être parfaite.

4ème sous-section—Portiques

La question semble avoir particulièrement attiré les Britanniques. On cite plusieurs séries d'essais d'Hendry. Dans l'un—voir fig. 11—on trouve *une égalisation des moments avant la ruine* pour laquelle le moment du genou dépassait notablement le moment sous la charge.

Conclusions pour la 11ème section

Il semble qu'on peut conclure comme suit:

A condition de compter avec les moments de plastification *vrais*, la théorie de l'égalisation des moments est vérifiée dans les portiques (hyperstaticité interne); elle ne l'est pas entièrement dans les poutres continues (hyperstaticité extérieure): dans ce cas il se forme des jarrets dès le début de la plastification d'une section.

12ème Section: Laminés percés de trous. Néant.

13ème Section: Poutres composées de plats soudés

On cite une série d'essais de portiques dus à Hendry pour lesquels la ruine est intervenue au moment de l'égalisation des moments pour la valeur du moment plastique *vrai.*

14ème Section: Poutres composées de plats rivés

On ne peut citer qu'un essai de Kazinczy avec poutre continue sur trois appuis mais pour lequel on manque par trop d'éléments de détails.

15ème Section: Pièces rapportées sur les semelles des laminés. Néant.

16ème Section: Influence de l'effort tranchant

On cite plusieurs séries d'essais de portiques, dus à Hendry, dont quelques résultats sont représentés aux figs. 12, 13 et 14. Elles montrent:

fig. 12, des variations linéaires des diagrammes: charges-moments;
fig. 13, un huit fermé, c'est-à-dire ruine par égalisation des moments après une égalisation préalable;
fig. 14, un cas où la charge étant très près du genou, le moment sous la charge n'a pas pu se développer complètement et où la ruine est intervenue quand le moment du genou a atteint la valeur du moment plastique vrai dans la section.

17ème et 18ème Sections: Phénomènes de flambement et sections dissymétriques. Néant.

19ème et 20ème Sections: Sollicitations cycliques

On aborde un point *capital* concernant l'adaptation de plasticité dans les poutres hyperstatiques *quand les charges sont variables ou mobiles*: Il s'agit du problème du "cumul des déformations plastiques" analogue à celui que nous avons traité dans le chapitre 1er avec les essais de la 4ème série.

Un examen serré de la proposition théorique bien connue de Hans Bleich nous a conduit aux conclusions suivantes:

La méthode de H. Bleich tend à améliorer le procédé de l'égalisation des moments élastiques; en fait cela ne doit être possible que dans certaines conditions qu'il reste à préciser. Il faut distinguer au moins deux cas:

1° La disposition des travées et des charges est telle que l'intervention des contraintes résiduelles les plus favorables modifie peu l'égalisation des moments selon la méthode habituelle: autrement dit les moments aux points les plus chargés, calculés en élasticité, sont très voisins.

Dans ces conditions il est probable qu'on atteindra assez aisément un état voisin de l'égalisation des moments plastiques vrais, cela dépendra d'une part, comme on l'a vu dans les essais des 11ème et 13ème sections, des répartitions de travées et d'autre part de l'étendue du domaine dans lequel les moments ondulent.

2° Au contraire les moments aux points les plus chargés sont assez différents pour que les contraintes résiduelles de H. Bleich modifient assez sensiblement l'égalisation habituelle. Dans ce cas, on peut concevoir que le point le plus chargé se plastifiera entièrement avant que n'intervienne la plastification de soulagement d'un point moins chargé, sauf pour les sections à grand coefficient de forme (marge de plastification élevée). Autrement dit l'égalisation envisagée ne se produira probablement pas pour des sections telles que I ou H et il y aura sans doute ruine par divergence des déformations pour des valeurs des charges plus faibles que celles calculées. Au contraire pour des sections à grand coefficient de forme on tendra vraisemblablement vers l'égalisation des moments plastiques vrais et les valeurs calculées seront sans doute dépassées. *De nombreux paramètres sont susceptibles d'intervenir et, a priori, la question n'est pas simple à résoudre.*

Le 1° est sensiblement confirmé par un essai de Klöppel où la valeur de Bleich a été dépassée d'au moins 35%; le 2° par des essais de la Chambre Syndicale des Constructeurs Métalliques Français destinés à vérifier une théorie corrective due à Dutheil.

Le tableau, ci-après, donne en fonction des valeurs des limites élastiques de l'acier des profilés:

colonne 2: les valeurs du moment élastique, en cm. T;

colonnes 3, 4, 5: les valeurs théoriques, en T, des charges pour lesquelles le moment sur appui égalerait: le moment élastique, le moment critique de Dutheil,* le moment plastique théorique;

colonnes 6, 7, 8: les valeurs théoriques, en T, des charges donnant l'égalisation, dans le cas de charge le plus défavorable, des moments sur appuis et sous la charge fixe avec: le moment élastique, le moment de Dutheil, le moment plastique théorique;

colonnes 9, 10: les valeurs théoriques, en T, des charges donnant l'égalisation des valeurs extrêmes des moments sur appui et sous la charge fixe avec: le moment élastique (méthode de H. Bleich), le moment critique de Dutheil (méthode Bleich corrigée par Dutheil);

* Le moment critique de Dutheil est le moment élastique majoré d'un coefficient de forme égal à 1,20; 1,425; 1,10 et 1,10 respectivement.

colonne 11: les valeurs expérimentales, en T, de la charge marquant la fin du domaine de proportionnalité.

colonnes 12, 13: les valeurs expérimentales, en T, des charges pour lesquelles la divergence semble s'être produite; d'après l'estimation du Laboratoire et d'après la nôtre.

1	2	3	4	5	6	7	8	9	10	11	12	13
■ recuit .	249,1	10,7	12,9	16,1	15,5	18,6	23,3	12,2	14,6	11	18	17
◆ recuit .	173,7	7,5	10,7	15,0	10,8	15,4	21,6	8,6	12,1	12,5	17	15
H . .	238,0	10,2	11,3	11,9	14,8	16,3	17,2	11,7	21,8	9	11,5	10
H recuit .	227,7	9,8	10,8	11,4	14,2	15,6	16,5	11,2	12,3	9,5	11,0	10

On voit qu'au point de vue des premières plastifications les prévisions de la colonne 3 ne sont pas (sauf pour le losange) trop éloignées de la réalité, par excès pour les H comme souvent déjà vu.

Au point de vue de la ruine par divergence on voit nettement apparaître les deux groupes que la discussion laissait prévoir:

(*a*) Pour les H, les charges sont très voisines de celles pour lesquelles le moment sur appuis égale le moment élastique ou le moment critique de Dutheil (cols. 3 ou 4) et légèrement *inférieures* au calcul de Bleich (col. 9).

(*b*) Pour le carré et le losange, au contraire, les charges sont voisines de celles pour lesquelles le moment sur appui est égal au moment plastique théorique (col. 5) et *très supérieures* aux calculs de Bleich ou de Dutheil (cols. 9 ou 10): cela tient évidemment à l'énorme réserve de plastification.

En conclusion, pour les cas de la pratique, tels que I et H, on voit qu'ici le calcul de Bleich est probablement trop optimiste, alors que dans l'exemple de Klöppel il était excessivement pessimiste.

La question est donc bien aussi compliquée que notre raisonnement permettait de l'envisager: *il faut tenir compte de la forme des sections*, de la *répartition des travées*, de la *position des charges et des rapports entre les valeurs des différentes charges.*

Il est souhaitable que de nombreuses expériences soient systématiquement entreprises.

Sous-chapitre II—Essais de fatigue

On ne trouve que des essais de Graf et de Wilson plus un essai de la Chambre Syndicale des Constructeurs Métalliques Français sur un assemblage par soudure bout à bout.

A part les essais isostatiques sur laminés bruts où l'auteur allemand n'a obtenu qu'une ruine plastique tandis que l'auteur américain obtenait des ruptures, les autres essais sont complémentaires et laissent beaucoup de lacunes. Les expériences les plus complètes sont celles de Wilson sur des semelles additionnelles soudées sur des laminés: il nous semble que l'on peut en tirer confirmation de la supériorité de semelles additionnelles de toute la longueur du laminé soudées par cordons continus d'une part, et de l'infériorité de plaquettes ou de semelles partielles soudées ainsi que de soudures sur des zones tendues, d'autre part.

Pour le reste les limites d'endurance, par exemple à 2 millions de répétitions, présentent une telle dispersion des valeurs qu'il est difficile, en l'état actuel, de tirer de conclusions nettes. Tout ce qu'on peut affirmer c'est que, dès qu'il y a une entaille

quelconque, la ruine survient par *rupture* et pour des valeurs des contraintes à la Navier *nettement inférieures* à la limite élastique de l'acier utilisé. On ne peut plus dès lors envisager, à proprement parler, de théorie de l'adaptation en flexion basée sur la plastification.

CHAPITRE III—CONCLUSIONS

On traitera d'abord des points qui paraissent acquis, ensuite de ceux qui prêtent encore à discussion ou n'ont pas été suffisamment traités.

1ÈRE PARTIE—POINTS ACQUIS

Si l'on met à part les essais de fatigue sur poutres présentant des entailles (le mot étant pris ici au sens le plus large) pour lesquelles l'adaptation de plastification ne semble pas jouer au sens où l'on entend généralement ces termes, les essais français et etrangers analysés aux chapitres II et III permettent de tirer les conclusions suivantes, en distinguant par nature de poutres:

1° *Laminés bruts*

(*a*) La plastification commence pour des valeurs des contraintes à la Navier inférieures à la limite élastique. Ceci n'empêche pas le laminé de se comporter élastiquement une fois la déformation permanente acquise et stabilisée; dans les poutres continues cette déformation se manifeste par des jarrets sous les charges ou sur les appuis.

(*b*) Si les précautions sont prises pour éviter les flambements locaux des semelles et des âmes comprimées et s'il n'existe pas de fortes charges concentrées à proximité d'appuis, la ruine intervient par plastification totale. Le moment atteint dans la section la plus exposée, ou moment plastique vrai, dépasse de plusieurs pour cent (10 à 20 en moyenne) le moment calculé d'après la théorie élémentaire du matériau idéalement plastique.

(*c*) Dans les systèmes hyperstatiques les moments sous les points les plus chargés et sur les appuis ou les genoux ont bien tendance à s'égaliser, la valeur commune étant celle du moment plastique vrai. Cette égalisation peut être atteinte dans les portiques; elle l'est rarement d'une manière parfaite dans les poutres continues: il y a là des circonstances défavorables dues probablement aux appuis. Enfin dans les cas de sollicitations conduisant au cumul des rotations plastiques, il n'est pas exclu que, dans certaines circonstances encore mal connues, la ruine survienne, par divergence des déformations, pour des valeurs relativement faibles.

(*d*) En définitive il semble qu'au regard des questions de sécurité les contraintes maxima réglementaires pourraient être fixées à des valeurs élevées dépendant:

de la dispersion des valeurs des limites élastiques conventionnelles (et non des limites de rupture) en différents points des laminés,
de la forme des sections,
éventuellement de la taille des laminés,
de l'isostaticité ou de l'hyperstaticité du système (poutres continues ou portiques),
dans certains cas de la nature des sollicitations (par exemple possibilité du cumul des rotations plastiques dans les systèmes hyperstatiques).

Des dispositions constructives appropriées, variables avec la taille des laminés, telles que raidisseurs dans les zones comprimées, devraient alors être prises pour éviter des flambements locaux des semelles et des âmes comprimées.

2° *Poutres composées de tronçons de laminés bruts assemblés par soudure bout à bout*

Si les soudures sont convenables et le mode de soudage approprié, il semble que de telles poutres peuvent être utilisées exactement comme des laminés bruts.

Celà est bien net dans les systèmes isostatiques. Les essais manquent dans les systèmes hyperstatiques; il semble toutefois que les conclusions peuvent être étendues dans ce cas à condition de ne pas disposer les soudures sur les appuis. Telle est, du moins, la tendance française: elle ne semble pas être générale à l'etranger.

3° *Poutres, à profil constant, composées de plats assemblés par soudures longitudinales continues*

Compte tenu du nombre limité d'essais probants il semble que les conclusions du 1° (laminés bruts) peuvent être également adoptées, tout au moins dans les systèmes isostatiques.

Toutefois ici le moment plastique vrai dans la section est sensiblement égal au moment calculé d'après la théorie du matériau idéalement plastique.

4° *Laminés percés de trous, poutres chaudronnées (rivées), laminés complétés par des semelles additionnelles rivées*

Il n'existe pas d'essais hyperstatiques. En isostatique la question n'est pas encore suffisamment éclaircie pour permettre des conclusions nettes. Sauf les cas bien précisés où les trous étaient poinçonnés sans alésage et où la ruine a été provoquée par une rupture brutale, il semble que l'adaptation de plastification joue; mais les domaines d'utilisation restent à préciser.

5° *Poutres composées de plats soudés et laminés complétés par des semelles additionnelles soudées*

La question est loin d'être éclaircie.

Il semble bien que le seul cas net soit celui où, en isostatique, ces semelles ont la longueur totale du laminé: la plastification est alors intégrale. Au contraire les semelles de longueur partielle semblent être nettement défavorables: celà dépend de plusieurs facteurs qui sont mal précisés.

2ème Partie—Questions restant à résoudre

En plus des points de la 1ère partie encore mal précisés on aura remarqué que de nombreux points restent à étudier, tels que:

l'influence de l'effort tranchant,
les phénomènes de flambement,*
l'influence du temps sur certaines accommodations élastiques,
le cumul des déformations plastiques dans les poutres continues.

De nombreux essais n'ont même pas été tentés. La plastification des sections dissymétriques n'a été réalisée qu'une seule fois. Il n'y a pas d'essais avec semelle partielle soudée sur un seul côté, soit tendu, soit comprimé. Il n'y a jamais eu d'essais de fatigue commencés par une plastification lente: ces essais seraient pourtant de première utilité pour essayer de résoudre le conflit qui oppose les écoles opposées affirmant ou niant l'existence des phénomènes de fatigue dans les ponts et dans les charpentes métalliques, sans que les arguments avancés de part et d'autre soient réellement convaincants.

* A cet égard les nouvelles recherches théoriques et expérimentales de Stüssi sur le flambement des plaques seront sans doute du plus grand secours.

Enfin l'essai le plus intéressant à réaliser, malgré son évidente difficulté, celui de poutres continues sous charges roulantes: ici intervient au minimum les phénomènes hyperstatiques, le cumul des déformations plastiques, l'influence de l'effort tranchant.

En conclusion il apparaît qu'il reste de nombreux essais systématiques à entreprendre. La tâche dépasse les possibilités d'un seul organisme ou d'un seul pays. C'est pourquoi nous souhaiterions qu'à l'issue de la discussion du Thème AI3 de ce Congrès, une sous-commission établisse un vaste programme de recherches (basé ou non sur la classification adoptée dans le cours du présent mémoire) et le répartisse entre les Membres de notre Association. Rendez-vous serait pris dans quatre ans, au prochain Congrès, pour tirer les conclusions.

Nous insistons sur la nécessité de détailler minutieusement les circonstances de chaque expérience.

BIBLIOGRAPHIE

ALBERS. *Stahlbau*, 9.6.1939.
BAKER, J. F. *J. Inst. Civ. Engrs.*, **31**, No. 3, 1948–49.
The Structural Engineer, **27**, No. 10, 1949.
BLEICH, F. *Ossature Métallique*, février 1934.
BLEICH, H. *Bauingenieur*, 1932, p. 161.
BRYLA et CHMIELOWIEC. Congrès de Berlin, Rapport final, 1938, pp. 561 et 766.
DAWANCE. *Annales de l'I.T.B.T.P.* (Institut Technique du Bâtiment et des Travaux Publics), Construction Métallique No. 6, mai 1950.
DUTHEIL. *Annales de l'I.T.B.T.P.*, Théories et Méthodes de Calcul No. 2, janvier 1948.
Ossature Métallique, 1949, No. 3, p. 143.
GRAF. *Stahlbau*, 26.10.1934, 24.4.1936 et 15.1.1937.
Bauingenieur, 16.9.1938 et 5.2.1942.
HARTMANN. *Schweizerische Bauzeitung*, 18.2.1933.
HENDRY. *The Structural Engineer*, octobre et décembre 1950.
KAYSER. *Stahlbau*, 26.2.1937.
KAZINCZY. Congrès de Berlin, Rapport final, 1938, p. 56.
KLÖPPEL. Congrès de Berlin, Rapport final, 1938, p. 77.
LAZARD, A. *Mémoires de l'A.I.P.C.*, **X**, p. 101.
Travaux, mai 1950; novembre et décembre 1951.
LEVI, R. Congrès de Berlin, Publication préliminaire, 1936, p. 81.
MAIER-LEIBNITZ. *Bautechnik*, 1928, cahiers 1 et 2 (pp. 11 et 27).
Stahlbau, 25.9.1936.
Congrès de Berlin, Publication préliminaire, p. 101.
Congrès de Berlin, Rapport final, p. 70.
PATTON et GORBUNOW. *Stahlbau*, 3.1.1936.
SCHREINER. *Stahlbau*, 30.9.1938.
STÜSSI et KOLLBRUNNER. *Bautechnik*, 17.5.1935.
Congrès de Berlin, Publication préliminaire, 1936, p. 121.
Congrès de Berlin, Rapport final, 1938, p. 74.
WILSON. Bulletin 377 de la Station Expérimentale de l'Illinois, 22.1.1948.

Résumé

Se basant sur les derniers essais français sur des laminés bruts I et H de différentes tailles sollicités isostatiquement jusqu'à la ruine dans des conditions très diverses, et étudiant la dispersion des aciers, les contraintes préalables, la non-conservation des sections planes, l'importance des volumes plastifiés, l'existence de compressions transversales, le flambement des zones comprimées, l'article conclut que, pour des laminés bruts sollicités isostatiquement:

la ruine plastique survient, si les précautions nécessaires sont prises contre le flambement, pour une valeur supérieure à celle qu'on peut calculer en admettant la plastification totale d'un acier idéalement plastique;

le laminé s'accommode élastiquement après un nombre très faible de répétitions des sollicitations. Il est possible d'en déduire un procédé systématique de prédéformation en vue de travailler sous contraintes élevées. A ce sujet le temps semble jouer un rôle important mais encore mal défini.

Elevant le débat à toutes les poutres à âme pleine en acier doux et passant en revue les essais antérieurs généralement exécutés sur petits échantillons, l'article cherche à distinguer les points définitivement acquis de ceux qui prêtent à discussion ou n'ont pas encore été suffisamment traités. Parmi ces derniers on relève plus particulièrement:

l'effet de l'effort tranchant,
l'effet des surcharges roulantes sur poutres continues,
les études sur profils dissymétriques.

En conclusion l'article propose qu'une sous-commission du Congrès dresse un programme des essais restant à réaliser et les répartisse entre les divers membres de l'Association Internationale.

Summary

Based on the latest French tests with plain rolled I and H joists of various sizes, isostatically loaded up to failure under very different conditions, and by studying the dispersion of the steel, the residual stresses, the non-conservation of plane sections, the size of the plastified volumes, the existence of transverse compressions and the buckling of the compressed zones, the author of the paper comes to the conclusion that, for plain rolled joists isostatically loaded:

if the required precautions against buckling are taken, plastic failure happens for a load which is higher than that which can be calculated by supposing the total plastification of an ideally plastic steel;

the rolled joist adapts itself flexibly after very few repetitions of the loads. It is possible from this fact to deduce a method of systematic prestraining in order to work under high stresses. Time seems here to play a part which is important but has not yet been clearly defined.

By extending the discussion to all plate-web girders in mild steel and by surveying previous tests which generally were made on joists of small cross-section, this paper tries to distinguish the points which are definitively established from those which are still disputable or have not yet been sufficiently treated.

Among the latter, particular emphasis is put on:

the effect of shearing-stress,
the effect of rolling loads on continuous girders,
the studies on unsymmetrical sections.

It is finally proposed that a sub-committee of the Congress should assume the task of establishing a programme for the tests which are still to be made and allotting these to different members of the International Association.

Zusammenfassung

Der Aufsatz stützt sich auf die neuesten französischen Versuche an unbearbeiteten normalen und Breitflansch-I-Walzträgern unterschiedlicher Grösse, die bei statisch

bestimmter Anordnung unter sehr verschiedenen Bedingungen bis zum Versagen beansprucht wurden und untersucht die Streuungen in der Stahl-Qualität, die inneren Spannungen, das Nicht-Ebenbleiben der Querschnitte, das Ausmass der plastifizierten Querschnittsteile, das Auftreten von Quer-Kontraktionen und das Ausknicken der Druckzonen. Für statisch beanspruchte und statisch bestimmt gelagerte unbearbeitete Walzträger kommt der Verfasser zu den nachstehenden Schlussfolgerungen:

Wenn die notwendigen Vorkehrungen gegen Ausknicken getroffen sind, tritt das plastische Versagen für einen Wert ein, der höher ist als derjenige, den man unter der Voraussetzung totaler Plastifizierung eines ideal-plastischen Stahles errechnen kann.

Der Träger erfährt nach einer sehr geringen Zahl wiederholter Beanspruchungen eine elastische Anpassung. Daraus kann ein systematisches Vorverformungs-Verfahren zwecks Zulassung höherer Nutzspannungen abgeleitet werden. In diesem Zusammenhang scheint der Faktor Zeit eine wichtige, aber noch ungenau definierte Rolle zu spielen.

Durch Erweiterung der Diskussion auf sämtliche Vollwandträger aus Flusstahl und an Hand eines Überblicks über die früheren, hauptsächlich an kleinen Probeträgern durchgeführten Versuche wird versucht, die endgültig gelösten Fragen von denjenigen zu trennen, die noch umstritten oder ungenügend untersucht sind. Unter den letzteren werden insbesondere erwähnt:

der Einfluss der Querkraft,
der Einfluss der beweglichen Lasten auf durchlaufende Träger,
die Untersuchung unsymmetrischer Profile.

Als Schlussfolgerung schlägt der Verfasser vor, dass ein Unter-Ausschuss des Kongresses ein Programm der noch durchzuführenden Versuche aufstellen und diese unter verschiedene Mitglieder der Internationalen Vereinigung verteilen soll.

Leere Seite
Blank page
Page vide

AI 3

Experimental investigations into the behaviour of continuous and fixed-ended beams

Recherches expérimentales sur le comportement des poutres continues ou encastrées à leur extrémités

Experimentelle Untersuchungen über das Verhalten durchlaufender und eingespannter Balken

M. R. HORNE, M.A., Ph.D., A.M.I.C.E.
Cambridge University

1. Introduction

The behaviour beyond the elastic limit of mild-steel beams subjected to pure bending moments or bending moments combined with shear forces has been studied by Ewing (1903), Robertson and Cook (1913) and many others. The various theories suggested and the experimental evidence relating to them have been reviewed by Roderick and Phillipps (1949). It appears that, when considering annealed beams, the most satisfactory theory is that in which it is assumed that initially plane sections remain plane during bending, the longitudinal stress being related to the longitudinal strain as in a tension or compression test (see Roderick, 1948). Good correlation between bending and tension tests may be obtained if due regard is paid to the upper yield stress and to the rate of straining in the plastic range. The influence of shear forces has been investigated experimentally by Baker and Roderick (1940) and Hendry (1950) and theoretically by Horne (1951). It has been shown that, for practical purposes, shear forces have negligible effect on the behaviour of a beam. The stress distributions are also modified in the vicinity of concentrated loads, and this has been investigated experimentally by Roderick and Phillipps (1949) and theoretically by Heyman (unpublished). The simple plastic theory has also been found to apply approximately to rolled steel sections (Maier-Leibnitz, 1936), although correlation between bending and tension tests is here more difficult due to the variation in properties of the steel over any cross-section.

The simple plastic theory leads to important deductions regarding the behaviour of continuous and fixed-ended beams and rigid-jointed unbraced structures such as building frames. Due to the considerable pure plastic deformation which mild steel

can undergo (of the order of 1 % strain, or ten times the strain at the commencement of yield), the curvature of the longitudinal centre line of an initially straight beam increases rapidly with practically no increase of bending moment as the section becomes fully plastic. The bending moment then approaches the "full plastic" value (see Roderick, 1948), and although at extremely high curvatures the beam may develop a higher moment of resistance due to strain hardening, the full plastic moment may be regarded as the highest moment to which the beam may be subjected and still retain its usefulness. When beams are continuous over a number of supports or *encastré* (i.e. fixed in position and direction at their ends), the high curvature which occurs in the vicinity of fully plastic sections enables the applied loads to be increased until the full plastic moment is reached at a sufficient number of sections for a "mechanism" to be formed, these sections being regarded as "hinges" with constant moments of resistance. Similar considerations apply to rigid-jointed unbraced frames as long as axial forces are small enough to have negligible effect on the bending moments in the members in which they occur. The application of such results to the calculation of collapse loads has been considered extensively by Bleich (1932), Baker (1949), Neal and Symonds (1950), Horne (1950) and others.

The above theoretical developments have been achieved by making certain extensions of the simple plastic theory as established by tests on simply supported members. The "plastic hinge" concept is only an approximation to the truth, corresponding as it does to infinite curvature at the assumed fully plastic sections. It is thus essential that these theoretical deductions should be tested experimentally. In the case of continuous beams, the simple plastic theory indicates that the order in which the spans are loaded, or the sinking of one support relative to the others, should have no effect on the value of the collapse load. In beams partially fixed against rotation at the ends, the degree of end restraint should similarly have no effect on the collapse loads as long as the moment of resistance of the end supports is at least equal to the full plastic moment of resistance of the beam. Moreover, the fact that full plasticity has been produced at some section or sections of a beam for one set of loads should not reduce the carrying capacity of that beam for any subsequent set.

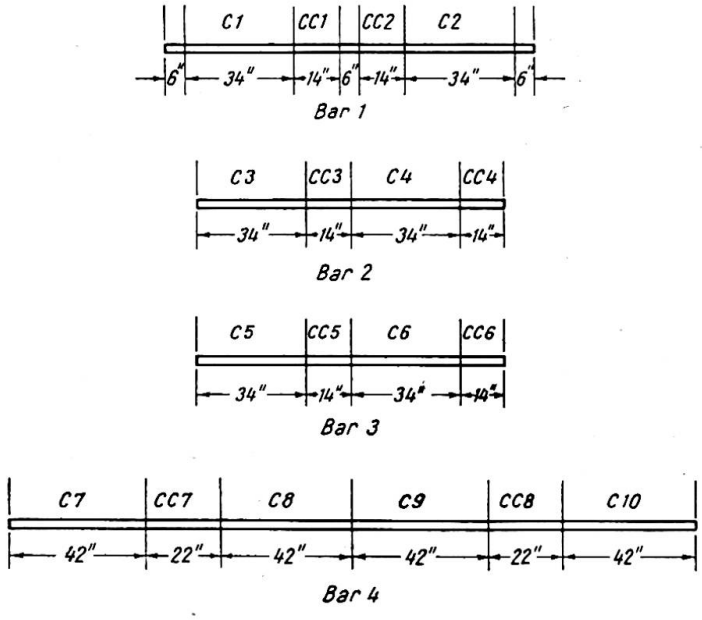

Fig. 1. Division of bars for continuous beam tests

While certain investigations on continuous beams have already been made by Maier-Leibnitz (1936) and Volterra (1943), no attempt to check these deductions systematically has yet been reported. It was for this reason that the investigations here described were undertaken.

2. Tests on continuous beams

(a) *Preparation of beams*

The beams were taken from 1-in. square bars of rolled mild steel in the "as received" condition, the bars being cut according to the scheme shown in fig. 1. All

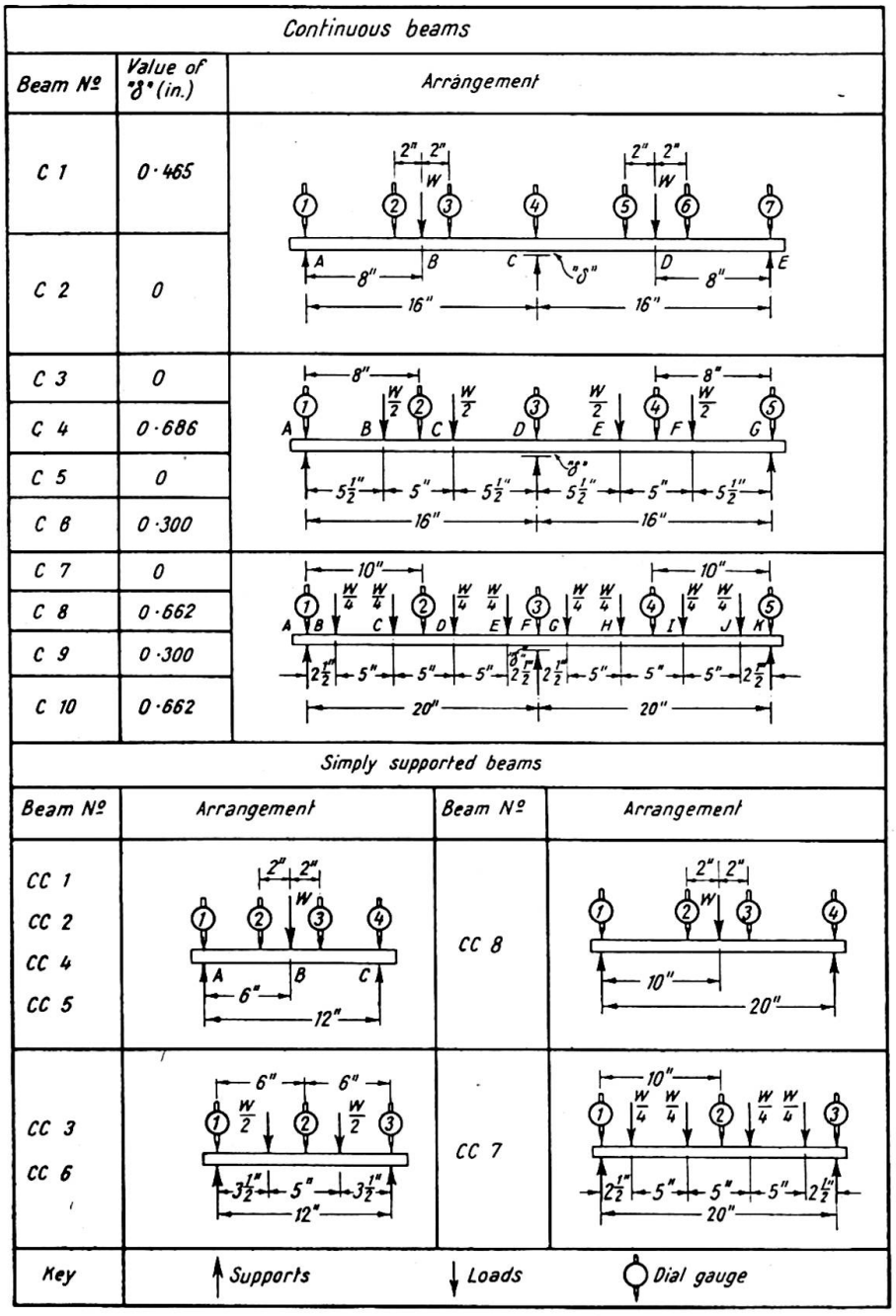

Fig. 2. Summary of continuous beam tests
(In beam CC8, for 2″ read 2½″)

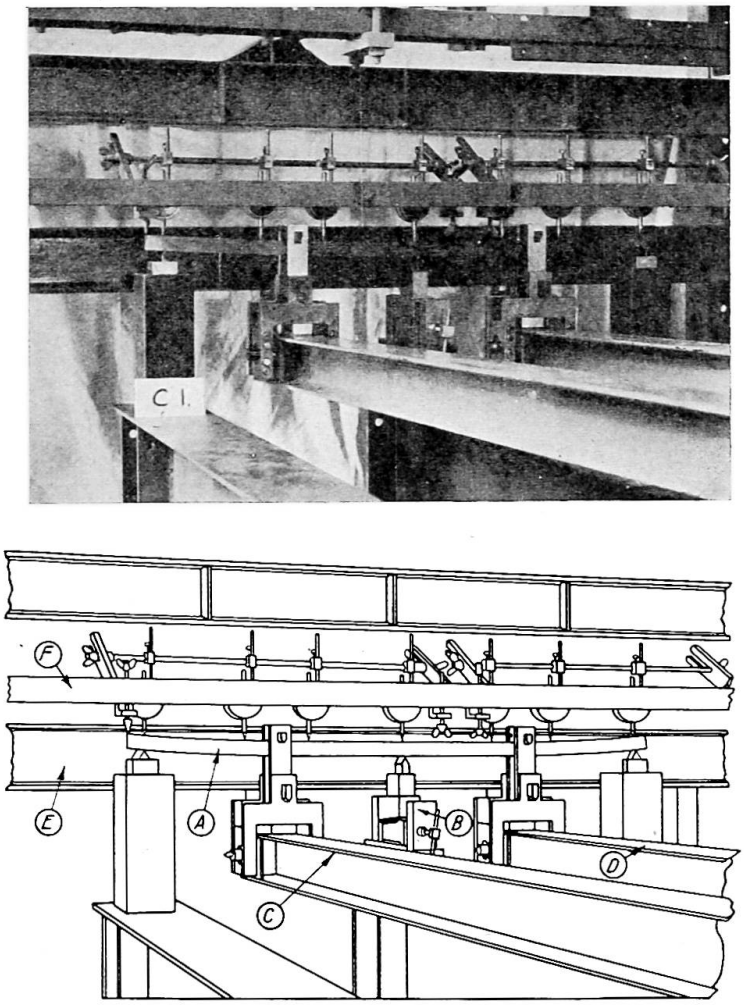

Fig. 3. Arrangement for testing continuous beams

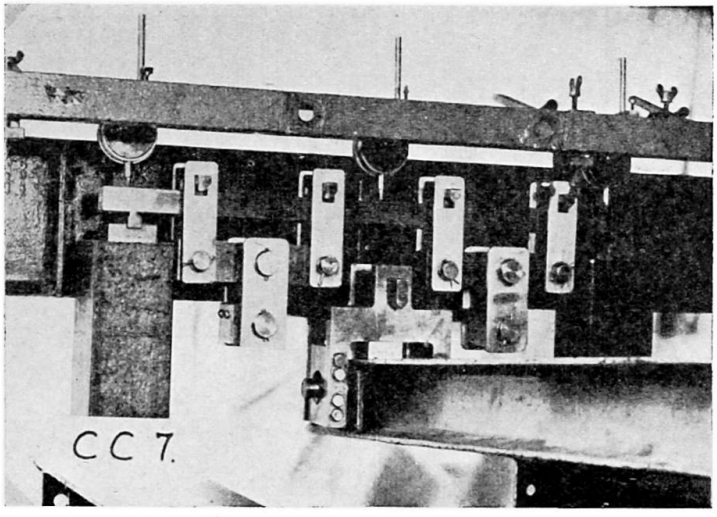

Fig. 4. Arrangement for testing simply supported beams

the beams were roughly planed to the required dimensions ($\frac{7}{8}$ in. square) and finished by surface grinding, thus imparting a polished surface which, as described below, enabled Lüders' wedges to be observed during the tests.

(b) *Description of tests*

The tests are summarised in fig. 2, which shows for each beam the positions of the supports, loads and dial gauges used to measure deflections. Some lengths were tested from each bar as continuous beams, while other lengths were tested as simply supported in order to obtain direct measurements of the full plastic moments. In some of the tests on the continuous beams, the central support was set a certain depth below the outer supports, and this is also indicated. Increasing loads were applied simultaneously to both spans of all the continuous beams except beam C5, in which span AD (see fig. 2) was loaded to collapse with only a small load on span DG. For all beams, when collapse had occurred in one span, the load on the other span was further increased until it also collapsed.

The tests were performed in a dead-load testing frame, a full description of which has been given by Baker and Roderick (1942). The arrangement for testing the continuous beam C1 is shown in fig. 3, in which A is the beam supported on knife-edges and B is a block by means of which it is possible to adjust the height of the central knife-edge. The load is applied by the levers C and D whose fulcra react against the member E, while the dial gauges for measuring deflections are supported on an independent frame of which F is a member. The simply supported beam CC7 was tested as shown in fig. 4, which also shows the linkage used to distribute the load from the lever equally to four knife-edges acting on the upper surface of the beam.

During the tests, as long as the beams remained elastic, finite increments of load were added at intervals of approximately two minutes, the dial gauges being read between each increment. After the first signs of creep had been observed, the addition of each load increment was delayed until no dial gauge showed a rate of increase greater than 10^{-4} in. per minute. Loading was continued until collapse occurred, this being characterised by a large increase of deflection for a small increase of load.

(c) *Test results*

The test results for all the beams are summarised in Table I, and are grouped according to the bar from which the beams were cut. The mean dimensions are given in columns 3 and 4. In the case of the simply supported beams, the values of the modulus of elasticity E calculated from the linear portions of the load deflection curves are given in column 5. The values of E quoted for the continuous beams are the mean of the values obtained for the simply supported beams cut from the same bar. Column 6 gives the collapse loads. In the case of the continuous beams, the mean of the values for the two spans is given; in no case did the difference between these values exceed 3·3%. Values of the full plastic moments may be deduced from the collapse loads by means of the simple plastic theory, giving the lower yield stresses quoted in column 7 of Table I. Assuming that each bar is of uniform material, the agreement between these stresses for beams cut from the same bar is a check on the accuracy of the simple plastic theory. The percentage variations of these yield stresses as compared with the average for the bar are given in column 9.

It has been shown by Heyman (to be published) that the assumption made in the simple plastic theory that there is no restraint in directions perpendicular to the longitudinal axis of a beam is invalidated in the vicinity of heavy load concentrations. This tends to increase the full plastic moment except where the maximum moment

TABLE I

	1	2	3	4	5	6	7	8	9	10	11	12
							Analysis by simple plastic theory ignoring the effect of load concentration			Analysis in which allowance is made for the effect of load concentration		
	Bar No.	Beam No.	Mean Width, in.	Mean Depth, in.	Estimated Modulus of Elasticity E, tons/in.^{2}	Load, tons	Lower Yield Stress, tons/in.^{2}	Mean Lower Yield Stress for bar, tons/in.^{2}	Per cent Difference	Lower Yield Stress, tons/in.^{2}	Mean Lower Yield Stress for bar, tons/in.^{2}	Per cent Difference
1	1	C1	0·875	0·876	13,360	1·125	17·83	18·02	−1·1	16·53	16·71	−1·1
2		C2	0·875	0·876	13,360	1·138	18·04		0·1	16·72		0·1
3		CC1	0·876	0·876	13,380	1·000	17·90		−0·7	16·59		−0·7
4		CC2	0·876	0·876	13,340	1·025	18·33		1·7	16·99		1·7
5	2	C3	0·875	0·875	13,120	1·560	19·03	18·34	3·8	17·96	17·48	2·7
6		C4	0·875	0·875	13,120	1·525	18·60		1·4	17·55		0·4
7		CC3	0·875	0·875	13,010	1·680	17·43		−5·0	17·43		−0·3
8		CC4	0·875	0·875	13,220	1·020	18·32		−0·1	16·98		−2·9
9	3	C5	0·875	0·875	12,930	1·225	14·93	14·91	0·1	14·09	14·21	−0·8
10		C6	0·875	0·874	12,930	1·230	15·01		0·7	14·16		−0·4
11		CC5	0·875	0·875	13,270	0·850	15·26		2·3	14·14		−0·5
12		CC6	0·875	0·875	12,590	1·380	14·44		−3·2	14·44		1·6
13	4	C7	0·875	0·876	12,945	1·670	18·13	17·84	1·6	16·46	16·60	−0·8
14		C8	0·876	0·875	12,945	1·670	18·12		1·6	16·45		−0·9
15		C9	0·876	0·876	12,945	1·650	17·92		0·4	16·27		−2·0
16		C10	0·876	0·876	12,945	1·700	18·38		3·0	16·69		0·5
17		CC7	0·875	0·875	13,060	1·150	17·16		−3·8	17·16		3·4
18		CC8	0·875	0·875	12,830	0·580	17·30		−3·0	16·54		−0·4

occurs uniformly over some length of the beam. This explains the lower than average yield stresses obtained for beams CC3, CC6 and CC7 (Table I, column 7). Roderick and Phillipps (1949) found that in their tests a satisfactory empirical allowance could be made for this effect by assuming that collapse was delayed until the full plastic moment had been reached at a section a distance away from the concentrated load equal to half the depth of the beam. The yield stresses for all the beams corresponding to this assumption are shown in column 10 of Table I, and the percentage variations from the mean values for separate bars are given in column 12.

There does not appear, from the figures given in columns 9 and 12 of Table I, to be any distinct advantage in accepting the complications introduced by Roderick and Phillipps. In either case the agreement is as good as could reasonably be expected, taking into account probable variations in yield stress in the bars. Ignoring signs, the mean values of the percentage variations given in columns 9 and 12 are 1·87 and 1·18 respectively. The application of the "t" test for the difference between means gives $t=1{\cdot}646$, corresponding to a probability of 0·12 that the difference between the means is due entirely to random causes. The improvement achieved with the second method of analysis, although discernible, is not therefore outstandingly significant. In their tests on simply supported beams, Roderick and Phillipps (1949) obtained much improved agreement by using this method, but it is to be noted that while these investigators tested carefully heat-treated beams, the tests here described were performed with the steel in the "as received" condition.

In a further attempt to decide between the two methods of analysis, tension tests were carried out on three specimens. Since the mean yield stresses given by the second method (column 11, Table I) are lower than those given by the first (column 8), it should thus be possible to reach some significant conclusion. The first two specimens (CT1 and CT2) were taken one from each end of beam C8, while the third (CT3) was taken from one end of beam C9. The specimens had a gauge length of 2·00 in. and a diameter of 0·282 in., and were tested in the Quinney Autographic Machine (see Quinney, 1938). The upper and lower yield stresses and the rates of strain in the plastic range are given in Table II. Calculations show that, during the

TABLE II

Tension Specimen	Upper Yield Stress, tons/in.^{2}	Lower Yield Stress, tons/in.^{2}	Rate of Strain in Plastic Range/sec. $10^{-6}\times$
CT1	22·48	17·99	18·20
CT2	19·53	17·32	0·767
CT3	22·31	18·16	18·20

beam tests, the mean rate of strain in the extreme fibres of the most highly stressed sections varied between $0{\cdot}7\times10^{-6}$ and $2{\cdot}0\times10^{-6}$ per sec. Hence the appropriate lower yield stress for bar 4 (see fig. 1) would be about 17·40 tons/in.^{2} Since the values obtained by the two methods of analysis were 17·84 and 16·60 tons/in.^{2} (columns 8 and 11 of Table I), the result is again inconclusive.

As an example of the load-deflection curves obtained, those for beams C1 and C2 are presented in figs. 5 and 6 respectively. In the case of beam C2, a theoretical load-deflection curve for dial gauges 3 and 5 has been calculated by means of the simple plastic theory, and is seen to be in good agreement with the observed values.

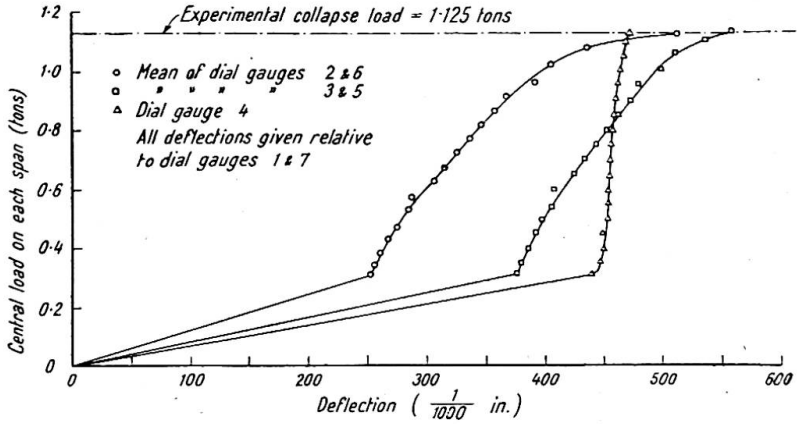

Fig. 5. Load-deflection curves for Beam C1

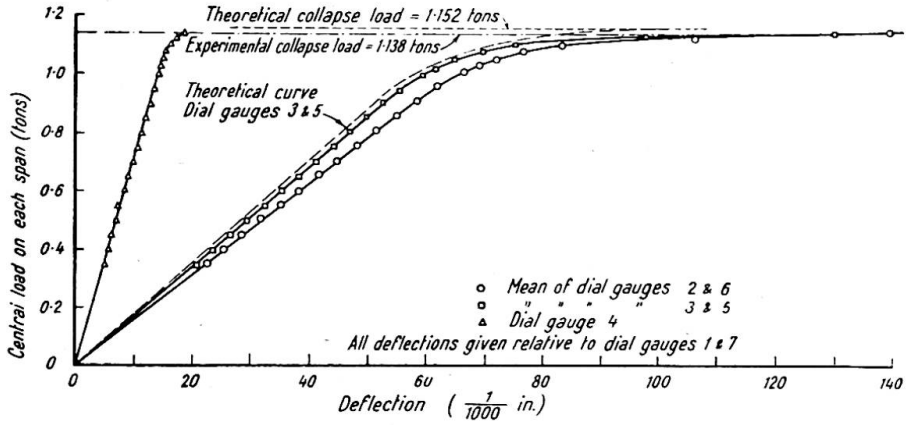

Fig. 6. Load-deflection curves for beam C2

In testing beams C1, C4, C8 and C10, the central support was set at such a distance below the outer supports that yield stress under a sagging bending moment was reached in the extreme fibres of the central section of the beam before contact occurred. As the loads on these beams were further increased, the central bending moment first decreased to zero and then increased until at collapse full plasticity under a hogging bending moment occurred over the central support. Simultaneously the position of the maximum sagging moment moved along the beam, as can be seen most clearly in the cases of beams C4 and C8. Thus in beam C4 (see fig. 2), a certain amount of yield under sagging moment occurred first at C and E, and finally at B and F, where full plastic moments developed at collapse. This may be traced in the appearance of Lüders' wedges on the side face of part of beam C4 after testing (fig. 7), in contrast to the absence of such wedges except at B and D on the face of beam C3, for which the supports were initially level. It will be observed from Table I that the sinking of the support and the occurrence of Lüders' wedges along the beam did not lead to any significant decrease in the carrying capacity of beam C4 as compared with beam C3. Similar remarks apply to beam C8, in which the maximum sagging moment moved first to sections E and G (see fig. 2), then to sections D and H, until finally full plastic moments were reached at collapse at

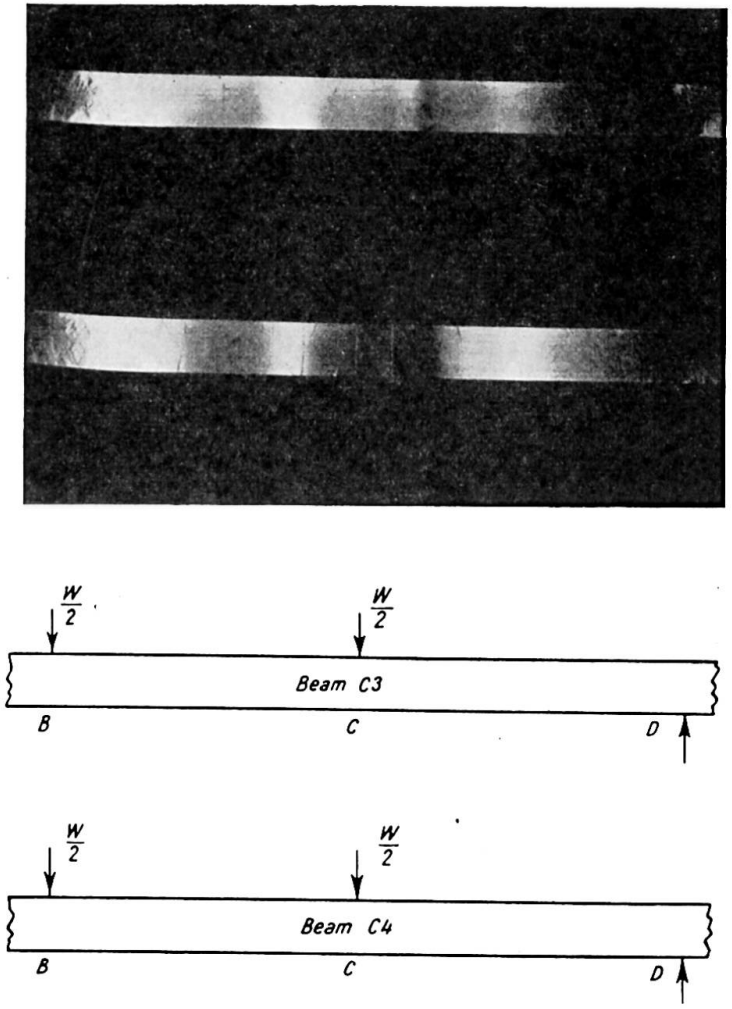

Fig. 7. Comparison of Lüders' wedges on beams C3 and C4

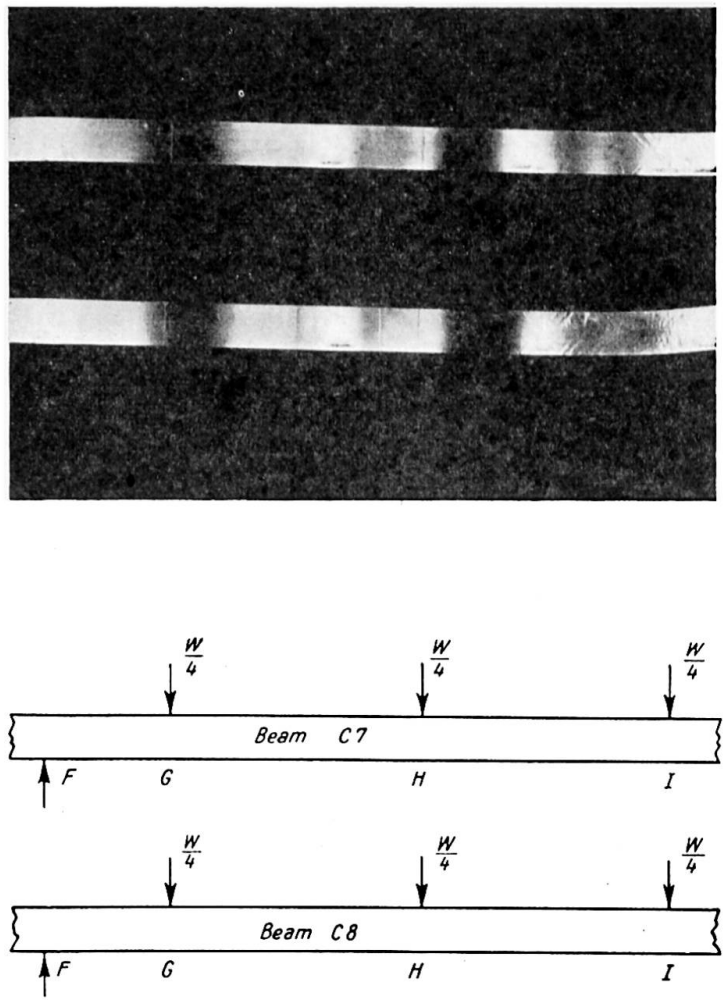

Fig. 8. Comparison of Lüders' wedges on beams C7 and C8

sections C and I. The side faces of parts of beams C7 and C8 after testing are compared in fig. 8. The theoretically deduced values of the moments at various sections of beam C8 at all stages of loading up to the collapse load are shown in fig. 9, and the progressive movement of the positions of the maximum sagging moments is apparent.

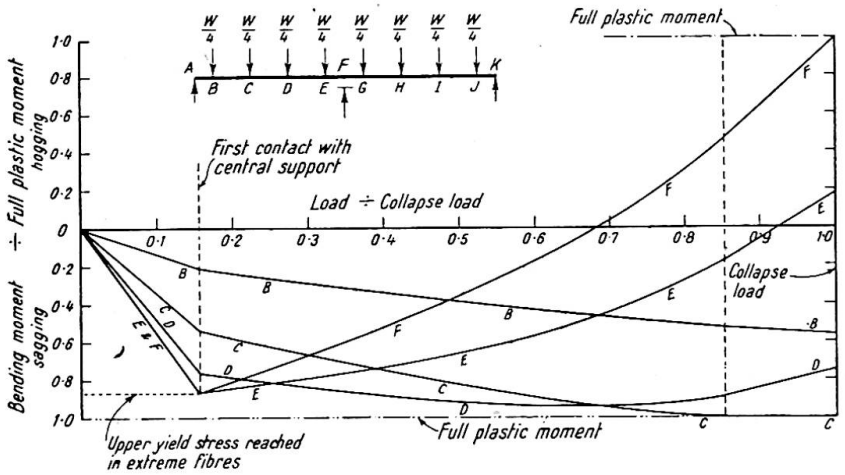

Fig. 9. Theoretical bending moment curves for beam C8

In test C5, the supports were at the same level, and equal loads of 0·50 tons were applied to each span. The load on span DG (fig. 2) was then kept constant while that on span AD was increased until collapse occurred at 1·20 tons. Finally the load on span DG was increased until this part of the beam also failed at a load of 1·25 tons.

3. Tests on fixed-ended beams

(a) *Preparation of beams*

The beams were all prepared from the same black mild-steel plate (dimensions 17 in. × 2 in. × $\frac{1}{4}$ in.) by cutting longitudinally (in the direction of rolling) into strips. The small size of the beams ($\frac{1}{4}$ in. × $\frac{1}{4}$ in. section) made it desirable to anneal at 900° C. and cool in air in order to reduce some of the effects of rolling and work-hardening. The beams were bent about axes perpendicular to the plane of the original plate.

(b) *Description of tests*

The tests are summarised in fig. 10. The beams E1–6 were tested over a span of 6·0 in. between end fittings which provided moments of resistance proportional to the rotations of the end sections of the beam. If a moment M lb. in. at the end of a beam corresponded to a rotation of θ radians, then $\theta = KM$ where K had the values for each beam given in the second column of fig. 10. The simply supported beams EC1 and EC2 had a span of 4·0 in. Fig. 10 shows the positions of the dial gauge used to measure deflections and of the mirror gauges used to measure rotations.

Tests E1, E2 and E3 were conducted to investigate the effect of various degrees of end fixity. Beams E4, E5 and E6 were subjected to loads at several sections (1, 2, 3 in fig. 10) in turn, each load being just sufficient according to the simple theory, to bring about collapse.

The arrangement for testing those beams which had the highest degree of end

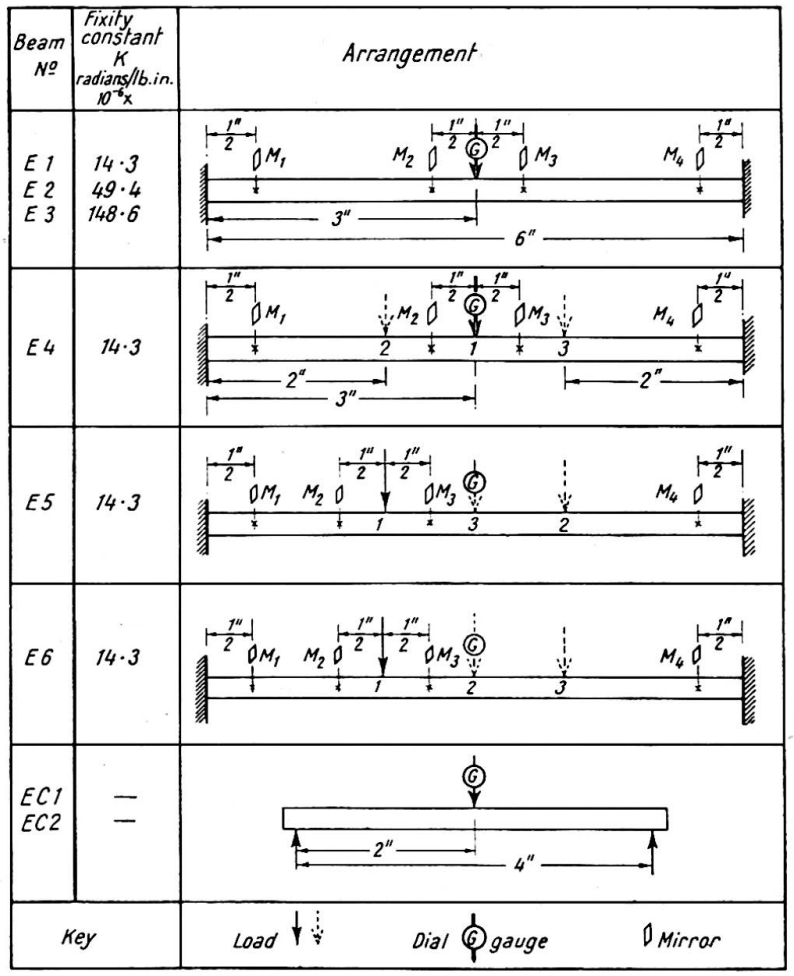

Fig. 10. Summary of tests on fixed-ended beams

fixity (beams E1, E4, E5 and E6) is shown in fig. 11, the load being applied by a chain acting through a yoke. The arrangement for testing beams E2 and E3 is shown in fig. 12, the clamping blocks on the end fittings having been removed for the sake of clarity.

During all the tests, load increments were made at approximately two-minute intervals until creep was first observed. Before each subsequent increment, the rate of creep on the dial gauge was allowed to drop to 10^{-4} in. during any two-minute interval.

(c) *Test results*

Beams E1, E2, E3, EC1 and EC2

The results are summarised in Table III, and columns 1 to 4 require no explanation. The end-fixity constants for the partially fixed-ended beams are given in column 5, from which it is possible to calculate the theoretical ratio of end to central moments for a central point load in the elastic range (column 6). The collapse loads are given in column 7, from which the lower yield stresses may be calculated by means of the simple plastic theory (see Table III, column 7). The percentage differences from the mean are given in column 10.

On the basis of the method suggested by Roderick and Phillipps for allowing for load concentration, these same collapse loads give the yield stresses shown in

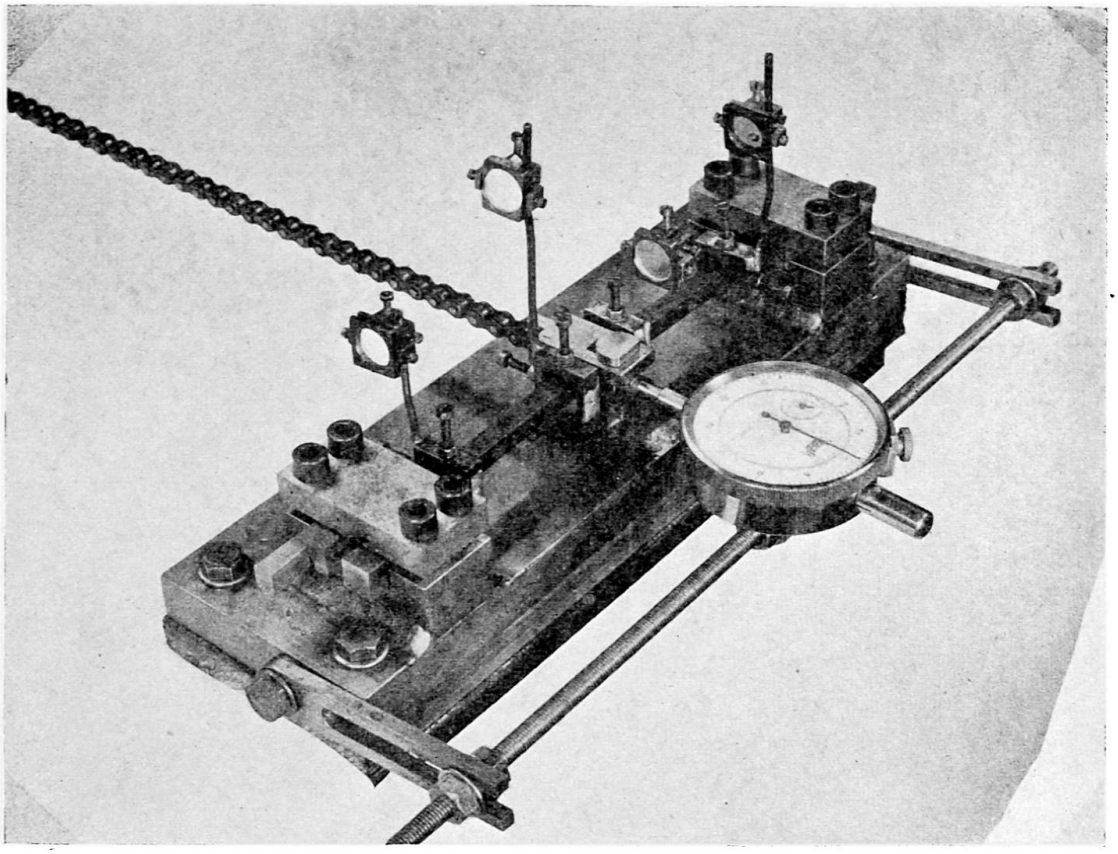

Fig. 11. Arrangement for testing fixed-ended beams

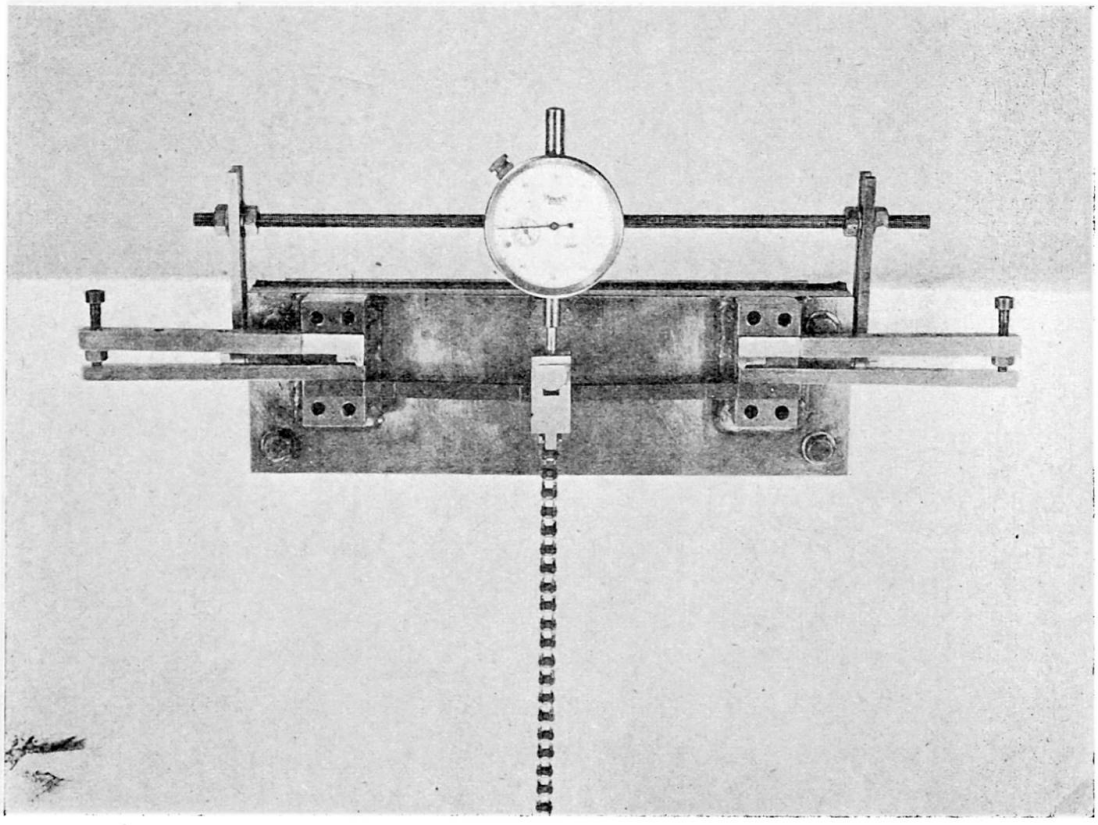

Fig. 12. Method of obtaining reduced end fixity

TABLE III

	1	2	3	4	5	6	7	8	9	10	11	12	13
								Analysis by simple plastic theory ignoring the effect of load concentration			Analysis in which allowance is made for the effect of load concentration		
	Beam No.	Mean Width, in.	Mean Depth, in.	Estimated Modulus of Elasticity E, tons/in.^{2}	End Fixity Constant K, radians/ lb. in. $10^{-6}\times$	Ratio of End Moment to Central Moment in Elastic Range	Collapse Load, lb.	Lower Yield Stress, tons/in.^{2}	Mean Lower Yield Stress, tons/in.^{2}	Per cent Difference	Lower Yield Stress, tons/in.^{2}	Mean Lower Yield Stress, tons/in.^{2}	Per cent Difference
1	E1	0·254	0·253	13,440	14·3	0·912	258	21·3		−3·4	20·4		−2·6
2	E2	0;249	0·255	13,440	49·4	0·746	263	21·8		−1·2	20·9		−0·3
3	E3	0·250	0·256	13,440	148·6	0·490	269	22·0	22·1	−0·3	21·1	21·0	0·7
4	EC1	0·246	0·252	13,140	—	—	199	22·8		3·4	21·4		2·2
5	EC2	0·247	0·250	13,730	—	—	194	22·4		1·5	21·0		0

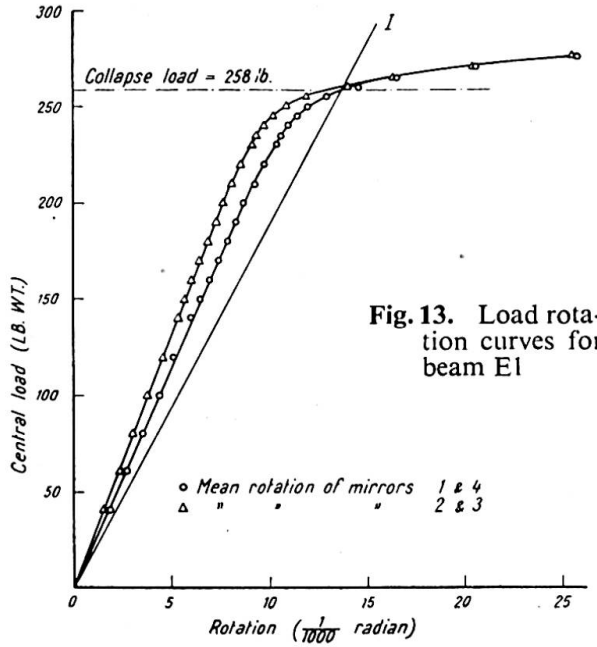

Fig. 13. Load rotation curves for beam E1

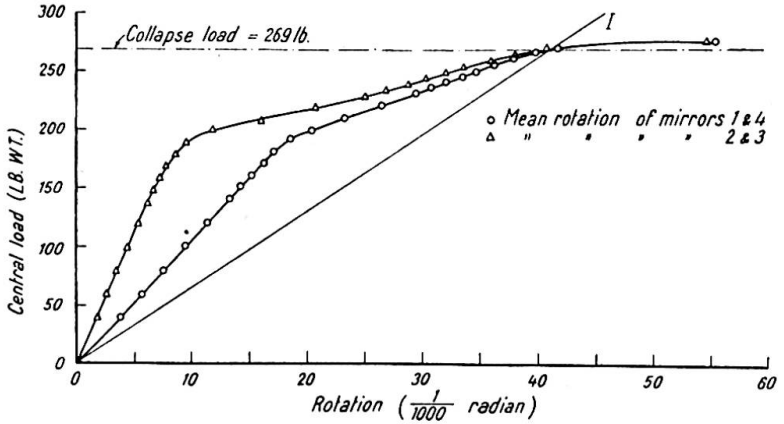

Fig. 14. Load rotation curves for beam E3

column 11, and the percentage differences from the mean are given in column 13. There is a certain improvement in the agreement between the yield stress values as compared with those given in column 8.

Load rotation curves are given for beams E1 and E3 in figs. 13 and 14 respectively. These curves do not indicate such definite collapse loads as obtained for the $\frac{7}{8}$-in. square beams described above. This may be due to strain hardening, and in order to obtain a consistent interpretation of test results, the collapse loads have been determined as follows.

Taking the value for the modulus of elasticity given in column 4 of Table III, and assuming some value for the collapse load, it is possible to calculate by means of the simple plastic theory of bending the rotation at any section of the beam when it is just about to collapse. Then the relationship between the assumed collapse load and the rotation is obtained as a straight line OI (figs. 13 and 14), and the collapse load is taken as the intersection of this line with the experimental load rotation curve. The figure quoted for any beam in column 7 of Table III is the mean of the three values obtained from the central deflection and the two pairs of mirrors (M_1, M_4 and M_2, M_3).

In the case of beam E1, the end moments were in the elastic range almost equal to the central moments (see column 6 of Table III), and the full plastic moment was reached at all three sections at practically the same load. With beam E3, however, the end moments were in the elastic range less than half the central moment, and the load rotation curves (fig. 14) indicate that full plastic moment was reached at the centre at a load of about 200 lb. Thereafter the rotations increased almost linearly with load up to 255 lb., soon after which full plastic moments developed at the ends and collapse occurred.

Beams E4, E5 and E6

The results for beams E4, E5 and E6 are summarised in Tables IV and V. Sufficient load was applied successively to the three loading positions (see fig. 10) to produce full plastic moments at the ends and under the load. Values of the lower yield stress calculated on the basis of the simple plastic theory are given in column 8 of Table IV.

TABLE IV

	1	2	3	4	5	6	7	8
	Beam No.	Mean Width, in.	Mean Depth, in.	Estimated Modulus of Elasticity, E, tons/in.^{2}	End Fixity Constant K, radians/lb. in. 10^{-6} ×	Order of Loading Positions	Maximum Load Actually Applied	
							Load, lb.	Corresponding Lower Yield Stress, tons/in.^{2}
1	E4	0·249	0·255	13,440	14·3	C	260·0	21·5
2						D	292·5	21·5
3						E	292·5	21·5
4	E5	0·248	0·253	13,440	14·3	D	287·5	21·6
5						E	287·5	21·6
6						C	255·6	21·6
7	E6	0·247	0·254	13,440	14·3	D	285·0	21·3
8						C	253·3	21·3
9						E	285·0	21·3

TABLE V

	1	2	3	4	5	6	7	8	9
	Beam No.	Quantity	Unit	1st Load Position		2nd Load Position		3rd Load Position	
				Observed Maximum	Calculated Value at Collapse	Observed Maximum	Calculated Value at Collapse	Observed Maximum	Calculated Value at Collapse
1	E4	Central deflection	in. $\times 10^{-3}$	60·0	45·5	66·1	87·2	89·7	100·0
2		Rotation θ_1	radians $\times 10^{-3}$	18·1	13·6	30·9	46·4	28·7	31·6
3		,, θ_2	,,	18·8	13·6	22·7	39·4	10·1	15·0
4		,, θ_3	,,	17·5	13·6	4·0	15·0	29·7	39·4
5		,, θ_4	,,	18·4	13·6	22·0	22·9	46·5	53·5
6	E5	Central deflection	in. $\times 10^{-3}$	50·1	63·1	71·3	83·7	83·5	86·3
7		Rotation θ_1	radians $\times 10^{-3}$	29·2	39·6	26·8	29·7	32·8	32·5
8		,, θ_2	,,	31·4	39·6	7·5	15·1	11·3	13·7
9		,, θ_3	,,	9·3	15·1	27·1	39·6	12·5	13·7
10		,, θ_4	,,	12·2	15·1	35·6	44·1	33·9	35·2
11	E6	Central deflection	in. $\times 10^{-3}$	50·3	62·1	66·2	65·8	77·9	94·2
12		Rotation θ_1	radians $\times 10^{-3}$	28·1	39·0	27·4	27·6	27·2	31·5
13		,, θ_2	,,	31·4	39·0	14·3	13·5	7·8	14·9
14		,, θ_3	,,	10·0	14·9	11·0	13·5	25·4	39·0
15		,, θ_4	,,	11·7	14·9	20·5	17·8	36·5	49·1

It is possible by means of the simple plastic theory to calculate the theoretical deflections and rotations at collapse for the various positions of the load. These calculated values are compared with those observed in Table V. The rotations θ_1, θ_2, θ_3 and θ_4 refer respectively to mirrors M_1, M_2, M_3 and M_4. Except for the first loading position practically all the observed deflections and rotations are less than the calculated values. Hence the ability of a beam to sustain a given ultimate load is not adversely affected by the attainment of the full plastic moment at various sections due to other critical load distributions. This is true whatever the order in which the loads are applied.

Tension tests

Tension tests were performed on four specimens, of diameter 0·178 in. and gauge length 0·70 in., in a Hounsfield Tensometer. Specimens ET1 and ET2 were cut from the ends of beam E2 after testing, and specimens ET3 and ET4 were cut from the ends of beam E6. The upper and lower yield stresses obtained are given in Table VI.

TABLE VI

Tension Specimen	Upper Yield Stress, tons/in.^{2}	Lower Yield Stress, tons/in.^{2}
ET1	21·68	20·88
ET2	21·57	20·57
ET3	22·70	20·56
ET4	21·08	20·17

The lower yield stresses are in good agreement with each other, and have a mean value of 20·54 tons/in.^{2} Considering beams E1, E2, E3, EC1 and EC2 (see Table III), the method of analysis suggested by Roderick and Phillipps gives a mean yield stress in closer agreement with the yield stress from the tension tests than is obtained when the simple plastic theory is applied.

4. CONCLUSIONS

The general agreement between the values of the lower yield stress calculated from the collapse loads for both the continuous and the fixed-ended beams is satisfactory and shows that the simple plastic theory gives predictions of the collapse loads of such beams with sufficient accuracy for practical purposes. The method of allowing for stress concentration suggested by Roderick and Phillipps (1949) does not lead to any distinct improvement for the continuous beams, but does lead to slightly better agreement for the fixed-ended beams. The tension tests carried out in connexion with the continuous beams did not establish any conclusive results, but with the fixed-ended beams tension tests favoured the method of Roderick and Phillipps.

The tests on the continuous beams confirm that the predictions of the plastic theory are not upset by sinking of supports, even if sinking is sufficient to cause yield in the beam. The plastic theory is equally successful for all the load distributions investigated, and the failure of one span does not decrease the ultimate carrying capacity of an adjacent span.

The tests on the fixed-ended beams show that ultimate carrying capacity is independent of the degree of rigidity of the end connections as long as these are capable of resisting the full plastic moment. The carrying capacity is not adversely affected when full plastic moments are produced at a number of sections by different successive load distributions, and this is true whatever the order in which the loads are applied.

The work described in this paper was carried out at the Engineering Laboratory, Cambridge University, and forms part of a general investigation into the behaviour of rigid-frame structures under the direction of Professor J. F. Baker, Head of the Department of Engineering.

References

BAKER, J. F. *J. Inst. Struct. Engrs.*, **27**, 397, 1949.
BAKER, J. F., and RODERICK, J. W. *Trans. Inst. Welding*, **3**, 83, 1940; **5**, 97, 1942.
BLEICH, H. *Der Bauingenieur*, **19/20**, 261, 1932.
EWING, A. *The Strength of Materials*, Cambridge U.P., 1903.
HENDRY, A. W. *Civil Engineering and Public Works Review*, **45**, 172, 1950.
HEYMAN, J. "The Determination by Relaxation Methods of Elasto-Plastic Stresses in Two Transversely Loaded Beams" (unpublished).
HORNE, M. R. *J. Inst. Civ. Engrs.*, **34**, 174, 1950.
HORNE, M. R. *Proc. Roy. Soc. A*, **207**, 216, 1951.
MAIER-LEIBNITZ, H. Proc. Int. Assn. Bridge Struct. Engng., Berlin, 1936.
NEAL, B. G., and SYMONDS, P. S. *J. Inst. Civ. Engrs.*, **35**, 21, 1950.
QUINNEY, H. *Engineering*, **145**, 309, 1938.
ROBERTSON, A., and COOK, G. *Proc. Roy. Soc. A*, **88**, 462, 1913.
RODERICK, J. W. *Phil. Mag.*, **39**, 529, 1948.
RODERICK, J. W., and PHILLIPPS, I. H. *Research, Engineering Structures Supplement*, **9**, 1949.
VOLTERRA, E. *J. Inst. Civ. Engrs.*, **20**, 349, 1943.

Summary

According to the simple plastic theory, the collapse loads of mild-steel continuous and fixed-ended beams may be calculated by considering merely the requirements of equilibrium in relation to the external loads and the full plastic moments of resistance of the beams. It follows that sinking of supports, order of loading and degree of end fixity should have no influence on such collapse loads. In order to check these deductions, tests were performed on $\frac{7}{8}$-in. square beams continuous over two spans and on $\frac{1}{4}$-in. square single-span beams provided with varying degrees of end fixity. The influence of various types of loading and of varying orders of application of the loads were investigated. Control tests were performed on similar simply supported members, and tension tests carried out at controlled rates of strain on material taken from unyielded sections of the beams.

The results give consistent confirmation of the simple plastic theory, and show conclusively that the collapse loads may be calculated with sufficient accuracy for practical purposes by this means. During the loading of a continuous beam in which one support is initially lower than the others, there is, according to the simple plastic theory, a progressive movement of the sections of maximum sagging moments along the beam. This is demonstrated in the tests by the appearance of Lüders' wedges on the polished surfaces of the $\frac{7}{8}$-in. square beams.

Résumé

Suivant la théorie simple de la plasticité, les charges de rupture des poutres en acier doux, continues ou encastrées à leurs extrémités, peuvent être calculées par simple considération des exigences d'équilibre corrélativement aux charges extérieures et aux pleins moments plastiques de résistance des poutres. Il en résulte que l'affaissement des appuis, l'ordre de mise en charge et le degré de rigidité aux extrémités ne doivent exercer aucune influence sur ces charges de rupture. Pour vérifier ces déductions, des essais ont été effectués sur des poutres carrées de $\frac{7}{8}$ in. (22,2 mm.), continues sur deux portées, ainsi que sur des poutres carrées de $\frac{1}{4}$ in. (6,35 mm.) sur portée simple, avec différents degrés de rigidité aux extrémités. On a étudié l'influence de divers types de charges et de divers ordres de mise en charge. Des essais ont été effectués, à titre de contrôle, sur des éléments simplement posés sur leur appuis; on a également procédé à des essais de traction, sous des taux de tension contrôlés, sur des éprouvettes prélevées sur des sections n'ayant subi aucune déformation.

Les résultats obtenus fournissent une bonne confirmation de la théorie simple de la plasticité et montrent d'une manière concluante que les charges de rupture peuvent être calculées avec une précision suffisante pour les besoins de la pratique, d'après la méthode ci-dessus. Au cours de la mise en charge d'une poutre continue dont un appui est initialement plus bas que les autres, il se produit, suivant la théorie simple de la plasticité, un déplacement progressif des sections présentant les moments maxima d'affaissement, le long de la poutre. Ceci est mis en évidence, au cours des essais, par l'apparition de figures de Luders sur les surfaces polies des poutres carrées de $\frac{7}{8}$ in.

Zusammenfassung

Nach der einfachen Plastizitätstheorie können die Bruchlasten von durchlaufenden und eingespannten Balken aus Flusstahl allein aus der Betrachtung der Gleichgewichtsbedingungen bezüglich der äusseren Lasten und der vollen plastischen Widerstandsmomente der Balken berechnet werden. Es folgt daraus, dass Auflagersenkungen, Lastanordnung und Einspannungsgrad keinen Einfluss auf solche Bruchlasten haben sollten. Zur Ueberprüfung dieser Feststellungen wurden Versuche an über zwei Felder durchlaufenden, $\frac{7}{8}$ in. (22,2 mm.) starken und an einfeldrigen, verschieden stark eingespannten, $\frac{1}{4}$ in. (6,35 mm.) starken Rechteck-Balken durchgeführt. Die Einflüsse verschiedener Arten von Lasten und verschiedener Formen der Last-Aufbringung wurden untersucht. Zur Kontrolle wurden Untersuchungen an entsprechenden einfach gelagerten Balken gemacht und unter kontrollierten Spannungen Zugversuche an Material aus unverformten Trägerteilen ausgeführt.

Die ermittelten Resultate bedeuten eine gute Bestätigung der einfachen Plastizitätstheorie und zeigen überzeugend, dass die Bruchlasten mit für praktische Bedürfnisse genügender Genauigkeit nach dieser Methode berechnet werden können. Während der Belastung eines durchlaufenden Balkens, bei dem ein Auflager von Anfang an tiefer liegt als die anderen, ergibt sich, in Uebereinstimmung mit der einfachen Plastizitätstheorie, entlang dem Balken ein fortlaufendes Fliessen der Zonen grösster Momentenbeanspruchung infolge Einsenkung. Dies zeigt sich im Versuch durch das Auftreten von Fliessfiguren von Lüders auf den polierten Oberflächen der $\frac{7}{8}$ in. Rechteckbalken.